

**Nutritional limitation of iron and methionine.
Physiological consequences and new evasion
strategies in staphylococci.**

Dissertation

der Mathematisch-Naturwissenschaftlichen Fakultät
der Eberhard Karls Universität Tübingen
zur Erlangung des Grades eines
Doktors der Naturwissenschaften
(Dr. rer. nat.)

vorgelegt von
Angelika Müller-Jochim
aus Sigmaringen

Tübingen
2020

Gedruckt mit Genehmigung der Mathematisch-Naturwissenschaftlichen Fakultät der
Eberhard Karls Universität Tübingen.

Tag der mündlichen Qualifikation:

01.12.2020

Stellvertretender Dekan:

Prof. Dr. József Fortágh

1. Berichterstatter:

Dr. Simon Heilbronner

2. Berichterstatter:

Prof. Dr. Friedrich Götz

Table of contents

| | |
|--|-----|
| Table of contents | 3 |
| Summary | 4 |
| Zusammenfassung | 5 |
| Chapter 1 – General Introduction | 7 |
| Chapter 2..... | 27 |
| An ECF-type transporter scavenges heme to overcome iron-limitation in <i>Staphylococcus lugdunensis</i> | 27 |
| Chapter 3..... | 67 |
| Methionine limitation impairs pathogen expansion and biofilm formation capacity ... | 67 |
| Chapter 4 – General Discussion..... | 102 |
| Contributions to publications..... | 117 |
| Curriculum vitae..... | 118 |

Summary

Gram-positive cocci are a major cause of healthcare associated infections. *Staphylococcus aureus* and *Staphylococcus lugdunensis* represent prominent species. Additionally, Gram-negative bacteria as *Pseudomonas aeruginosa* and *Escherichia coli* frequently cause infections. With the emerge of multi drug resistant strains, the development of new antibacterial agents against Gram-positive and Gram-negative pathogens becomes increasingly urgent. To maintain proliferation, bacteria need to adapt to different parameters as e.g. varying nutrient availability. During invasive disease, the access to trace nutrients such as iron (Fe) is actively limited by the host. This strategy is referred to as “nutritional immunity”. Besides trace metals like Fe, several metabolites as e.g. the amino acid methionine, are essential for bacterial growth and their availability in the human host is scarce. During infection bacteria either need efficient acquisition systems or must rely on the *de novo* synthesis of such nutrients.

Here we provide insight into the unique role of an iron regulated ABC transporter from the energy-coupling factor type (ECF) in *S. lugdunensis* which is involved in heme acquisition. We showed that the Lha transporter is specific for heme and recombinant substrate-specific protein LhaS accepts heme from various hemoproteins. By creating isogenic mutants and recombinant expression of Lha we showed that its function is independent of the well-studied heme acquisition system Isd and allows usage of human cells as a source of iron. Our investigations revealed a new strategy of nutritional heme acquisition to overcome host-induced iron limitation. Additionally we investigated the importance of the methionine biosynthesis pathway for bacterial growth and biofilm formation. We found methionine auxotrophic mutants of *S. aureus*, *E. coli* and *P. aeruginosa* to depend on exogenous concentrations of methionine exceeding those reported for human serum. Growth characteristics and biofilm formation was impaired in auxotrophic strains of *S. aureus* and *P. aeruginosa*. Our studies suggest primary metabolic pathways as interesting targets for antimicrobial therapy.

Zusammenfassung

Gram-positive Kokken sind eine der Hauptursachen für Infektionen im Gesundheitswesen. *Staphylococcus aureus* und *Staphylococcus lugdunensis* repräsentieren prominente pathogene Spezies. Zusätzlich verursachen häufig Gram-negative Bakterien, wie *Pseudomonas aeruginosa* und *Escherichia coli* Infektionen. Mit dem Aufkommen multiresistenter Stämme wird die Entwicklung neuer Antibiotika gegen Gram-positive, sowie Gram-negative Krankheitserreger immer dringlicher. Um ihr Wachstum aufrecht erhalten zu können, müssen sich Bakterien an verschiedene Parameter anpassen, wie z.B. variierende Nährstoffverfügbarkeit. Während einer invasiven Erkrankung wird der Zugang zu Spurenelementen wie Eisen (Fe) vom Wirt aktiv limitiert. Diese Strategie wird als „nutritional immunity“ bezeichnet. Neben Spurenmetallen wie Fe können mehrere Metabolite wie z.B. die Aminosäure Methionin für das Bakterienwachstum essenziell sein. Auch ihre Verfügbarkeit im menschlichen Körper ist knapp. Daher benötigen Bakterien während einer Infektion entweder effiziente Aufnahmesysteme oder müssen sich auf die *de-novo* Synthese solcher Nährstoffe verlassen. Hier geben wir einen Einblick in die einzigartige Rolle eines eisenregulierten ABC-Transporters vom „energy-coupling factor“ Typ (ECF) in *S. lugdunensis*, welcher an der Häm-Aufnahme beteiligt ist. Wir haben gezeigt, dass der Lha-Transporter spezifisch für Häm ist und dass das rekombinante substratspezifische Protein LhaS Häm von verschiedenen Hämoproteinen akzeptiert. Durch die Generierung isogener Mutanten und die rekombinante Expression von Lha haben wir gezeigt, dass seine Funktion unabhängig vom gut untersuchten Häm-Aufnahmesystem Isd ist und Lha die Verwendung menschlicher Zellen als Eisenquelle ermöglicht. Unsere Untersuchungen ergaben eine neue Strategie der Häm-Aufnahme zur Überwindung der durch den Wirt verursachten Eisenlimitierung. Zusätzlich untersuchten wir die Bedeutung des Methionin-Biosynthesewegs für das Bakterienwachstum und die Biofilmbildung. Wir beobachteten, dass auxotrophe Methionin-Mutanten von *S. aureus*, *E. coli* und *P. aeruginosa* von exogenen Methionin-Konzentrationen abhängen, die die für menschliches Serum angegebenen Konzentrationen überschreiten. Das Wachstum und die Biofilmbildung waren bei auxotrophen *S. aureus* und *P. aeruginosa* Stämmen beeinträchtigt. Unsere Studien

legen nahe, dass primäre Stoffwechselwege interessante Ziele für antimikrobielle Therapien sind.

Chapter 1 – General Introduction

Staphylococci

Bacteria belonging to the staphylococcal species are Gram-positive, non-motile cocci whose DNA has a low G+C content from 30-40% [1]. The 0.5-1.5 µm small cocci divide in four planes to form grape shaped cell aggregates. *Staphylococci* colonize birds and mammals but are often found to colonize the human body, too. Several different species were identified all over the human body e.g. on the skin and in the nasal cavities [2]. Staphylococci are facultative anaerobe, catalase-positive and not able to form spores. Furthermore, they are oxidase-positive and tolerant to high salt concentrations. Due to the ability to produce coagulase, *Staphylococci* are divided into coagulase-negative (CoNS) and coagulase-positive (CoPS) strains [3].

Staphylococcus aureus

Staphylococcus aureus is the only human associated coagulase positive *staphylococcus*. It is one of the major human pathogens and a human commensal. About 30 % of the human population is constantly colonized by *S. aureus*, mainly in the anterior nares [4]. On solid media *S. aureus* colonies appear in a golden colour which is attributed to the membrane bound carotenoid staphyloxanthin [5]. *S. aureus* is equipped with an arsenal of virulence factors, amongst them are secreted exotoxins such as phenyl soluble modulins (PSMs) and leukocidins [6, 7]. The toxic shock syndrome toxin 1 (TSST1), for example, causes a high release of cytokines which leads to the toxic shock syndrome [8]. By consumption of adulterated food, *S. aureus* enterotoxins can cause food poisoning [9]. The cell wall associated MSCRAMMs (microbial surface components recognizing adhesive matrix molecules) represent a second group of virulence factors. They are involved in cell attachment to host molecules such as collagen and fibronectin [10]. With its numerous virulence factors *S. aureus* can cause several diseases ranging from minor skin infections to endocarditis and blood stream infections [11, 12]. Additionally, it is one of the most frequent causes of biofilm related infections [13]. The rise of *S. aureus* antibiotic

resistance is a major concern and methicillin resistant *S. aureus* (MRSA) strains are common. About 22% of the reported *S. aureus* infections in hospitals in the United States, Canada, and Latin America are caused by *S. aureus* MRSA isolates [14]. This resistance to the entire class of β -Lactam antibiotics is mediated by a penicillin insensitive penicillin-binding protein (PBP2A). Usually β -Lactam antibiotics as e.g. methicillin function by inhibiting the function of the penicillin-binding protein (PBP) which is necessary for bacterial peptidoglycan biosynthesis. But the insensitive PBP2A, encoded by *mecA* is able to fulfill its role in peptidoglycan biosynthesis even in the presence of a β -Lactam antibiotic [15]. In the past years, every introduction of a novel antibiotic compound was followed by the emerge of antibiotic resistant bacteria. For that reason, a desperate need for novel antibiotics becomes more and more evident [16].

Pseudomonas aeruginosa

P. aeruginosa counts to the major human pathogens and causes a wide range of infections such as endocarditis and cystic fibrosis (CF). Besides the human body, the usual habitat of *P. aeruginosa* is water, soil, and vegetation. It is a Gram-negative bacillus belonging to the family *Pseudomonaceae* and due to its single polar flagellum, it is motile. Amongst their many virulence factors are endo- and exotoxin production, as well as the ability to form biofilms [17]. Biofilm formation often results in antimicrobial resistance and *Pseudomonas* biofilms are frequently associated within the lungs of cystic fibrosis patients [18, 19].

Staphylococcus lugdunensis

Staphylococcus lugdunensis belongs to the coagulase-negative *staphylococci* (CoNS). Colony pigmentation of *S. lugdunensis* varies from unpigmented, over slightly cream-colored to golden [20]. Due to the expression of a fibrinogen-binding protein, *S. lugdunensis* can easily be mistaken for *S. aureus*. This protein triggers a false positive result in agglutination tests using latex particles coated with fibrinogen. This test is routinely used to distinguish *S. aureus* and CoNS [21]. *S. lugdunensis* is a commensal of the human skin, where it can be found frequently in moist areas like e.g. the perineum, under the large toenail and the inguinal fold [22]. Additionally,

S. lugdunensis can colonize the human anterior nares and competes with *S. aureus* for this niche [23]. In the past, *S. lugdunensis* has been described as a “wolf in sheep’s clothing”. Although CoNS are regarded as less pathogenic, *S. lugdunensis* is counted as a human pathogen that is involved in nosocomial and community-acquired infections [21]. It causes not only skin and soft tissue infections [24], but also severe infections such as bloodstream infections [25] and infective endocarditis [26] have been reported. Full genome sequencing of two *S. lugdunensis* strains revealed several virulence factors that might contribute to severe courses of diseases [27, 28]. The encoded fibrinogen-binding protein (Fbl) facilitates binding to human host tissue [29]. The existence of the *ica* genes allow biofilm formation conferring protection to rough environmental conditions [27, 30]. The pathogenicity of *S. lugdunensis* has several times been reported to cohere with the production of biofilm within medical devices or host tissues [30]. Additionally, the *S. lugdunensis* genome contains genes encoding hemolytic peptides called *S. lugdunensis* synergistic hemolysin (*slush*). SLUSH shows synergistic hemolytic activity with the *S. aureus* β -toxin [31]. A feature that *S. lugdunensis* shares with *Staphylococcus caprae* and *Staphylococcus capitis* [32, 33], when compared with other CoNS, is the expression of the iron-regulated surface determinant (Isd) locus. The Isd system enables *S. lugdunensis* to acquire iron from host hemoproteins like hemoglobin [27].

Clinical importance

Multidrug resistant pathogens are emerging over the years. We are in need of antibacterial agents against Gram-positive and Gram-negative pathogens. *Enterococcus faecium*, *S. aureus*, *Klebsiella pneumoniae*, *Acinetobacter baumannii*, *P. aeruginosa* and *Enterobacter* species belong to the so-called “ESKAPE” pathogens due to extensive antibiotic resistances. Most hospital infections in the USA were caused by these species [34]. For example, increasing number of reports about vancomycin resistance among *E. faecium* strains (VRE), methicillin resistant *S. aureus* strains (MRSA), carbapenem resistant *K. pneumoniae*, *Escherichia coli*, and *Acinetobacter* strains, carbapenem and quinolone resistant *P. aeruginosa* and carbapenem resistant *Enterobacter* species emerge and point up the urgency of the situation [35].

P. aeruginosa causes diseases like endocarditis or cystic fibrosis (CF), where it often forms biofilms. Besides their ability to form biofilms, *P. aeruginosa* possess several additional virulence factors including exotoxin and endotoxin production, as well as an antiphagocytic property [17, 18]. Due to its extended resistance to antibiotics and its ability to cause chronic infections it plays a major role in the healthcare system.

Enterobacteriaceae species as *Escherichia coli* form a substantial part of the human gut microbiota and live as apathogenic commensals. But virulent *E. coli* strains can lead to numerous diseases e.g. gastroenteritis and urinary tract infections, as well as peritonitis. Virulence factors and antibiotic resistance genes are often encoded on mobile genetic elements giving the threat of spreading resistances [36]. New antimicrobial agents to treat infections are desperately needed. Therefore, our knowledge of bacterial virulence factors and bacterial pathogenesis needs to be broadened.

Biofilm formation

Bacterial biofilms can be defined as communities of sessile microbes [37]. The bacteria colonize implanted medical devices and initiate the onset of severe infections as osteomyelitis in orthopaedical patients [38]. Biofilms are structured organizations of bacteria embedded in a matrix of extracellular polymeric substances (EPS) [39]. Biofilm formation can be divided into three phases i) initial attachment, ii) biofilm maturation and iii) detachment. MSCRAMMs mediate primary attachment to a polymer surface e.g. to a medical device coated with host matrix molecules. Biofilm maturation depends on adhesive matrix molecules like polysaccharide intercellular adhesins (PIA). These polysaccharides are produced by the *icaADBC* gene products and mediate cell-cell contact. PIA-independent biofilms are also described and are based on the production of the accumulation associated protein (Aap) [40] or the MSCRAMM SasG [39]. Besides exopolysaccharides and proteins, also extracellular DNA (eDNA) is a major part of bacterial biofilms. It is either derived from lysed bacterial cells as proposed for *S. aureus* or released from small membrane vesicles as it was shown for *P. aeruginosa* [40-42]. However, the importance of eDNA for biofilm maturation is still not fully investigated. Especially in *P. aeruginosa* biofilms exopolysaccharides play a major role. Three important polysaccharides involved in biofilm structure and antibiotic resistance are Psl, Pel and alginate [43]. Psl mediates cell-cell or cell-surface contact

[44], and Pel is involved in antibiotic resistance and a major factor for solid-surface biofilm formation [45, 46]. Alginate production is mainly associated with cystic fibrosis infections and contributes to biofilm stability by affecting the water and nutrient storage inside biofilms [47, 48]. Biofilm detachment relies on the expression of extracellular proteases, PSMs and nucleases and during detachment the released cells can spread further to new sites [49].

Nutritional immunity

Bacteria rely on certain nutrients in their environment because they are auxotrophic for diverse vitamins or transition metals. For example, iron (Fe) is an essential molecule for all living organisms. It is crucial for several metabolic processes such as respiration, DNA replication and glycolysis [50, 51]. Depending on the pH, iron can be present in two oxidation states, ferrous (Fe^{2+}) or ferric (Fe^{3+}) iron. Under physiological pH conditions ferrous iron is oxidized to ferric iron, which is virtually insoluble. Additionally, free iron is toxic due to the ability to form oxygen radicals. Hence, in the host iron is mostly bound to proteins or complexed in heme as the prosthetic group of hemoproteins such as hemoglobin or myoglobin [50, 52]. Most bacterial organisms require 10^{-5} to 10^{-7} M iron for survival. This is 10^{11} - 10^{12} fold higher than free iron is available in the host [50, 53, 54].

Although iron is an abundant molecule within the human body, it is hardly available to invading microorganisms as it is complexed to iron binding proteins [55]. Most iron within the human host is localized within erythrocytes. Hemoglobin within erythrocytes contains heme as prosthetic group. Heme complexes an iron atom in the center of a porphyrin molecule. Hemoglobin functions as an oxygen-delivery and carbon dioxide-removal system [56]. But also, myoglobin located in the muscle tissues contains heme. To access this iron source, bacteria need to lyse erythrocytes or muscle cells, to extract and import heme and finally to release the metal ion. Additionally, iron is stored intracellularly in the storage protein ferritin e.g. in liver cells. [57].

Especially during infection, the mechanism referred to as “nutritional immunity” restricts not only iron availability but also all other transition metals as e.g. zinc (Zn) and manganese (Mn). Bacterial proliferation is reduced by hindering the access to trace metals via high affinity binding vertebrate proteins in body fluids and tissues, or by utilizing the toxicity of transition metals [58, 59]. Several host mechanisms for

withholding iron have evolved. Free hemoglobin is sequestered by the host protein haptoglobin and heme is captured by hemopexin. Any Fe^{3+} in serum is bound by transferrin and in secreted fluids as saliva, sweat, lacrimal fluid and breast milk by lactoferrin. Additionally, albumin, citrate and amino acids can sequester free iron in serum [56, 60].

To overcome such barriers, some pathogens have evolved sophisticated systems for iron acquisition during colonization and infection. There are five general mechanisms to overcome nutritional immunity. For example, *Borrelia burgdorferi* diminishes its need for iron by eliminating most enzymes that need Fe as a cofactor and instead uses manganese (Mn) as cofactor for the metalloenzymes left [61].

The other mechanisms involve siderophore production, expression of lactoferrin and transferrin receptors, transporters for ferric and ferrous iron and heme acquisition systems.

Siderophores are small (200 - 2000 Da) secreted secondary metabolites with a high affinity towards Fe^{3+} . Association constants up to 10^{50} have been reported, which is even higher than that of lactoferrin and transferrin. This enables bacteria to extract Fe from those host proteins. Siderophores are produced under low iron conditions by a wide range of bacteria and more than 500 siderophores are known so far [56, 62, 63]. Because these compounds are too big for diffusion, import of iron-saturated forms is managed by specialized transporters. In Gram-negative bacteria transport is carried out by the TonB-ExbB-ExbD system to manage outer membrane transport. Once in the periplasm siderophores were captured by substrate binding proteins of ABC transporters and shuttled into the cytoplasm. In Gram-positive bacteria ABC transporter systems with substrate-binding lipoproteins mediate siderophore transport. For example, the two transporter systems Hts and Sir of *S. aureus* transport the siderophores staphyloferrin A and staphyloferrin B, respectively, into the cell [64, 65]. However, it has been shown that host protein lipocalin 2 binds bacterial siderophores from the catecholate-type e.g. produced by *E. coli* and therefore prevents siderophore iron acquisition of certain pathogens [66].

Even though siderophores enable bacteria to sequester iron from transferrin and lactoferrin, some bacteria evolved receptors to directly use transferrin or lactoferrin as iron source. By expressing TbpA and TbpB during iron limitation bacteria utilize transferrin as iron source. TbpA mediates the transport and TbpB captures holo-transferrin. Hence, iron is extracted and further imported into the cell [67, 68].

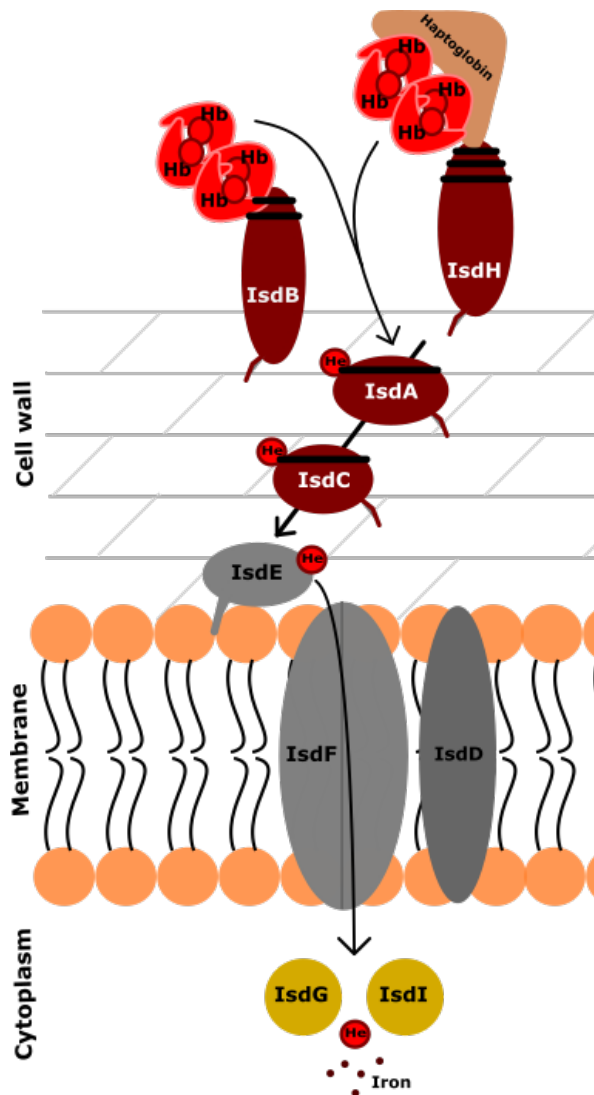


Figure 1 Schematic drawing of *S. aureus* Isd system. Hb- hemoglobin; He- heme; black lines indicate NEAT domains

Additionally, there is the transport of free Fe^{2+} . Many bacterial pathogens express the ferrous iron transporter system (Feo). By expression of the *feo* genes they shuttle free Fe^{2+} into the cytoplasm [69]. Last, bacteria can acquire iron from heme or hemoproteins. The Isd systems (iron-regulated surface determinant) of *S. lugdunensis* and *S. aureus* are well-studied heme acquisition systems. *S. aureus* encodes four cell surface receptors (IsdABCH) shown in Figure 1, that bind host hemoproteins. It has one membrane transporter (IsdEF) for nutrient transport, a sortase (SrtB) and two cytoplasmic proteins (IsdGI) [70]. The transpeptidase SrtA covalently links IsdABH to the peptidoglycan layer of the cell wall, so that they are displayed on or near the cell surface. Whereas IsdC is linked via SrtB the *isd* encoded sortase, to the cell envelope and does not reach out into the extracellular milieu [71, 72].

IsdABCH possess one to three near transporter domains (NEAT) which enable hemoglobin or heme binding. For example, IsdB captures hemoglobin, whereas IsdH binds both hemoglobin and haptoglobin. In contrast IsdA and IsdC bind only heme [72-75]. After hemoglobin is captured by IsdB or IsdH, heme gets extracted and shuttled over the cell wall by IsdC to a membrane-located ABC transporter IsdEF, which passes heme into the cytoplasm, where heme is degraded by the monooxygenases IsdG or IsdI to release the nutritional iron [75, 76].

Besides the direct heme uptake systems, bacteria can express hemophores able to bind exogenous heme. These secreted heme-binding proteins are recognized by special receptors for heme import. For example, *P. aeruginosa* encodes for such an hemophore-mediated uptake system called HasA. HasA binds heme from

hemoglobin, leghemoglobin, myoglobin and hemopexin. The rate of heme dissociation from hemoglobin almost equals the acquisition rate of HasA, which proposes a passive binding of heme [77, 78]. Pathogens do not only depend on nutritional iron but also on several other trace metals like zinc and manganese. Those trace metals are included in sequestration mechanisms of the innate immune system and scarce in human body fluids. Also, Mn and Zn serve as catalytic cofactors for several metalloenzymes [79, 80]. To hinder bacterial Zn and Mn uptake the protein calprotectin of human neutrophils serves as an Mn^{2+} and Zn^{2+} chelator at the same time. It is a heterodimer with two binding sites, one shows high affinity to Mn^{2+} and to Zn^{2+} and the other only for Mn^{2+} . Additionally, calprotectin exhibits proinflammatory properties [80, 81]. Our current molecular knowledge points towards an ongoing battle for trace nutrients between the infecting microbes and their hosts.

***S. lugdunensis* heme acquisition**

Heme acquisition systems of *S. lugdunensis* and *S. aureus* are well studied. Both encode an iron regulated surface determinant (Isd) locus. It facilitates heme acquisition and can therefore be regarded as an adaptation to an invasive lifestyle. The gene expression is controlled by the ferric uptake regulator (Fur). Fe ions bind to Fur and trigger dimerization of two Fur molecules, these bind to *fur* boxes in the DNA and block transcription. During iron starvation the repressor dissociates from its consensus sequence, leading to an increased gene expression [82, 83]. The Isd locus of *S. lugdunensis* comprises 13 genes, *isdBJCKEFLG*, *srtB*, and an autolysin. IsdB, IsdJ and IsdC are cell wall-anchored and possess 2, 2 and 1 NEAT domains (**near transporter domains**), respectively. NEAT domains enable hemoglobin or heme binding. For example, IsdB has two NEAT domains, IsdB-N1 and IsdB-N2. IsdB-N1 binds hemoglobin resulting in a conformational change of the protein that facilitates heme extraction. The second NEAT domain IsdB-N2 binds heme, and starts passage across the cell wall and membrane [84]. IsdB is processed by sortase A and binds hemoglobin, whereas IsdC can only bind heme and is linked to the peptidoglycan by sortase B. In comparison to *S. aureus*, *S. lugdunensis* does not encode for an haptoglobin-binding protein comparable to IsdH. The proposed transport mechanism starts with hemoglobin binding and heme extraction by IsdB. Heme is passed to IsdC and further to IsdE. IsdE is the membrane-anchored lipoprotein of the transporter

IsdEFL, enabling translocation. In the cytoplasm heme is degraded by the oxygenase IsdG to release the iron ion. The proteins IsdJ and K feature NEAT domains, too. They can bind heme, but their exact role in heme acquisition is not fully elucidated [27, 83, 85]. Additionally, three unknown genes encoding for an ABC transporter form the energy coupling factor type are present within the *isd* locus.

Energy coupling factor type ABC transporters

ABC transporters play an important role in nutrient recovery. They are indispensable for uptake of key nutrients such as carbohydrates and amino acids but also for trace nutrients such as metal ions or vitamins. Hence, bacteria have evolved multiple transporters to satisfy their needs. For example, *Listeria monocytogenes*, *Streptococcus pneumoniae* and *S. aureus* lack thiamin biosynthesis pathways and rely on efficient transporters for the uptake of this micronutrient. All three organisms encode for thiamin-specific transporters from the energy-coupling factor type (ECF) [86]. Amongst the many ABC transporter families, the ECF type ABC transporter family is an exceptional one. The first description of an ECF transporter was in 1979 by Henderson et al. They described a new transporter for folate in *Lactobacillus casei*. Several descriptions for novel micronutrient transporters followed, but only after 2009 they linked all the transporters to the previous findings of Henderson et al. [87, 88]. They are found in about 50% of all prokaryotic species. In contrast, amongst all eukaryotes only a single ECF transporter of unknown function is described for plant chloroplasts [89].

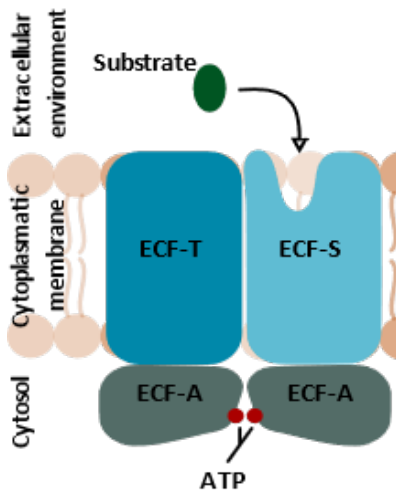


Figure 2 Schematic drawing of an ECF transporter

ECF transporters, as shown in Figure 2, are described to transport micronutrients [86] like thiamin [90] and riboflavin [91], as well as metal ions like nickel and cobalt [92, 93]. According to their genetic organization, ECF transporters are divided into two groups. Genes of group I ECF transporters are located in one operon while genes of group II ECF transporters are scattered through the chromosome [88]. Transporters of the ECF-type consist of three components, a substrate binding protein called S-component (ECF-S), an ATPase (ECF-A) and a transmembrane domain (ECF-T). The latter two built the ECF module. Key of substrate transport is a highly hydrophobic membrane protein (S-component), which is the only part that mediates substrate specificity. So far about 27 S-components, each specific for a particular substrate, have been identified [94]. In type I each S-component has its own ECF module. Although S-components share low sequence identity (10-20 %), in type II ECF transporters several S-components with different substrate specificities share one ECF module for transport [86]. However, crystal structures of S-components revealed that their overall 3D structure, with its six to seven α -helices crossing the membrane, is similar [95]. This could explain how different S-components manage transport through the same ECF module. Generally, S-components show a high substrate specificity and bind their substrates with an affinity in the low nanomolar to picomolar range [96]. Crystal structures of ECF-transporters revealed a stoichiometry of 1:1:1:1 (ECF-S: -T: -A: -A) for a heterodimer, or 1:1:2 for a homodimer module. One S-component together with one ECF-T protein and two ATPase proteins, either in a homo- or heterodimer, builds the functional ECF transporter [97]. Besides the type I and type II ECF transporters of several *Chlamydia* species and cyanobacteria encode for solitary S-components. These are described to be specific for biotin and *in vitro* experiments showed that they can mediate transport of biotin into the cell. It remains unclear how transport can be executed in the absence of ECF modules [98]. One can speculate whether there are further proteins involved [86].

Methionine limitation

Rapid adaption to changing environmental conditions is key to maintain proliferation. Bacteria need to adapt to different parameters such as temperature, light intensity, presence or absence of noxious agents, or varying nutrient availability. Investigations revealed that bacteria can change their growth rates when facing a change of nutrient availability by e.g. adapting their proteome composition [99-101]. Depending on their surrounding they need different sets of nutrient acquisition systems [102]. Besides trace metals like Fe and Mn, several metabolites are essential for bacterial growth, and their availability in human body fluids and on body surfaces is scarce. One example is the amino acid methionine. The proteinogenic amino acid (AA) is especially important for bacterial protein biosynthesis. It is necessary for initiation and elongation of translation. Additionally, it is the precursor of the global methyl group donor S-adenosyl-L-methionine (SAM) and therefore needed for DNA methylation [103, 104]. Even bacterial chemotaxis is affected by methionine limitation. It has been shown that methionine limitation abolishes chemotaxis in *E. coli* [105, 106]. The concentrations of free methionine in human body fluids depends on the diet and can vary significantly. Human serum has been reported to contain 25 to 48 μM methionine depending on the human donor and method of measurement. Human urine showed way lower concentrations of 6.1 μM [107, 108]. Krismer *et al.* investigated the nutritional composition of nasal secretions and their importance on *S. aureus* nasal colonization. Methionine was not detected in nasal fluids suggesting that *S. aureus* relies on the *de novo* synthesis of methionine during nasal colonization. Accordingly, a methionine auxotrophic mutant of *S. aureus* was shown to be attenuated in a cotton rat model of nasal colonization [109]. This finding underlines the importance of methionine biosynthesis or environmental availability for bacterial proliferation. Although bacteria can import exogenous methionine, most species encode for methionine biosynthesis genes [110, 111]. This suggests a crucial importance of the *de novo* biosynthesis to guarantee sufficient intracellular pools of methionine and that the methionine biosynthesis pathway might be an attractive target for antibiotic intervention. However, effectiveness of inhibition will most likely depend on external availability and it is unclear how much methionine is needed for bacterial proliferation during infection. Therefore, more, and detailed investigations about bacterial methionine requirements during infection are needed.

S. aureus, *P. aeruginosa* and *E. coli* do all possess a methionine biosynthesis pathway although they differ in methionine biosynthesis enzymes. It has been shown that methionine biosynthesis mutants are attenuated in growth in methionine depleted medium [109] but the extracellular concentrations that can complement auxotrophy are unclear. However, limited amounts of methionine are present in the human body during infection, therefore information of methionine needs is crucial if the antibacterial potential of methionine biosynthesis blockers is to be judged. Since the methionine biosynthesis pathway is common in most human pathogens be an underestimated drug target. Due to limited treatment possibilities we need to promote investigations concerning screening of new antimicrobial compounds and new drug targets, like the methionine biosynthesis pathway. Therefore, more detailed knowledge about the needs and utilization of methionine during infection of different pathogens is needed.

Methionine biosynthesis

The methionine biosynthesis pathway shown in Figure 3 is well studied in many

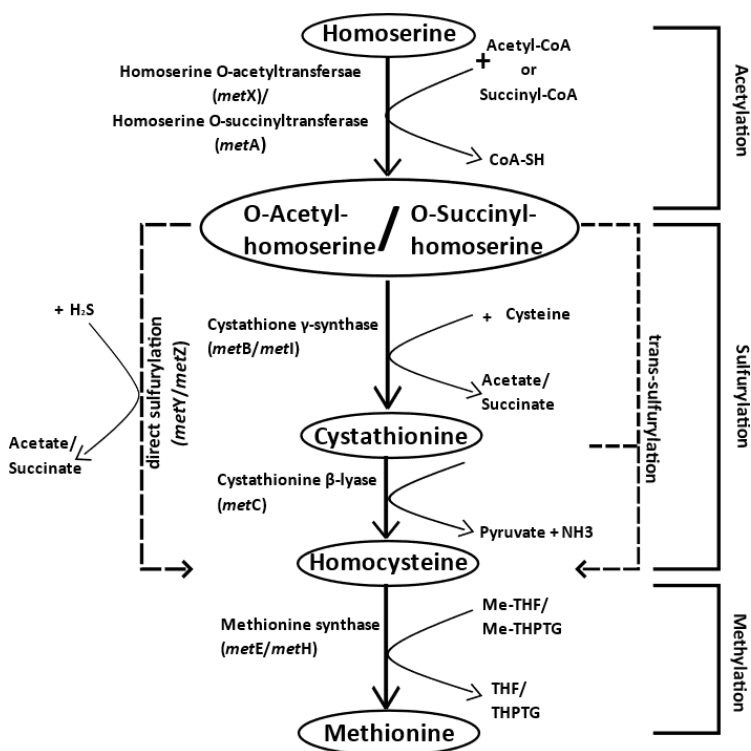


Figure 3 Schematic diagram of the bacterial methionine biosynthesis pathways. Me-THF, 5-methyl-tetrahydrofolate; Me-THPTG, 5-methyl-tetrahydropteroyl

bacterial species. The common precursor is homoserine, which is derived from aspartate. Methionine biosynthesis can be divided into three important steps: i) the acetylation step, ii) the sulfurylation and iii) the methylation step. In different species, the acetylation reaction can be performed by two unrelated proteins, MetA or MetX. The MetA class enzymes can use either succinyl-coenzyme A or acetyl-coenzyme A for activation of homoserine. *S. aureus* employs a MetX class enzyme using

acetyl-coenzyme A. This first acetylation step transfers a succinyl- or acetyl group to produce either O-succinyl-homoserine or O-acetyl-homoserine. The most common sulfurylation steps among different bacteria are direct sulfurylation and trans-sulfurylation, both yielding homocysteine. The one step direct sulfurylation reaction is carried out by MetY and MetZ class enzymes. For example, *Pseudomonas aeruginosa* uses hydrogen sulfide in the direct sulfurylation reaction to build homocysteine in single reaction. Trans-sulfurylation is carried out by e.g. *S. aureus* and *E. coli*. In the first part of the trans-sulfurylation O-acetyl-homoserine or O-succinyl-homoserine together with cysteine is converted to cystathionine by the cystathionine- γ -synthase (MetB/MetI). In this process a thiol group from cysteine is transferred to homoserine. In the following reaction cystathionine is cleaved to form homocysteine. This reaction is catalyzed by a cystathionine β -lyase encoded by *metC*. During the methylation step, methionine synthases like MetE and MetH class enzymes, either one of the methyl group donors, 5-methyl-tetrahydrofolate or 5-methyl-tetrahydropteroyltri-L-glutamate, to methylate homocysteine and produce methionine [104, 109, 112].

Methionine biosynthesis as a putative target for antibiotics

The bacterial methionine biosynthesis pathways seems to be promising targets for antibiotic treatment, since they are omnipresent in prokaryotes [104]. This suggests that inhibitors might have a broad target spectrum. Additionally, mammalian cells lack this biosynthesis pathway and exclusively rely on their diet for methionine supply. To date, the potential of the methionine biosynthesis pathway as a drug target has probably been underestimated, as antibiotic screening approaches are carried out in complex media containing high methionine concentrations. Under these conditions, blocking of methionine biosynthesis is not effective. This might be during colonization and infection, because body fluids contain low methionine concentrations and bacteria most likely rely on the *de novo* synthesis of methionine [109].

By targeting the methionine biosynthesis, one could affect a wide array of bacterial properties including protein biosynthesis and S-Adenosyl-methionine (SAM) biosynthesis. Down the line, methionine deficiency would also affect synthesis of DNA, since SAM is delivering the methyl group for DNA methylation [113]. Similarly it would influence the synthesis of sulfur containing compounds, like e.g. iron-sulfur cluster proteins as bacterial nitrogenases [114]. Additionally, SAM is involved in polyamine

biosynthesis and thereby important for expression of virulence genes [115]. This suggests that depletion of intracellular methionine pools will most likely result in pleiotropic effects on the bacterial physiology.

Besides the importance of methionine during nasal colonization, Krismer *et al.* also reported the activity of the cystathionine γ -synthase inhibitor L-propargylglycine (PG). It blocks the first step of the trans-sulfurylation reaction catalyzed by MetI that converts O-succinyl-CoA and cysteine to cystathionine. L-propargylglycine inhibited *S. aureus* growth in methionine depleted medium, mimicking conditions in the human nose [109]. However, L-propargylglycine also inhibits the cystathionine γ -lyase, catalyzing the reverse reaction in mammalian cells. This makes L-propargylglycine toxic to eukaryotic cells, limiting its therapeutic potential [116-118].

References

1. Rosypal, S., A. Rosypalova, and J. Horejs, *The classification of micrococci and staphylococci based on their DNA base composition and adansonian analysis*. J Gen Microbiol, 1966. **44**(2): p. 281-92.
2. Kloos, W.E. and T.L. Bannerman, *Update on clinical significance of coagulase-negative staphylococci*. Clin Microbiol Rev, 1994. **7**(1): p. 117-40.
3. Harris, L.G., S.J. Foster, and R.G. Richards, *An introduction to Staphylococcus aureus, and techniques for identifying and quantifying S. aureus adhesins in relation to adhesion to biomaterials: review*. Eur Cell Mater, 2002. **4**: p. 39-60.
4. Wertheim, H.F., et al., *The role of nasal carriage in Staphylococcus aureus infections*. Lancet Infect Dis, 2005. **5**(12): p. 751-62.
5. Marshall, J.H. and G.J. Wilmoth, *Pigments of Staphylococcus aureus, a series of triterpenoid carotenoids*. J Bacteriol, 1981. **147**(3): p. 900-13.
6. Dinges, M.M., P.M. Orwin, and P.M. Schlievert, *Exotoxins of Staphylococcus aureus*. Clin Microbiol Rev, 2000. **13**(1): p. 16-34, table of contents.
7. Wang, R., et al., *Identification of novel cytolytic peptides as key virulence determinants for community-associated MRSA*. Nat Med, 2007. **13**(12): p. 1510-4.
8. Marrack, P. and J. Kappler, *The staphylococcal enterotoxins and their relatives*. Science, 1990. **248**(4959): p. 1066.
9. Harris, T.O., W.O. Hufnagle, and M.J. Betley, *Staphylococcal-Enterotoxin Type-a Internal Deletion Mutants - Serological Activity and Induction of T-Cell Proliferation*. Infection and Immunity, 1993. **61**(5): p. 2059-2068.
10. Foster, T.J., et al., *Adhesion, invasion and evasion: the many functions of the surface proteins of Staphylococcus aureus*. Nat Rev Microbiol, 2014. **12**(1): p. 49-62.

11. Gorwitz, R.J., et al., *Changes in the prevalence of nasal colonization with Staphylococcus aureus in the United States, 2001-2004*. J Infect Dis, 2008. **197**(9): p. 1226-34.
12. Archer, G.L., *Staphylococcus aureus: a well-armed pathogen*. Clin Infect Dis, 1998. **26**(5): p. 1179-81.
13. Bryers, J.D., *Medical biofilms*. Biotechnol Bioeng, 2008. **100**(1): p. 1-18.
14. Diekema, D.J., et al., *Survey of infections due to Staphylococcus species: frequency of occurrence and antimicrobial susceptibility of isolates collected in the United States, Canada, Latin America, Europe, and the Western Pacific region for the SENTRY Antimicrobial Surveillance Program, 1997-1999*. Clin Infect Dis, 2001. **32 Suppl 2**: p. S114-32.
15. Pinho, M.G., H. de Lencastre, and A. Tomasz, *An acquired and a native penicillin-binding protein cooperate in building the cell wall of drug-resistant staphylococci*. Proc Natl Acad Sci U S A, 2001. **98**(19): p. 10886-91.
16. Clatworthy, A.E., E. Pierson, and D.T. Hung, *Targeting virulence: a new paradigm for antimicrobial therapy*. Nat Chem Biol, 2007. **3**(9): p. 541-8.
17. Iglewski, B.H., *Pseudomonas*, in *Medical Microbiology*, 4th and S. Baron, Editors. 1996: Galveston (TX).
18. Drenkard, E. and F.M. Ausubel, *Pseudomonas biofilm formation and antibiotic resistance are linked to phenotypic variation*. Nature, 2002. **416**(6882): p. 740-3.
19. Cabeen, M.T., S.A. Leiman, and R. Losick, *Colony-morphology screening uncovers a role for the Pseudomonas aeruginosa nitrogen-related phosphotransferase system in biofilm formation*. Mol Microbiol, 2016. **99**(3): p. 557-70.
20. Fleurette, J., et al., *Clinical isolates of Staphylococcus lugdunensis and S. schleiferi: bacteriological characteristics and susceptibility to antimicrobial agents*. Res Microbiol, 1989. **140**(2): p. 107-18.
21. Frank, K.L., J.L. Del Pozo, and R. Patel, *From clinical microbiology to infection pathogenesis: how daring to be different works for Staphylococcus lugdunensis*. Clin Microbiol Rev, 2008. **21**(1): p. 111-33.
22. Bieber, L. and G. Kahlmeter, *Staphylococcus lugdunensis in several niches of the normal skin flora*. Clin Microbiol Infect, 2010. **16**(4): p. 385-8.
23. Zipperer, A., et al., *Human commensals producing a novel antibiotic impair pathogen colonization*. Nature, 2016. **535**(7613): p. 511-6.
24. Herchline, T.E. and L.W. Ayers, *Occurrence of Staphylococcus lugdunensis in consecutive clinical cultures and relationship of isolation to infection*. J Clin Microbiol, 1991. **29**(3): p. 419-21.
25. Pfaller, M.A., et al., *Survey of blood stream infections attributable to gram-positive cocci: frequency of occurrence and antimicrobial susceptibility of isolates collected in 1997 in the United States, Canada, and Latin America from the SENTRY Antimicrobial Surveillance Program. SENTRY Participants Group*. Diagn Microbiol Infect Dis, 1999. **33**(4): p. 283-97.
26. Vandenesch, F., et al., *Endocarditis due to Staphylococcus lugdunensis: report of 11 cases and review*. Clin Infect Dis, 1993. **17**(5): p. 871-6.
27. Heilbronner, S., et al., *Genome sequence of Staphylococcus lugdunensis N920143 allows identification of putative colonization and virulence factors*. FEMS Microbiol Lett, 2011. **322**(1): p. 60-7.
28. Tse, H., et al., *Complete genome sequence of Staphylococcus lugdunensis strain HKU09-01*. J Bacteriol, 2010. **192**(5): p. 1471-2.

29. Mitchell, J., A. Tristan, and T.J. Foster, *Characterization of the fibrinogen-binding surface protein Fbl of Staphylococcus lugdunensis*. *Microbiology*, 2004. **150**(Pt 11): p. 3831-3841.
30. Argemi, X., et al., *Kinetics of biofilm formation by Staphylococcus lugdunensis strains in bone and joint infections*. *Diagn Microbiol Infect Dis*, 2017. **88**(4): p. 298-304.
31. Donvito, B., et al., *Synergistic hemolytic activity of Staphylococcus lugdunensis is mediated by three peptides encoded by a non-agr genetic locus*. *Infect Immun*, 1997. **65**(1): p. 95-100.
32. Zheng, B., et al., *Whole-Genome Sequence of Multidrug-Resistant Staphylococcus caprae Strain 9557, Isolated from Cerebrospinal Fluid*. *Genome Announc*, 2015. **3**(4).
33. Sun, Z., et al., *Determining the Genetic Characteristics of Resistance and Virulence of the "Epidermidis Cluster Group" Through Pan-Genome Analysis*. *Front Cell Infect Microbiol*, 2020. **10**: p. 274.
34. Rice, L.B., *Federal funding for the study of antimicrobial resistance in nosocomial pathogens: no ESKAPE*. *J Infect Dis*, 2008. **197**(8): p. 1079-81.
35. Boucher, H.W., et al., *Bad bugs, no drugs: no ESKAPE! An update from the Infectious Diseases Society of America*. *Clin Infect Dis*, 2009. **48**(1): p. 1-12.
36. Kaper, J.B., J.P. Nataro, and H.L. Mobley, *Pathogenic Escherichia coli*. *Nat Rev Microbiol*, 2004. **2**(2): p. 123-40.
37. Lister, J.L. and A.R. Horswill, *Staphylococcus aureus biofilms: recent developments in biofilm dispersal*. *Front Cell Infect Microbiol*, 2014. **4**: p. 178.
38. Arciola, C.R., et al., *Interactions of staphylococci with osteoblasts and phagocytes in the pathogenesis of implant-associated osteomyelitis*. *Int J Artif Organs*, 2012. **35**(10): p. 713-26.
39. Arciola, C.R., et al., *Biofilm formation in Staphylococcus implant infections. A review of molecular mechanisms and implications for biofilm-resistant materials*. *Biomaterials*, 2012. **33**(26): p. 5967-82.
40. Otto, M., *Staphylococcal infections: mechanisms of biofilm maturation and detachment as critical determinants of pathogenicity*. *Annu Rev Med*, 2013. **64**: p. 175-88.
41. Kadurugamuwa, J.L. and T.J. Beveridge, *Virulence factors are released from Pseudomonas aeruginosa in association with membrane vesicles during normal growth and exposure to gentamicin: a novel mechanism of enzyme secretion*. *J Bacteriol*, 1995. **177**(14): p. 3998-4008.
42. Whitchurch, C.B., et al., *Extracellular DNA required for bacterial biofilm formation*. *Science*, 2002. **295**(5559): p. 1487.
43. Ryder, C., M. Byrd, and D.J. Wozniak, *Role of polysaccharides in Pseudomonas aeruginosa biofilm development*. *Curr Opin Microbiol*, 2007. **10**(6): p. 644-8.
44. Ma, L., et al., *Analysis of Pseudomonas aeruginosa conditional psl variants reveals roles for the psl polysaccharide in adhesion and maintaining biofilm structure postattachment*. *J Bacteriol*, 2006. **188**(23): p. 8213-21.
45. Friedman, L. and R. Kolter, *Two genetic loci produce distinct carbohydrate-rich structural components of the Pseudomonas aeruginosa biofilm matrix*. *J Bacteriol*, 2004. **186**(14): p. 4457-65.
46. Colvin, K.M., et al., *The pel polysaccharide can serve a structural and protective role in the biofilm matrix of Pseudomonas aeruginosa*. *PLoS Pathog*, 2011. **7**(1): p. e1001264.

47. Govan, J.R. and V. Deretic, *Microbial pathogenesis in cystic fibrosis: mucoid Pseudomonas aeruginosa and Burkholderia cepacia*. Microbiol Rev, 1996. **60**(3): p. 539-74.
48. Sutherland, I., *Biofilm exopolysaccharides: a strong and sticky framework*. Microbiology (Reading), 2001. **147**(Pt 1): p. 3-9.
49. Speziale, P. and J.A. Geoghegan, *Biofilm formation by staphylococci and streptococci: structural, functional, and regulatory aspects and implications for pathogenesis*. Front Cell Infect Microbiol, 2015. **5**: p. 31.
50. Schaible, U.E. and S.H. Kaufmann, *Iron and microbial infection*. Nat Rev Microbiol, 2004. **2**(12): p. 946-53.
51. Weinberg, E.D., *Microbial pathogens with impaired ability to acquire host iron*. Biometals, 2000. **13**(1): p. 85-9.
52. Kaplan, J., *Mechanisms of cellular iron acquisition: another iron in the fire*. Cell, 2002. **111**(5): p. 603-6.
53. Weinberg, E.D., *Iron and infection*. Microbiol Rev, 1978. **42**(1): p. 45-66.
54. Andrews, S.C., A.K. Robinson, and F. Rodriguez-Quinones, *Bacterial iron homeostasis*. FEMS Microbiol Rev, 2003. **27**(2-3): p. 215-37.
55. Andreini, C., et al., *Metal ions in biological catalysis: from enzyme databases to general principles*. J Biol Inorg Chem, 2008. **13**(8): p. 1205-18.
56. Cassat, J.E. and E.P. Skaar, *Iron in infection and immunity*. Cell Host Microbe, 2013. **13**(5): p. 509-519.
57. Harrison, P.M. and P. Arosio, *The ferritins: molecular properties, iron storage function and cellular regulation*. Biochim Biophys Acta, 1996. **1275**(3): p. 161-203.
58. Zwilling, B.S., et al., *Role of iron in Nramp1-mediated inhibition of mycobacterial growth*. Infect Immun, 1999. **67**(3): p. 1386-92.
59. Hood, M.I. and E.P. Skaar, *Nutritional immunity: transition metals at the pathogen-host interface*. Nat Rev Microbiol, 2012. **10**(8): p. 525-37.
60. Schaible, U.E., et al., *Correction of the iron overload defect in beta-2-microglobulin knockout mice by lactoferrin abolishes their increased susceptibility to tuberculosis*. J Exp Med, 2002. **196**(11): p. 1507-13.
61. Posey, J.E. and F.C. Gherardini, *Lack of a role for iron in the Lyme disease pathogen*. Science, 2000. **288**(5471): p. 1651-3.
62. Schalk, I.J., *Metal trafficking via siderophores in Gram-negative bacteria: specificities and characteristics of the pyoverdine pathway*. J Inorg Biochem, 2008. **102**(5-6): p. 1159-69.
63. Schwyn, B. and J.B. Neilands, *Universal chemical assay for the detection and determination of siderophores*. Anal Biochem, 1987. **160**(1): p. 47-56.
64. Beasley, F.C., et al., *Staphylococcus aureus transporters Hts, Sir, and Sst capture iron liberated from human transferrin by Staphyloferrin A, Staphyloferrin B, and catecholamine stress hormones, respectively, and contribute to virulence*. Infect Immun, 2011. **79**(6): p. 2345-55.
65. Letain, T.E. and K. Postle, *TonB protein appears to transduce energy by shuttling between the cytoplasmic membrane and the outer membrane in Escherichia coli*. Mol Microbiol, 1997. **24**(2): p. 271-83.
66. Flo, T.H., et al., *Lipocalin 2 mediates an innate immune response to bacterial infection by sequestering iron*. Nature, 2004. **432**(7019): p. 917-21.
67. Noinaj, N., S.K. Buchanan, and C.N. Cornelissen, *The transferrin-iron import system from pathogenic Neisseria species*. Mol Microbiol, 2012. **86**(2): p. 246-57.

68. Retzer, M.D., et al., *Discrimination between apo and iron-loaded forms of transferrin by transferrin binding protein B and its N-terminal subfragment*. Microb Pathog, 1998. **25**(4): p. 175-80.
69. Cartron, M.L., et al., *Feo--transport of ferrous iron into bacteria*. Biometals, 2006. **19**(2): p. 143-57.
70. Skaar, E.P. and O. Schneewind, *Iron-regulated surface determinants (Isd) of Staphylococcus aureus: stealing iron from heme*. Microbes Infect, 2004. **6**(4): p. 390-7.
71. Mazmanian, S.K., et al., *An iron-regulated sortase anchors a class of surface protein during Staphylococcus aureus pathogenesis*. Proc Natl Acad Sci U S A, 2002. **99**(4): p. 2293-8.
72. Mazmanian, S.K., et al., *Passage of heme-iron across the envelope of Staphylococcus aureus*. Science, 2003. **299**(5608): p. 906-9.
73. Dryla, A., et al., *Identification of a novel iron regulated staphylococcal surface protein with haptoglobin-haemoglobin binding activity*. Mol Microbiol, 2003. **49**(1): p. 37-53.
74. Torres, V.J., et al., *Staphylococcus aureus IsdB is a hemoglobin receptor required for heme iron utilization*. J Bacteriol, 2006. **188**(24): p. 8421-9.
75. Pilpa, R.M., et al., *Functionally distinct NEAT (NEAr Transporter) domains within the Staphylococcus aureus IsdH/HarA protein extract heme from methemoglobin*. J Biol Chem, 2009. **284**(2): p. 1166-76.
76. Haley, K.P. and E.P. Skaar, *A battle for iron: host sequestration and Staphylococcus aureus acquisition*. Microbes Infect, 2012. **14**(3): p. 217-27.
77. Anzaldi, L.L. and E.P. Skaar, *Overcoming the heme paradox: heme toxicity and tolerance in bacterial pathogens*. Infect Immun, 2010. **78**(12): p. 4977-89.
78. Yukl, E.T., et al., *Kinetic and spectroscopic studies of hemin acquisition in the hemophore HasAp from Pseudomonas aeruginosa*. Biochemistry, 2010. **49**(31): p. 6646-54.
79. Hantke, K., *Bacterial zinc uptake and regulators*. Curr Opin Microbiol, 2005. **8**(2): p. 196-202.
80. Kehl-Fie, T.E., et al., *Nutrient metal sequestration by calprotectin inhibits bacterial superoxide defense, enhancing neutrophil killing of Staphylococcus aureus*. Cell Host Microbe, 2011. **10**(2): p. 158-64.
81. Hsu, K., et al., *Anti-Infective Protective Properties of S100 Calgranulins*. Antiinflamm Antiallergy Agents Med Chem, 2009. **8**(4): p. 290-305.
82. Coy, M. and J.B. Neilands, *Structural dynamics and functional domains of the fur protein*. Biochemistry, 1991. **30**(33): p. 8201-10.
83. Zapotoczna, M., et al., *Iron-regulated surface determinant (Isd) proteins of Staphylococcus lugdunensis*. J Bacteriol, 2012. **194**(23): p. 6453-67.
84. Gianquinto, E., et al., *Interaction of human hemoglobin and semi-hemoglobins with the Staphylococcus aureus hemophore IsdB: a kinetic and mechanistic insight*. Sci Rep, 2019. **9**(1): p. 18629.
85. Heilbronner, S., et al., *Competing for Iron: Duplication and Amplification of the isd Locus in Staphylococcus lugdunensis HKU09-01 Provides a Competitive Advantage to Overcome Nutritional Limitation*. PLoS Genet, 2016. **12**(8): p. e1006246.
86. Slotboom, D.J., *Structural and mechanistic insights into prokaryotic energy-coupling factor transporters*. Nat Rev Microbiol, 2014. **12**(2): p. 79-87.
87. Henderson, G.B., E.M. Zevely, and F.M. Huennekens, *Coupling of energy to folate transport in Lactobacillus casei*. J Bacteriol, 1979. **139**(2): p. 552-9.

88. Rodionov, D.A., et al., *A novel class of modular transporters for vitamins in prokaryotes*. J Bacteriol, 2009. **191**(1): p. 42-51.
89. Voith von Voithenberg, L., et al., *A Novel Prokaryote-Type ECF/ABC Transporter Module in Chloroplast Metal Homeostasis*. Front Plant Sci, 2019. **10**: p. 1264.
90. Erkens, G.B. and D.J. Slotboom, *Biochemical characterization of ThiT from Lactococcus lactis: a thiamin transporter with picomolar substrate binding affinity*. Biochemistry, 2010. **49**(14): p. 3203-12.
91. Karpowich, N.K., J. Song, and D.N. Wang, *An Aromatic Cap Seals the Substrate Binding Site in an ECF-Type S Subunit for Riboflavin*. J Mol Biol, 2016. **428**(15): p. 3118-30.
92. Bao, Z., et al., *Structure and mechanism of a group-I cobalt energy coupling factor transporter*. Cell Res, 2017. **27**(5): p. 675-687.
93. Rodionov, D.A., et al., *Comparative and functional genomic analysis of prokaryotic nickel and cobalt uptake transporters: evidence for a novel group of ATP-binding cassette transporters*. J Bacteriol, 2006. **188**(1): p. 317-27.
94. Rempel, S., W.K. Stanek, and D.J. Slotboom, *ECF-Type ATP-Binding Cassette Transporters*. Annu Rev Biochem, 2019. **88**: p. 551-576.
95. Finkenwirth, F., F. Kirsch, and T. Eitinger, *Complex Stability During the Transport Cycle of a Subclass I ECF Transporter*. Biochemistry, 2017. **56**(34): p. 4578-4583.
96. Duurkens, R.H., et al., *Flavin binding to the high affinity riboflavin transporter RibU*. J Biol Chem, 2007. **282**(14): p. 10380-6.
97. ter Beek, J., et al., *Quaternary structure and functional unit of energy coupling factor (ECF)-type transporters*. J Biol Chem, 2011. **286**(7): p. 5471-5.
98. Finkenwirth, F., F. Kirsch, and T. Eitinger, *Solitary BioY proteins mediate biotin transport into recombinant Escherichia coli*. J Bacteriol, 2013. **195**(18): p. 4105-11.
99. Ehrenberg, M., H. Bremer, and P.P. Dennis, *Medium-dependent control of the bacterial growth rate*. Biochimie, 2013. **95**(4): p. 643-58.
100. Kjeldgaard, N.O., O. Maaloe, and M. Schaechter, *The transition between different physiological states during balanced growth of Salmonella typhimurium*. J Gen Microbiol, 1958. **19**(3): p. 607-16.
101. Schaechter, M., O. Maaloe, and N.O. Kjeldgaard, *Dependency on medium and temperature of cell size and chemical composition during balanced growth of Salmonella typhimurium*. J Gen Microbiol, 1958. **19**(3): p. 592-606.
102. Scott, M., et al., *Interdependence of cell growth and gene expression: origins and consequences*. Science, 2010. **330**(6007): p. 1099-102.
103. Chiang, P.K., et al., *S-Adenosylmethionine and methylation*. FASEB J, 1996. **10**(4): p. 471-80.
104. Ferla, M.P. and W.M. Patrick, *Bacterial methionine biosynthesis*. Microbiology, 2014. **160**(Pt 8): p. 1571-1584.
105. Armstrong, J.B., *Chemotaxis and methionine metabolism in Escherichia coli*. Can J Microbiol, 1972. **18**(5): p. 591-6.
106. Springer, M.S., et al., *Role of methionine in bacterial chemotaxis: requirement for tumbling and involvement in information processing*. Proc Natl Acad Sci U S A, 1975. **72**(11): p. 4640-4.
107. Deakova, Z., et al., *Two-dimensional high performance liquid chromatography for determination of homocysteine, methionine and cysteine enantiomers in human serum*. J Chromatogr A, 2015. **1408**: p. 118-24.

108. Psychogios, N., et al., *The human serum metabolome*. PLoS One, 2011. **6**(2): p. e16957.
109. Krismer, B., et al., *Nutrient limitation governs Staphylococcus aureus metabolism and niche adaptation in the human nose*. PLoS Pathog, 2014. **10**(1): p. e1003862.
110. Kadner, R.J., *Regulation of methionine transport activity in Escherichia coli*. J Bacteriol, 1975. **122**(1): p. 110-9.
111. Kadner, R.J. and H.H. Winkler, *Energy coupling for methionine transport in Escherichia coli*. J Bacteriol, 1975. **123**(3): p. 985-91.
112. Schoenfelder, S.M., et al., *Methionine biosynthesis in Staphylococcus aureus is tightly controlled by a hierarchical network involving an initiator tRNA-specific T-box riboswitch*. PLoS Pathog, 2013. **9**(9): p. e1003606.
113. Reisenauer, A., et al., *Bacterial DNA methylation: a cell cycle regulator?* J Bacteriol, 1999. **181**(17): p. 5135-9.
114. Brzoska, K., S. Meczynska, and M. Kruszewski, *Iron-sulfur cluster proteins: electron transfer and beyond*. Acta Biochim Pol, 2006. **53**(4): p. 685-91.
115. Nazi, I., et al., *Role of homoserine transacetylase as a new target for antifungal agents*. Antimicrob Agents Chemother, 2007. **51**(5): p. 1731-6.
116. Johnston, M., et al., *Suicide inactivation of bacterial cystathionine gamma-synthase and methionine gamma-lyase during processing of L-propargylglycine*. Biochemistry, 1979. **18**(21): p. 4690-701.
117. Rao, A.M., M.R. Drake, and M.H. Stipanuk, *Role of the transsulfuration pathway and of gamma-cystathionase activity in the formation of cysteine and sulfate from methionine in rat hepatocytes*. J Nutr, 1990. **120**(8): p. 837-45.
118. Steegborn, C., et al., *Kinetics and inhibition of recombinant human cystathionine gamma-lyase. Toward the rational control of transsulfuration*. J Biol Chem, 1999. **274**(18): p. 12675-84

Chapter 2

An ECF-type transporter scavenges heme to overcome iron-limitation in *Staphylococcus lugdunensis*

Jochim A¹, Adolf LA¹, Belikova D¹, Schilling NA², Setyawati I³, Chin D⁴, Meyers S⁵, Verhamme P⁵, Heinrichs DE⁴, Slotboom DJ³ and Heilbronner S^{1,6,7*}

1 - Interfaculty Institute of Microbiology and Infection Medicine, Department of Infection Biology, University of Tübingen, Tübingen, Germany

2 - Institute of Organic Chemistry, University of Tübingen, Tübingen, Germany

3 - Groningen Biomolecular Sciences and Biotechnology Institute, University of Groningen, Groningen, The Netherlands

4 - Department of Microbiology and Immunology, University of Western Ontario, London, Ontario, Canada.

5 - Center for Molecular and Vascular Biology, KU Leuven, Belgium.

6 - German Centre for Infection Research (DZIF), Partner Site Tübingen, Tübingen, Germany

7 - (DFG) Cluster of Excellence EXC 2124 Controlling Microbes to Fight Infections

* Corresponding author

Abstract

Energy-coupling factor type (ECF-transporters) represent trace nutrient acquisition systems. Substrate binding components of ECF-transporters are membrane proteins with extraordinary affinity, allowing them to scavenge trace amounts of ligand. A number of molecules have been described as substrates of ECF-transporters, but an involvement in iron-acquisition is unknown. Host-induced iron limitation during infection represents an effective mechanism to limit bacterial proliferation. We identified the iron-regulated ECF-transporter Lha in the opportunistic bacterial pathogen *Staphylococcus lugdunensis* and show that the transporter is specific for heme. The recombinant substrate-specific subunit LhaS accepted heme from diverse host-derived hemoproteins. Using isogenic mutants and recombinant expression of Lha, we demonstrate that its function is independent of the canonical heme acquisition system Isd and allows proliferation on human cells as sources of nutrient iron. Our findings reveal a unique strategy of nutritional heme acquisition and provide the first example of an ECF-transporter involved in overcoming host-induced nutritional limitation.

Key words

Iron, heme, ECF-transporter, *Staphylococcus lugdunensis*, nutritional immunity

Background

Trace nutrients such as metal ions and vitamins are needed as prosthetic groups or cofactors in anabolic and catabolic processes and are therefore crucial for maintaining an active metabolism. Metal ions such as iron, manganese, copper zinc, nickel and cobalt must be acquired from the environment by all living organisms. In contrast many prokaryotes are prototrophic for vitamins like riboflavin, biotin, and vitamin B₁₂. However, these biosynthetic pathways are energetically costly [1], and prokaryotes have developed several strategies to acquire these nutrients from the environment. ABC transporters of the Energy-coupling factor type (ECF-transporters) represent highly effective trace nutrient acquisition systems [2, 3]. In contrast to the substrate-binding lipoproteins/periplasmic proteins of conventional ABC transporters, the specificity subunits of ECF transporters (ECF-S) are highly hydrophobic membrane proteins (6-7 membrane spanning helices) [2]. ECF-S subunits display a remarkably high affinity for their cognate substrates in the picomolar to the low nanomolar range,

which allows scavenging of smallest traces of their substrates from the environment [4]. Whether ECF type transporters can be used to acquire iron or iron-containing compounds is unknown.

The dependency of bacteria on trace nutrients is exploited by the immune system to limit bacterial proliferation by actively depleting nutrients from body fluids and tissues. This strategy is referred to as “nutritional immunity” [5, 6]. In this regard, depletion of nutritional iron ($\text{Fe}^{2+}/\text{Fe}^{3+}$) is crucial as iron is engaged in several metabolic processes such as DNA replication, glycolysis, and respiration [7, 8]. Extracellular iron ions are bound by high-affinity iron-chelating proteins such as lactoferrin and transferrin found in lymph and mucosal secretions and in serum, respectively. However, heme is a rich iron source in the human body and invasive pathogens can access this heme pool by secreting hemolytic factors to release hemoglobin or other hemoproteins from erythrocytes or other host cells. Bacterial receptors then extract heme from the hemoproteins. This is followed by import and degradation of heme to release the nutritional iron. To date, several heme acquisition systems of different Gram-positive and Gram-negative pathogens have been characterized at the molecular level (see [9] for an excellent review).

Staphylococci are a major cause of healthcare-associated infections that can lead to morbidity and mortality. The coagulase-positive *Staphylococcus aureus* represents the best-studied and most invasive species. Coagulase-negative staphylococci (CoNS) are regarded as less pathogenic than *S. aureus* and infections caused by CoNS are normally subacute and less severe. In this regard, the CoNS *Staphylococcus lugdunensis* represents an exception. *S. lugdunensis* infections frequently show a fulminant and aggressive course of disease that resembles that of *S. aureus*. Strikingly, *S. lugdunensis* is associated with a series of cases of infectious endocarditis [10]. The reasons for the apparently high virulence potential of *S. lugdunensis* remains largely elusive and few virulence factors have been identified so far. In this respect, it is interesting to observe that *S. lugdunensis*, unlike other staphylococci but similar to *S. aureus*, encodes an iron-dependent surface determinant locus (Isd) system [11, 12]. Isd facilitates the acquisition of heme from hemoglobin and can be regarded as a hallmark of adaption towards an invasive lifestyle. However, to ensure continuous iron acquisition within the host, many pathogens encode multiple systems to broaden the range of iron-containing molecules that can be acquired [13].

Here we report the identification of an iron-regulated ECF-type ABC transporter (named LhaSTA) in *S. lugdunensis*. We found LhaSTA to be specific for heme, thus representing a novel strategy to overcome nutritional iron limitation. Recombinant LhaS was able to take up heme from several host hemoproteins such as hemoglobin, myoglobin or hemopexin. Consistent with these data, LhaSTA expression allowed proliferation of *S. lugdunensis* in the presence of these iron sources as well as human erythrocytes or cardiac myelocytes as a sole source of nutrient iron. Our data indicate that LhaSTA function is independent of the presence of surface-displayed hemoprotein receptors suggesting Isd-independent acquisition of heme from host hemoproteins. Our work identifies LhaSTA as the first ECF transporter that facilitates iron acquisition, thus participating to overcome host immune defenses.

Results

LhaSTA encodes an iron regulated ECF transporter

The *isd* locus of *S. lugdunensis* shows several characteristics that distinguish it from the locus of *S. aureus*. Amongst these is the presence of three genes that encode a putative ABC transporter and are located between *isdJ* and *isdB* (Fig. 1A) [11]. Analysis of the open reading frame using Pfam [14] revealed that the three adjacent genes encode components of a putative ECF-transporter, namely a specificity subunit (*IhaS* - SLUG_00900), a transmembrane subunit (*IhaT* - SLUG_00910) and an ATPase (*IhaA* - SLUG_00920), and they might be part of a polycistronic transcript. The location within the *isd* operon suggested a role of the transporter in iron acquisition. Bacteria sense iron limitation using the ferric uptake repressor (Fur) which forms DNA-binding dimers in the presence of iron ions [15]. Under iron limitation, Fe dissociates from Fur and the repressor loses affinity for its consensus sequence (*fur* box) allowing transcription. Interestingly, a *fur*-box was located upstream of *IhaS* (Fig. 1A). qPCR analysis in *S. lugdunensis* N920143 revealed that the expression of *IhaS* and *IhaA* increased ~21 and ~12 fold, respectively, in the presence of the Fe-specific chelator EDDHA (Fig. 1B). The effect of EDDHA could be prevented by addition of FeSO₄ (Fig. 1B). This confirmed iron-dependent regulation and suggested that LhaSTA is involved in iron acquisition.

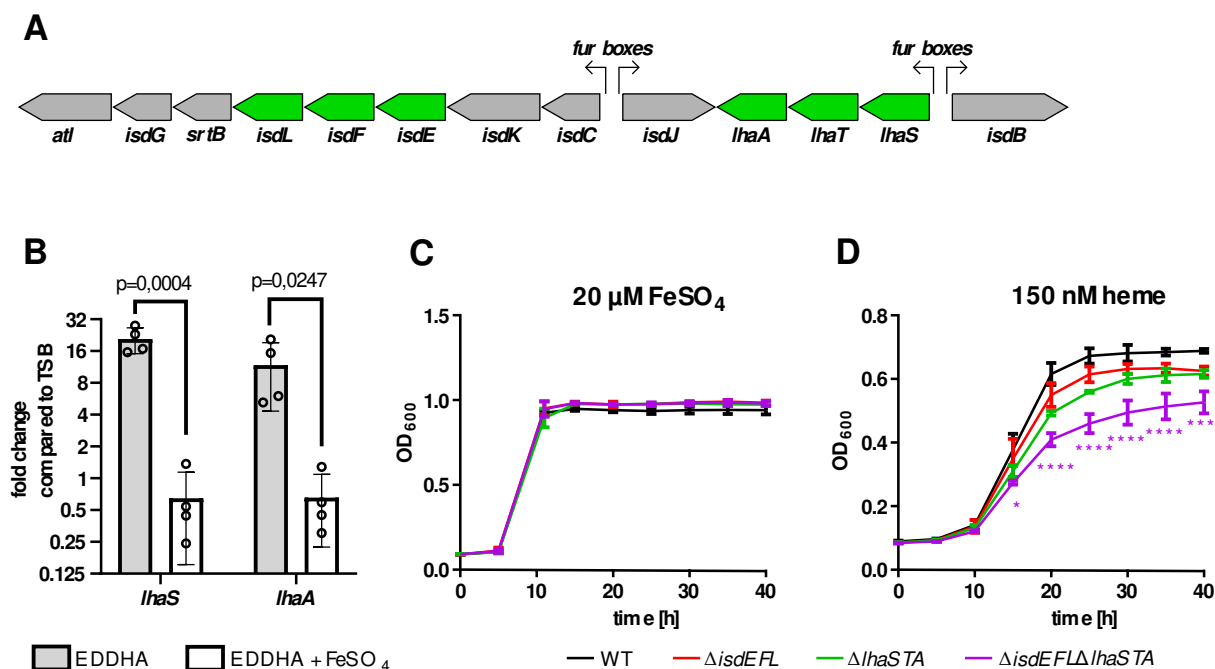


Figure 1 LhaSTA represents an iron-regulated heme transporter.

A) Schematic diagram of the *isd* operon of *S. lugdunensis* N920143. Coding sequences, direction of transcription and Fur-binding sites are indicated. ABC membrane-transporters are shown in green.

lhaS - SLUG_00900; *lhaT* - SLUG_00910; *lhaA* - SLUG_00920

B) Iron-regulated expression of Lha: *S. lugdunensis* was grown overnight in TSB, TSB + 200 µM EDDHA or TSB + 200 µM EDDHA + 200 µM FeSO₄. Gene expression was quantified by qPCR. Expression was normalized to 5srRNA and to the TSB standard condition using the $\Delta\Delta C_t$ method. Fold differences in gene expression are shown. Data represent mean and SD of four independent experiments. Statistical evaluation was performed using students unpaired t-test (*lhaS*: $t=7,045$, $df=6$; *lhaA*: $t=2,979$, $df=6$)

C/D Growth curves of *S. lugdunensis* N920143 and isogenic mutants. The wild type (WT) *S. lugdunensis* N920143 strain and the indicated isogenic null mutant strains were grown in the presence of 20 µM FeSO₄ (C) or 150 nM heme (D) as a sole source of iron. 500 µl of bacterial cultures were inoculated to an OD₆₀₀ = 0,05 in 48 well plates and OD₆₀₀ was monitored every 15 min using an Epoch1 plate reader. For reasons of clarity values taken every 5 hours are displayed. Mean and SD of three experiments are shown. Statistical analysis was performed using one-way ANOVA followed by Dunett's test for multiple comparisons. * - $p < 0,05$, **** $p < 0,00001$

LhaSTA allows bacterial proliferation on heme as a source of nutrient iron

LhaSTA is encoded within the *isd* operon and the Isd system facilitates the acquisition of heme from hemoglobin [12, 16]. Therefore, we speculated that LhaSTA might also be involved in the transport of heme. To test this, we used allelic replacement and created isogenic deletion mutants in *S. lugdunensis* N920143 lacking either *lhaSTA* or *isdEFL* the latter of which encodes the conventional lipoprotein-dependent heme transporter of the *isd* locus. Further we created a $\Delta lhaSTA\Delta isdEFL$ double mutant. In the presence of 20 μ M FeSO₄ all strains showed similar growth characteristics (Fig. 1C). The two single mutants had a slight growth defect compared to wild type when heme was the only iron source. However, the $\Delta lhaSTA\Delta isdEFL$ mutant showed a significant growth defect under these conditions (Fig. 1D). These data strengthen the hypothesis that LhaSTA is a heme transporter.

LhaS binds heme

To confirm the specificity of LhaSTA, we heterologously produced the substrate-specific component LhaS in *E. coli* and purified the protein. We observed that the recombinant protein showed a distinct red color when purified from *E. coli* grown in rich LB medium, which contains heme due to the presence of crude yeast extract [17] (Fig. 2A). The absorption spectrum of the protein showed a Soret peak at 415 nm and Q-band maxima at 537 and 568 nm, suggesting histidine coordination of the heme group. Both the visible color and the spectral peaks were absent when LhaS was purified from *E. coli* grown in heme-deficient RPMI medium (Fig. 2A). We conducted MALDI TOF analysis of holo-LhaS purified from *E. coli* grown in LB and identified two peaks, one of which corresponds to full length recombinant LhaS (24074.437 Da expected weight), and the other to heme (616,1767 Da expected weight). Importantly, the heme peak was not detectable when LhaS was purified from RPMI (Fig 2B and 2C). Furthermore, ESI MS confirmed the presence of heme only in LhaS samples purified from LB (Figure 2 - figure supplement 1). Using the extinction coefficients of LhaS and heme we calculated a heme-LhaS binding stoichiometry of 1:0.6 for the complex isolated from heme containing medium.

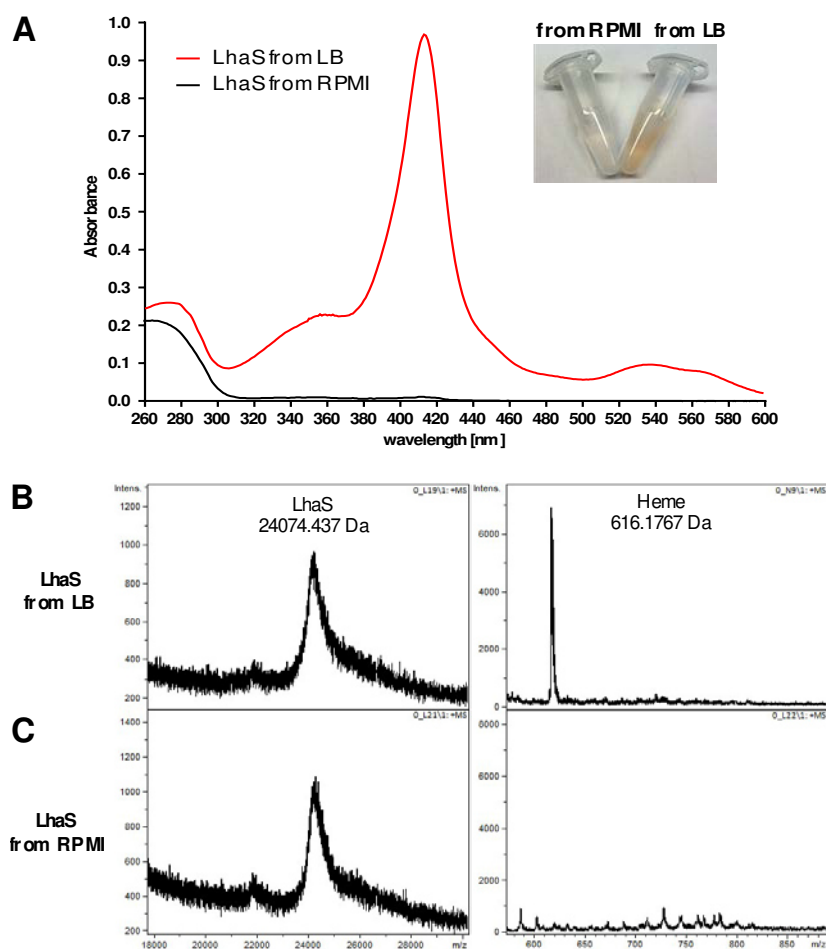


Figure 2 LhaS binds heme.

A) Ultraviolet-visible (UV-vis) spectrum of recombinant LhaS. C-terminal His-tagged LhaS was heterologously expressed in *E. coli* and purified from heme-containing LB medium or heme-free RPMI medium. The UV-vis spectrum of the purified LhaS was measured with a BioPhotometer.

B) and C) MALDI-TOF mass spectra of recombinant LhaS. LhaS (B) was purified out of LB medium and apo-LhaS (C) was purified out of RPMI medium. Mass spectra were recorded with a Reflex IV in reflector mode. All spectra are a sum of 50 shots. Prior to measurements the protein samples were mixed with a 2,5-dihydroxybenzoic acid matrix dissolved in water/acetonitrile/trifluoroacetic acid (50/49.05/0.05) at a concentration of 10 mg ml^{-1} and spotted onto the MALDI polished steel sample plate.

LhaSTA represents an iron acquisition system

Next, we sought to investigate whether LhaSTA represents a functional and autonomous iron acquisition system. LhaSTA is located within the *isd* locus of *S. lugdunensis*, which, besides the conventional heme membrane transporter IsdEFL,

also encodes the hemoglobin receptor LsdB and the cell wall-anchored proteins LsdJ and LsdC. Furthermore, the locus encodes the putative secreted/membrane-associated hemophore LsdK, whose role in heme binding or transport is currently unknown [16], and the autolysin *atl* remodeling the cell wall [18]. To study solely LhaSTA-dependent effects, we disabled all known heme import activity in *S. lugdunensis* by creation of a deletion mutant lacking the entire *isd* operon (from the *atl* gene to *isdB*, Fig. 1A). Then we expressed *lhaSTA* under the control of its native promoter on a recombinant plasmid in the Δisd background. *S. lugdunensis* has been reported to degrade nutritional heme in an LsdG-independent fashion due to an unknown enzyme (OrfX) [19]. Therefore, we speculated that heme degradation in this strain might still be possible. LhaSTA deficient and proficient strains showed comparable growth in the presence of $FeSO_4$ (Figure 1 - figure supplement 1). However, only the *lhaSTA* expressing strain was able to grow in the presence of heme as sole source of nutrient iron (Fig. 3A). To further support a role for LhaSTA in iron import, we isolated the cytosolic fraction of the strains prior and after incubation with heme and measured iron levels using the ferrozine assay [20]. Consistently, we found that LhaSTA expression increased cytosolic iron levels post incubation with heme (Fig. 3B). These data suggest that LhaSTA represents a “bona fide” and functional autonomous iron acquisition system.

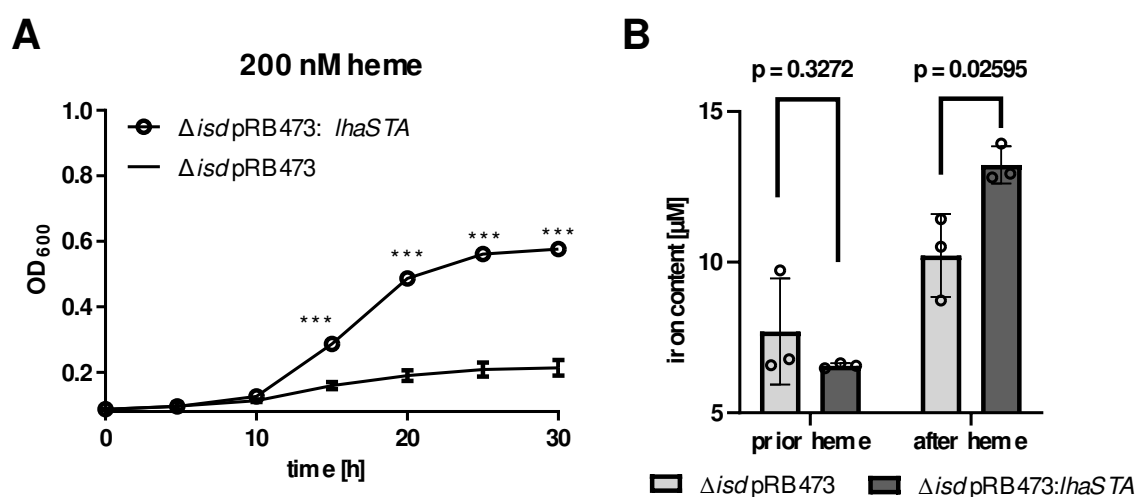


Figure 3 LhaSTA represents a functionally autonomous iron acquisition system.

A) LhaSTA-dependent proliferation. *S. lugdunensis* N920143 deletion mutant strains lacking the entire *isd* operon and expressing LhaSTA (Δisd pRB473:*lhaSTA*) or not (Δisd pRB473) from the plasmid pRB473 were grown in the presence of 200 nM heme as a sole source of

iron. 500 μ l of cultures were inoculated to an $OD_{600} = 0,05$ in 48 well plates and OD_{600} was monitored every 15 min using an Epoch1 plate reader. For reasons of clarity values taken every 5 hours are displayed. Mean and SD of three experiments are shown. Statistical analysis was performed using students unpaired t-test. *** $p < 0,0001$

B) Intracellular accumulation of iron. Strains were grown in iron limited medium to $OD_{600} = 0,6$ and 5 μ M heme were added for 3 h. Cell fractionation of 1 ml $OD_{600} = 50$ was performed and the iron content of the cytosolic fraction was determined using the ferrozine assay. Data represent the mean and SD of three independent experiments. Statistical analysis was performed using students unpaired t-test ($t=5,12729$, $df=4$).

LhaSTA enables acquisition of heme from various host hemoproteins

We wondered how *S. lugdunensis* might benefit from a heme specific ECF-transporter when a heme acquisition system is already encoded by the canonical Isd system. Indeed, Isd represents a highly effective heme acquisition system. Interactions between the surface receptor IsdB and the proteinaceous part of hemoglobin are thought to enhance heme release to increase its availability [21, 22]. The downside of this mechanism is the specificity for hemoglobin because heme derived from other host hemoproteins such as myoglobin remains inaccessible. In contrast, the HasA hemophore produced by Gram negative pathogens is reported to bind heme with sufficient affinity to enable heme acquisition from a range of host hemoproteins without the need of protein-protein interactions to enhance heme release [23, 24]. As ECF-transporters are known to have high affinity towards their ligands, we speculated that LhaS might represent a membrane-located high affinity 'hemophore' allowing heme acquisition from hemoproteins other than hemoglobin. We explored this idea using the hemoprotein myoglobin which is abundant in muscle tissues. Myoglobin was previously reported to not interact with *S. lugdunensis* IsdB [16] and is therefore unlikely to be a substrate for the Isd system. We analyzed the growth of the *S. lugdunensis* wild type (WT) strain as well as of the isogenic *lhaSTA* deficient strain (Fig 4A) on human hemoglobin (hHb) or on equine myoglobin (eqMb) as sole sources of nutrient iron (Fig. 4B). Unlike the WT strain, the *lhaSTA* deficient strain displayed a mild proliferation defect on hHb and a pronounced growth defect on equine eqMb (Fig. 4B). Interestingly, *lhaSTA* deficiency did not impact proliferation on hemoglobin-haptoglobin (Hb-Hap) complexes suggesting Isd-dependent acquisition of heme from Hb-Hap. These data strongly indicate that LhaSTA possesses a hemoprotein substrate

range that differs from that of the *Isd* system. To further validate this, we used the above-described *S. lugdunensis* *isd* mutant expressing *IhaSTA* (Fig. 4A) and tested its ability to proliferate on a range of different hemoproteins. (Fig. 4C). We found that *IhaSTA* expression enabled growth on hemoglobin (human and murine origin) and myoglobin (human and equine origin) as well as with hemopexin (Hpx). Consistent with the above observations, Hb-Hap complexes did not enable growth of the *IhaSTA* proficient strain strengthening the notion that Hb-Hap acquisition is *Isd*-dependent. These data further indicate that LhaSTA allows extraction and usage of heme from a diverse set of host hemoproteins, thus expanding the range of hemoproteins accessible to *S. lugdunensis*.

To confirm the activity of LhaSTA at the biochemical level, we isolated *E. coli*-derived membrane vesicles that carried apo-LhaS. Following incubation of the vesicles with or without different host hemoproteins, LhaS was purified using affinity chromatography. Heme saturation of LhaS was assessed using SDS-PAGE and tetramethylbenzidine (TMBZ) staining, a reagent that turns green in the presence of hemin-generated peroxides [25] (Fig. 4D). In the absence of hemoproteins during incubation, apo-LhaS did not stain with TMBZ, but TMBZ staining was observed after incubation with all the hemoproteins tested except for Hb-Hap. These data nicely correlate with the ability of the *IhaSTA* proficient strain to grow on all hemoproteins but Hb-Hap complexes.

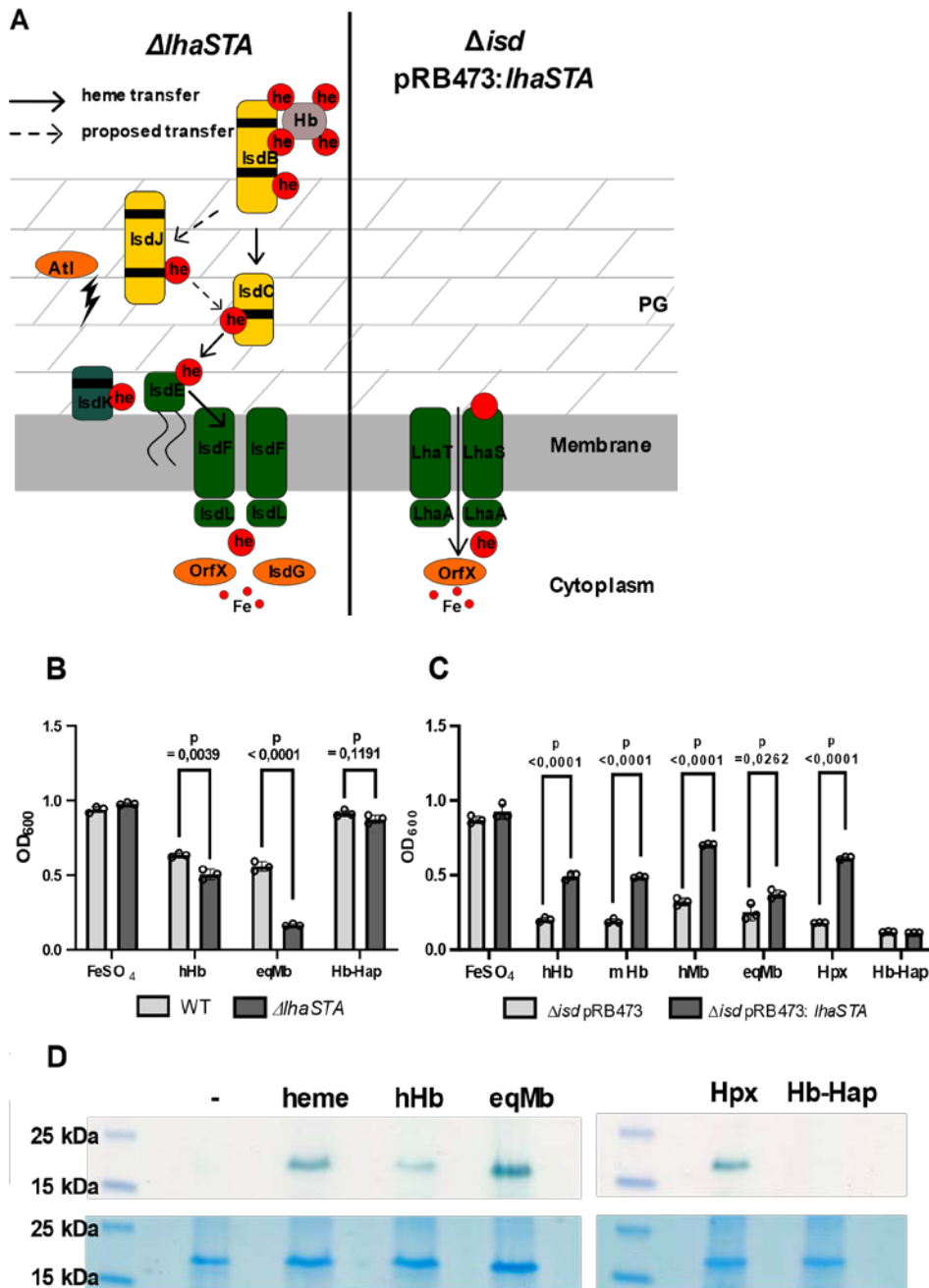


Figure 4 LhaSTA facilitates heme acquisition from a wide range of hemoprotein substrates.

A) Schematic diagram of known heme acquisition systems in the *S. lugdunensis* mutant strains lacking either the genes encoding LhaSTA ($\Delta lhaSTA$, left) or the entire *isd* operon and expressing LhaSTA from the plasmid pRB473 (Δisd pRB473: *lhaSTA*). ABC membrane transporters are shown in green. Cell wall-anchored proteins of the Lsd-system are shown in yellow. Heme/hemoglobin-binding NEAT motifs within each protein are indicated as black boxes. Black arrows indicate the transfer of heme. he: heme; hb: hemoglobin; PG: peptidoglycan.

B) Growth of *S. lugdunensis* N920143 wild type (WT) and Δ *lhaSTA*. Strains were grown in the presence of 20 μ M FeSO₄ or 2.5 μ g/ml human hemoglobin (hHb) or 10 μ g/ml equine myoglobin (eqMb) or 117 nM hemoglobin-haptoglobin complex (Hb-Hap) as a sole source of iron. 500 μ l of cultures were inoculated to an OD₆₀₀ = 0,05 in 48 well plates and OD₆₀₀ was measured after 30 h using an Epoch1 plate reader. Mean and SD of three experiments are shown. Statistical analysis was performed using students unpaired t-test. hHb - t=6,0007, df=4; eqMb - t=20,52, df=4; Hb-Hap - t=1,978, df=4.

C) Growth of *S. lugdunensis* N920143 Δ *isd* pRB473 and Δ *isd* pRB473:*lhaSTA*. Strains were grown in the presence of 20 μ M FeSO₄ or 2.5 μ g/ml hHb or 2.5 μ g/ml murine hemoglobin (mHb) or 10 μ g/ml human myoglobin (hMb) or 10 μ g/ml eqMb or 200 nM human hemopexin (Hpx) or 117 nM Hb-Hap as a sole source of iron. 500 μ l of cultures were inoculated to an OD₆₀₀ = 0,05 in 48 well plates and OD₆₀₀ was measured after 30 h using an Epoch1 plate reader. Mean and SD of three experiments are shown. Statistical analysis was performed using students unpaired t-test hHb - t=18,5, df=4; mHb - t=29,03, df=4; hMb - t=25,98, df=4; eqMb - t=3,442, df=4; Hpx - t=77,12 df=4; Hb-Hap t=2,758 df=4.

D) TMBZ-H₂O₂ stain of TGX gels for heme-associated peroxidase activity. Membrane vesicles were saturated with excess of hemoprotein (5.6 μ M heme, 476 μ g/ml hHb, 437 μ g/ml eqMb, 5.6 μ M Hpx, 476 μ g/ml Hb-Hap) or no hemoprotein (-) for 10 min at RT. LhaS was purified, 15 μ g protein was loaded on a TGX gel and stained for peroxidase activity with TMBZ-H₂O₂ (upper panel). Gels were destained and subsequently stained with BlueSafe (lower panel) to confirm the presence of the protein in all conditions.

LhaSTA allows usage of human host hemoproteins as an iron source

Usage of host derived hemoproteins requires the combined action of hemolytic factors to damage host cells as well as hemoprotein acquisition systems to use the released hemoproteins. Since we realized that the *S. lugdunensis* N920143 strain is non-hemolytic on sheep blood agar, we reproduced the Δ *isd* deletion as well as the plasmid-based expression of *lhaSTA* in the hemolytic *S. lugdunensis* N940135 strain. As for N920143, LhaSTA-dependent usage of hemoproteins was also observed in the N940135 background (Figure 4 - figure supplement 1).

We speculated that the expression of LhaSTA is beneficial to *S. lugdunensis* during invasive disease as it allows usage of a wide range of hemoproteins as iron sources. To test this, we attempted to establish septic disease models for *S. lugdunensis*. However, we found that *S. lugdunensis* N940135 was unable to establish systemic disease in mice. Even when infected with 3*10⁷ CFU/animal, mice did not

show signs of infection (weight loss / reduced movement). Three days post infection, the organs of infected animals showed low bacterial burdens frequently approaching sterility (Figure 5 - figure supplement 1) and the expression of LhaSTA did not increase the bacterial loads within the organs. We speculate that the presence of human-specific, but lack of mouse-specific virulence factors might reduce *S. lugdunensis* pathogenesis in mice. Little is known about virulence factors encoded by *S. lugdunensis*, however, human specific toxins that lyse erythrocytes to release nutritional hemoglobin have previously been described for *S. aureus* [26]. To further assess this, we performed hemolysis assays using human as well as murine erythrocytes (Figure 5 - figure supplement 2). Hemolytic activity of *S. lugdunensis* culture filtrates were low compared to those of *S. aureus*. Nevertheless, we observed lysis of human erythrocytes while murine erythrocytes were not affected by *S. lugdunensis* culture filtrates. This suggests human specific factors mediating host cell damage (Figure 5 - figure supplement 2).

Therefore, we used an *ex-vivo* model to investigate whether LhaSTA facilitates the usage of human cells as a source of iron. First, we supplied freshly isolated human erythrocytes as a source of hemoglobin. Figure 5A shows, that the presence of human erythrocytes allowed significantly improved growth of the *Isd* deficient but LhaSTA-expressing strain. Secondly, we used a human cardiac myocyte cell line as a source of iron. *S. lugdunensis* is associated with infective endocarditis and myocytes are a source of myoglobin which can be acquired via LhaSTA. Indeed, we found that *lhaSTA* expression enhanced the growth of *S. lugdunensis* in the presence of cardiac myocytes.

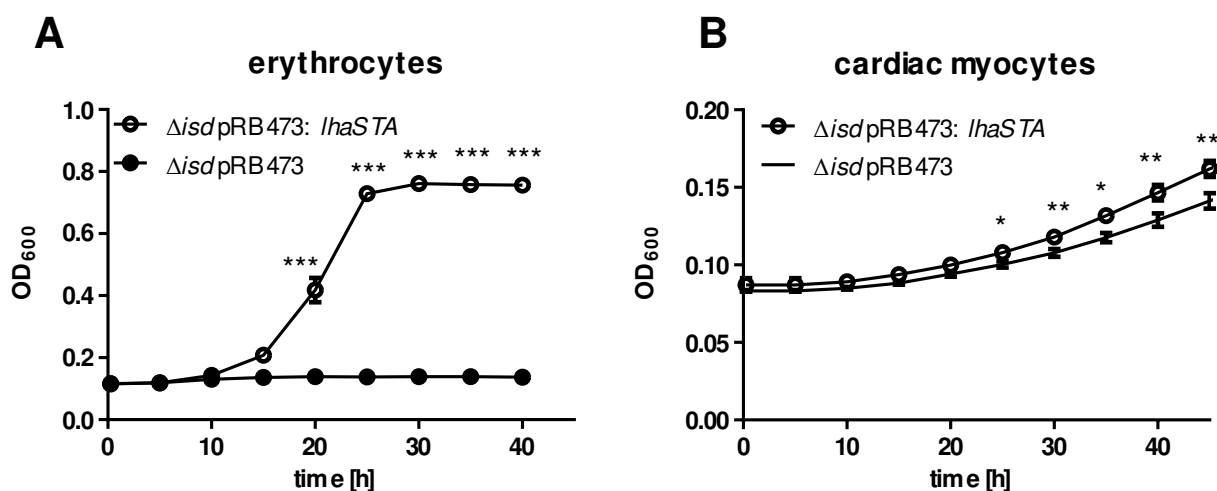


Figure 5 LhaSTA allows usage of host cells as an iron source.

A) Growth of *S. lugdunensis* N940135 $\Delta isd pRB473:lhaSTA$ and $\Delta isd pRB473$ on human erythrocytes. Strains were grown in the presence of freshly isolated human erythrocytes (10^5 cells/ml) as a sole source of iron. 500 μ l of cultures were inoculated to an $OD_{600} = 0,05$ in 48 well plates and OD_{600} was monitored every 15 min using an Epoch1 plate reader. For reasons of clarity values taken every 5 hours are displayed. Mean and SD of three experiments are shown. Statistical analysis was performed using students unpaired t-test. *** $p < 0,0001$

B) Growth of *S. lugdunensis* N940135 $\Delta isd pRB473$ and $\Delta isd pRB473:lhaSTA$ on human cardiac myocytes. Strains were grown in the presence of 40000 primary human cardiac myocytes per well as a sole source of iron. Cardiac myocytes were detached and washed once with RPMI+200 μ M EDDHA prior addition to the wells. 500 μ l of cultures were inoculated to an $OD_{600} = 0,05$ in 48 well plates and OD_{600} was monitored every 15 min using an Epoch1 plate reader. For reasons of clarity values taken every 5 hours are displayed. Mean and SD of three experiments are shown. Statistical analysis was performed using students unpaired t-test. * $p < 0,05$, ** $p < 0,01$

In conclusion, our results suggest that LhaSTA represents a novel broad-range heme-acquisition system that expands the hemoprotein substrate range accessible to *S. lugdunensis* to overcome nutritional iron restriction (Fig. 6).

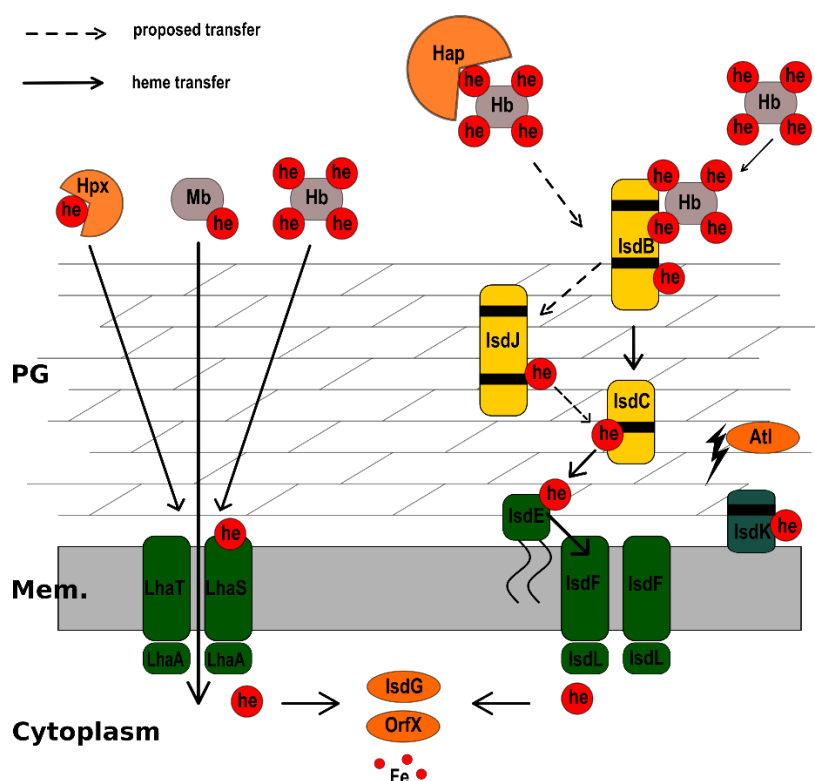


Figure 6 Model of heme acquisition in *S. lugdunensis*.

ABC membrane transporters are shown in green. Cell wall-anchored proteins of the Isd-system are shown in yellow. Heme/hemoglobin-binding NEAT motifs within each protein are indicated as black boxes. Black arrows indicated the transfer of heme. he: heme; hb: hemoglobin; PG: peptidoglycan; Mem: Membrane; Hap: Haptoglobin; Hpx:Hemopexin; AtI: Autolysin.

Discussion

Nutritional iron restriction represents an effective host strategy to prevent pathogen proliferation within sterile tissues. In turn, bacterial pathogens have developed a range of strategies to overcome nutritional iron limitation during infection. Amongst these is the production and acquisition of siderophores which scavenge the smallest traces of molecular iron to make it biologically available. The highly virulent *S. aureus* species produces the siderophores staphyloferrin A (SF-A) and staphyloferrin B (SF-B) which are important during infection [27, 28]. *S. lugdunensis* is associated with a series of cases of infective endocarditis and the course of disease mimics that of *S. aureus* endocarditis. In contrast to *S. aureus*, *S. lugdunensis* does not produce endogenous siderophores [29], suggesting that the iron requirements during infection must be satisfied through alternative strategies. Host hemoproteins

can be used by pathogens to acquire iron-containing heme and a plethora of hemoproteins are available during infection. Hemoglobin or myoglobin becomes available if the intracellular pool of the host is tapped by secretion of hemolytic factors. Alternatively, host hemopexin or hemoglobin-haptoglobin complexes involved in heme/hemoglobin turnover are extracellularly available to pathogens. Host hemoproteins are characterized by a remarkable affinity towards heme: Both, globin and hemopexin bind heme with dissociation constants (K_ds) smaller than 1 pM [30, 31]. The usage of heme by invasive pathogens is widely distributed, however, the molecular pathways and hemoprotein range availability differs dramatically (see [9] for an excellent review). Iron dependent surface determinant loci are used to acquire heme from hemoglobin by several Gram positive pathogens including *S. aureus* [32], *S. lugdunensis* [11, 12], *Bacillus anthracis* [33], *Streptococcus pyogenes* [34] and *Listeria monocytogenes* [35].

ABC transporters of the Energy-coupling factor type (ECF) are trace element acquisition systems [3, 4]. ECF-type transporters are characterized by high affinity towards their ligands and ECF systems specific for the vitamins riboflavin [36], folate [37], thiamine [38], biotin [39], cobalamine [40, 41], pantothenate [42, 43], niacin [44] and pyridoxamine [45] as well as for the trace metals nickel and cobalt [46, 47] have been described. However, ECF-transporters that allow iron acquisition have so far remained elusive.

Now we show that *S. lugdunensis* encodes the iron regulated ECF-transporter LhaSTA. LhaS binds heme and enables accumulation of iron within the cytoplasm. Therefore, the system represents a novel type of “bona fide” iron acquisition system. Recombinant LhaS acquired heme from human and murine hemoglobin, from human and equine myoglobin as well as from human hemopexin. The ability of LhaS to accept heme from several sources strongly suggest an affinity-driven mechanism relying on passive diffusion of heme between proteins rather than on active extraction. Such a mechanism has been suggested for HasA-type hemophores of Gram-negative pathogens such as *Serratia marcescens*, *Yersina pestis* and *Pseudomonas aeruginosa* [48, 49]. Similar to LhaS, HasA has been shown to possess a broad hemoprotein substrate range and allows the usage of hemoglobin from different species as well as myoglobin and hemopexin [48]. This ability of HasA was attributed to its high affinity towards heme (K_d = 0.2 nM) [23]. ECF-specificity subunits frequently possess K_ds towards their ligands in the low nanomolar to picomolar range [4],

supporting the idea that LhaS might directly accept heme from hemoproteins. We attempted isothermal titration calorimetry to determine the affinity of LhaS towards heme, but our efforts failed to deliver a precise K_d . However, co-purification of heme with heterologously expressed LhaS suggests that the off-rates are low, consistent with high-affinity binding. Therefore, the system might be superior to heme acquisition systems, which depend on specific interactions between bacterial hemoprotein-receptors and host hemoproteins to extract heme. The *S. aureus* Isd system is well-studied in this regard. The surface located receptor IsdB binds hemoglobin through its N-terminal NEAT domain (IsdB-N1). This binding is proposed to induce a steric strain that facilitates heme dissociation. Heme is then captured by the C-terminal NEAT domain (IsdB-N2) and transported across the cell wall and membrane [22, 28, 50-52]. Similarly, the secreted hemophores IsdX1 and IsdX2 of *Bacillus anthracis* possess NEAT motifs and perform the same two-step process as IsdB of *S. aureus* to acquire heme [53]. This mechanism harbours the disadvantage of facilitating heme acquisition only from a single hemoprotein. IsdB allows acquisition from hemoglobin but does not interact with myoglobin or hemopexin [51] and even hemoglobin from different species reduces the efficacy of the system [54, 55]. The same is true for IsdB of *S. lugdunensis* [16]. *Haemophilus influenzae* uses the specific interaction between the surface exposed receptor HxuA and hemopexin to facilitate heme dissociation. Heme is subsequently captured by HxuC [56, 57]. Again, the specificity for hemopexin prevents usage of other hemoproteins by HxuA. Specific interactions between LhaS and multiple host hemoproteins seem unlikely, suggesting that the superior affinity of LhaS towards the heme group bypasses the need for protein-protein interactions and enables usage of different hemoproteins. However, additional experimental evidence is required to strengthen this hypothesis of passive heme transfer.

The LhaSTA operon of *S. lugdunensis* is located within the *isd* operon which encodes the hemoglobin receptor IsdB, the cell wall-anchored, heme-binding proteins IsdJ and IsdC as well as the conventional heme membrane transporter IsdEFL. Deletion of *lhaSTA* in combination with *isdEFL* did not completely abrogate acquisition of free heme. A similar effect has been observed in *S. aureus* suggesting the presence of additional, low affinity heme transporters within these species [58]. Furthermore, a putative secreted/membrane associated hemophore (IsdK) is encoded within the operon [16]. Interestingly, we show LhaSTA to be functionally independent of the Isd cluster because LhaSTA-dependent usage of all host hemoproteins except for Hb-Hap

was observed in the absence of all Isd-associated proteins. This indicates that LhaSTA does not rely on Isd-dependent funneling of heme across the cell wall, but also raises interesting questions about the spatial organization of heme acquisition and donor proteins. For an efficient transfer of heme between host hemoproteins and LhaS one would expect that spatial proximity between the proteins is required. Yet, LhaS is situated in the bacterial membrane and host hemoproteins are too large (hemoglobin ~ 64-16 kd (tetramer-monomer), myoglobin ~16 kDa, Hemopexin-heme ~70,6 kDa) to readily penetrate the peptidoglycan layer of Gram-positive bacteria. However, it has been shown that staphylococcal peptidoglycan contains pores that might allow access of proteins to the bacterial membrane [59, 60]. Along this line, it is tempting to speculate that surface receptor-dependent acquisition of Hb-Hap might be needed as these complexes exceed 100 kDa and might be unable to access the bacterial membrane. However, we also observed that recombinant LhaS did not accept heme from Hb-Hap which might indicate that binding of haptoglobin to hemoglobin increases the strength of heme binding to the protein complex. Such an effect of haptoglobin is to our knowledge not known and might be interesting for further investigation.

We failed to establish a functional mouse model of systemic disease to study the *in vivo* role of LhaSTA for the pathogenicity of *S. lugdunensis*. The reasons for this can be plentiful as little is known about virulence factors of *S. lugdunensis*. Genome analysis showed that *S. lugdunensis* lacks the wide variety of virulence and immune evasion molecules found in *S. aureus* [11]. This is the most likely explanation for the apparent reduced virulence of *S. lugdunensis* in mice. Nevertheless, the co-existence of the Isd and LhaSTA heme-acquisition system in this species may represent a virulent trait and be required for invasive disease. In line with this, most *S. lugdunensis* strains are highly hemolytic on blood agar plates suggesting that the release of hemoproteins from host cells can be achieved by this species. The hemolytic SLUSH peptides [61] of *S. lugdunensis* resemble the β -PSMs of *S. aureus* [62]. Additionally, the sphingomyelinase C (β -toxin) is conserved in *S. lugdunensis* [11]. However, recent research suggested that *S. aureus* targets erythrocytes specifically using the bi-component toxins LukED and HlgAB recognising the DARC receptor [26]. This creates human specificity. Whether similar mechanisms are used by *S. lugdunensis* is unclear, but we found that, in contrast to human cells, *S. lugdunensis* failed to lyse murine erythrocytes. This suggests that host specific virulence factors are present in *S.*

lugdunensis. Bi-component toxin genes are not located in the chromosome but genes encoding a streptolysin-like toxin were identified [11].

We found that LhaSTA facilitated growth of *S. lugdunensis* in the presence of human cells such as erythrocytes and myelocytes strongly suggesting that the system allows usage of these cells during invasive disease.

Altogether our experiments identify LhaSTA as an ECF-transporter able to acquire iron and place this important class of nutrient acquisition system in the context of bacterial pathogens and immune evasion strategies. During the revision of this manuscript Chatterjee and colleagues published the identification of a heme-specific ECF transporter in streptococci [63]. In addition, a preprint manuscript that reports the identification of a heme-specific ECF transporter in *Lactococcus sakei* is present in bioarchives [64]. Although these transporters seem functionally redundant to the one of *S. lugdunensis* described here, the specificity subunits of the systems show remarkably little amino-acid sequence similarity. This suggests that the genes encoding them might have developed independently in bacterial species. This was also suggested for the cobalamin-specific components BtuM and CbrT which bind the same ligand despite little sequence conservation [40].

Additional experiments are required to determine whether heme-specific ECF transporters are also present in other bacterial pathogens and the biochemical properties of heme-binding need to be further characterized to better understand the role of these systems in overcoming nutritional iron limitation.

Methods

Table 1 Bacterial strains, plasmids and chemicals used in this study

| Key Resources Table | | | | |
|---|-------------|--|-------------|------------------------|
| Reagent type (species) or resource | Designation | Source or reference | Identifiers | Additional information |
| strain, strain background (<i>Staphylococcus lugdunensis</i>) | N940135 | National Reference Center for Staphylococci, | | |

| | | | | |
|---|----------------------------------|--|--------------------------|--|
| | | Lyon, France [11] | | |
| strain, strain background (<i>S. lugdunensis</i>) | N920143 | National Reference Center for Staphylococci, Lyon, France [11] | | |
| strain, strain background (<i>S. lugdunensis</i>) | N920143 <i>ΔisdEFL</i> | This paper | | Markerless deletion mutant of <i>isdEFL</i> |
| strain, strain background (<i>S. lugdunensis</i>) | N920143 <i>ΔlhaSTA</i> | This paper | | Markerless deletion mutant of <i>lhaSTA</i> |
| strain, strain background (<i>S. lugdunensis</i>) | N920143 <i>ΔisdEFLΔlhaSTA</i> | This paper | | Markerless double deletion mutant of <i>isdEFL</i> and <i>lhaSTA</i> |
| cell line (Human) | Human cardiac myocytes (HCM) | PromoCell | C-12810 | |
| recombinant DNA reagent | pQE-30 | Qiagen | | IPTG inducible expression plasmid |
| recombinant DNA reagent | pQE30:lhaS | This paper | | LhaS expressing plasmid for protein purification |
| recombinant DNA reagent | pRB473:lhaSTA | This paper | | LhaSTA expressing plasmid for complementation |
| recombinant DNA reagent | pIMAY (plasmid) | [65] | See material and methods | Thermosensitive vector for allelic exchange |

| | | | | |
|---------------------------|-----------------------------------|-----------------|--------------------------|---|
| recombinant DNA reagent | pIMAY: Δ <i>isd</i> | [16] | | Plasmid for the deletion of the entire <i>isd</i> locus |
| recombinant DNA reagent | pIMAY: Δ <i>isdEFL</i> | This study | | Plasmid for the deletion of conventional heme transporter <i>isdEFL</i> |
| recombinant DNA reagent | pIMAY: Δ <i>haST A</i> | This study | | Plasmid for the deletion of heme specific ECF-transporter |
| recombinant DNA reagent | pRB473 | [68] | | Expression plasmid without promotor region. |
| biological sample (Human) | Human hemoglobin | Own preparation | See material and methods | Sex male |
| biological sample (Human) | Porcine hemin | Sigma | 51280 | |
| biological sample (Human) | Human Myoglobin | Sigma Aldrich | M6036 | |
| biological sample (Horse) | Equine Myoglobin | Sigma Alrich | M1882 | |
| biological sample (Human) | Human Haptoglobin (Phenotype 1-1) | Sigma Aldrich | SRP6507 | |

| | | | | |
|---------------------------|---------------------------------------|---------------|------------------|--|
| biological sample (Human) | Human Hemopexin | Sigma Aldrich | H9291 | |
| chemical compound, drug | RPMI 1640 Medium | Sigma Aldrich | R6504-10L | |
| chemical compound, drug | Casamino acids | BACTO | 223050 | |
| chemical compound, drug | EDDHA | LGC Standarts | TRC-E335100-10MG | |
| chemical compound, drug | Dodecyl- β -D-maltosid (DDM) | Carl Roth | CN26.1 | |
| chemical compound, drug | 3,3',5,5'-tetramethylbenzidine (TMBZ) | Sigma Aldrich | 860336 | |
| chemical compound, drug | Profinity IMAC resin nickel charged | BIO RAD | 1560135 | |

Chemicals

If not stated otherwise, reagents were purchased from Sigma

Bacterial strains and growth in iron limited media

All bacterial strains generated and/or used in this study are listed in Table 1. For growth in iron limited conditions, bacteria were grown overnight in Tryptic Soy Broth (TSB) TSB (Oxoid). Cells were harvested by centrifugation, washed with RPMI containing 10 μ M EDDHA (LGC standards), adjusted to an $OD_{600} = 1$ and 2,5 μ l were used to inoculate 0,5 ml of RPMI+ 1 % casamino acids (BACTO) + 10 μ M EDDHA in individual wells of a 48 well microtiter plate (NUNC). As sole iron source 200 nm porcine hemin (Sigma), 2.5 μ g/ml human hemoglobin (own preparation), 10 μ g/ml human myoglobin

(Sigma) or equine myoglobin (Sigma), 117nM human haptoglobin-hemoglobin or 200 nM hemopexin-heme (Sigma) were added to the wells. Bacterial growth was monitored using an Epoch2 reader (300 rpm, 37°C). The OD₆₀₀ was measured every 15 minutes.

Creation of markerless deletion mutants in *S. lugdunensis*

For targeted deletion of *lhaSTA* and *isdEFL*, 500 bp DNA fragments upstream and downstream of the genes to be deleted were amplified by PCR. A sequence overlap was integrated into the fragments to allow fusion and creating an ATG-TAA scar in the mutant allele. The 1 kb deletion fragments were created using spliced extension overlap PCR and cloned into pIMAY. All the oligonucleotides are summarized in Supplementary File 1 Targeted mutagenesis of *S. lugdunensis* was performed using allelic exchange described elsewhere [65]. The plasmids and the primers used are listed in Table 1 and Supplementary File 1, respectively.

Heterologous expression of LhaS and membrane vesicle preparation

LhaS was overexpressed with a N-terminal deca-His tag using pQE-30 in *E. coli* XL1 blue in either Lysogeny broth (LB) medium or RPMI+1% casamino acids. 100 ml overnight culture in LB with 100 µg ml⁻¹ ampicillin was harvested by centrifugation and washed once in PBS. Cells were resuspended in 5 ml PBS and used for inoculation of 2 L RPMI + 1% casamino acids or LB medium. Cells were allowed to grow at 37°C to an OD₆₀₀ = 0.6 - 0.8. Expression was induced by adding 0.3 mM IPTG for 4 – 5 h at 25°C. Cells were harvested, washed with 50 mM potassium phosphate buffer (KPi) pH 7.5, and lysed through 3 rounds of sonification (Branson Digital Sonifier; 2 min, 30% amplitude), in presence of 200 µM PMSF, 1 mM MgSO₄ and DNaseI. Cell debris were removed by centrifugation for 30 min at 7000 rpm and 4°C. The supernatant was centrifuged for 2 h at 35000 rpm and 4 °C to collect membrane vesicles (MVs). The MV pellet was homogenized in 50 mM KPi pH 7.5 and flash frozen in liquid nitrogen, stored at -80°C and used for purification.

Purification of LhaS

His-tagged LhaS MVs were dissolved in solubilisationbuffer (50 mM KPi pH 7.5, 200 mM KCl, 200 mM NaCl, 1% (w/v) n-dodecyl-b-D-maltopyranosid (DDM, Roth) for 1 h at 4°C on a rocking table. Non-soluble material was removed by centrifugation at 35000 rpm for 30 min and 4°C. The supernatant was decanted into a poly-prep

column (BioRad) containing a 0.5 ml bed volume Ni²⁺-NTA sepharose slurry, equilibrated with 20 column volumes (CV) wash buffer (50mM KPi pH 7.5, 200mM NaCl, 50 mM imidazole, 0.04 % DDM) and incubated for 1 h at 4°C while gently agitating. The lysate was drained out of the column and the column was washed with 40 CV wash buffer. Bound protein was eluted from the column in 3 fractions with elution buffer (50mM KPi, pH 7.5, 200 mM NaCl, 350 mM imidazole, 0.04 % DDM). The sample was centrifuged for 3 min at 10.000 rpm to remove aggregates and loaded on a Superdex® 200 Increase 10/300 GL gel filtration column (GE Healthcare), which was equilibrated with SEC buffer (50mM KPi pH 7.5, 200 mM NaCl, 0.04% DDM). Peak fractions were combined and concentrated in a Vivaspin disposable ultrafiltration device (Sartorius Stedim Biotec SA).

MV saturation with hemoproteins

MVs (120 mg total protein content) from RPMI were thawed and incubated for 10 min at RT with each of the following molecules: 5.6 µM heme, 476 µg/ml human hemoglobin, 437 µg/ml equine myoglobin, 5.6 µM hemopexin-heme, 476 µg/ml hemoglobin-haptoglobin. Further purification was performed as described above. After Ni²⁺ affinity chromatography the protein was concentrated and used to measure the peroxidase activity of heme (TMBZ staining).

TMBZ staining of heme

Protein content was determined by Bradford analysis (BIORAD) according to the manufacturer's protocol. 15 µg protein sample was mixed 1:1 with native sample buffer (BIORAD) and loaded on a Mini-PROTEAN TGX Precast Gel (BIORAD). The PAGE was run at 4°C and low voltage for 2 h in Tris /Glycine buffer (BIORAD). The gel was rinsed with H₂O for 5 min and stained with 50 ml staining solution (15 ml 3,3',5,5'-tetramethylbenzidine (TMBZ) solution (6.3 mM TMBZ in methanol) +35 ml 0.25 M sodium acetate solution (pH 5)) for 1 h at room temperature (RT) while gently agitating. The gel was then incubated for 30 min at RT in the dark in presence of 30 mM H₂O₂. The background staining was removed by incubating the gel in a solution of isopropanol/0.25 M sodium acetate (3:7). Following scanning, the gel was completely destained in a solution of isopropanol/0.25 M sodium acetate (3:7) and stained with the BlueSafe stain (nzytech) for 10 min.

Preparation of human erythrocytes

Human blood was obtained from healthy volunteers and mixed 1:1 with MACS buffer (PBS w/o + 0.05 % BSA + 2 mM EDTA). Erythrocytes were pelleted by density gradient centrifugation in a histopaque blood gradient for 20 min 380 x g at RT. The erythrocyte pellet was washed 3 times with erythrocyte wash buffer (21 mM Tris, 4.7 mM KCl, 2 mM CaCl₂, 140.5 mM NaCl, 1.2 mM MgSO₄, 5.5 mM Glucose, 0.5 % BSA, pH 7.4). Cell count and viability was determined by using the trypan blue stain (BIO RAD).

Purification of human hemoglobin

Human/murine haemoglobin was purified by using standard procedures describe in detail elsewhere [66]

Preparation of saturated hemopexin and haptoglobin

Human hemopexin was dissolved in sterile PBS and saturated with porcine heme in a hemopexin: heme 1: 1.3 molar ratio for 1 h at 37°C. This was followed by 48 h dialysis in a Slide-a-Lyzer chamber (ThermoFisher) with one buffer (1 x PBS) change. Haptoglobin was saturated by mixing 4.7 µg/ml haemoglobin with 8.4 µg/ml human haptoglobin for 30 min at 37°C.

Quantification of intracellular iron

Bacteria were grown at 37°C in RPMI + 1% casamino acids to an OD₆₀₀= 0.6. An aliquot of the culture was collected prior addition of 5 µM heme and 25 µM EDDHA and further incubation at 37°C for 3 hours. At this time point bacteria were collected and resuspended in buffer WB (10 mM Tris-HCl, pH 7, 10 mM MgCl₂, 500 mM sucrose) to an OD₆₀₀ = 50. The bacterial pellet was collected by centrifugation at 8000 rpm for 7 min and resuspended in 1 ml buffer DB (10 mM Tris-HCl, pH 7, 10 mM MgCl₂, 500 mM sucrose, 0.6 mg/ml lysostaphin, 25 U/ml mutanolysin, 30 µl protease inhibitor cocktail (1 complete mini tablet dissolved in 1 ml H₂O (Roche), 1 mM phenylmethanesulfonylfluoride (Roth). The cell wall was digested by incubating at 37°C for 1.5 h, followed by centrifugation at 17000 x g for 10 min at 4°C. Pelleted protoplasts were washed with 1 ml buffer WB, centrifuged and resuspended in 200 µl buffer LB (100 mM Tris-HCl; pH 7, 10 mM MgCl₂, 100 mM NaCl, 100 µg/ml DNaseI, 1 mg/ml RNaseA). Protoplast lysis was performed through repeated cycles (3) of freezing and thawing. The lysate was centrifuged 30 min to pellet membrane fraction and recover

the supernatant, which contained the cytosolic fraction and was used for quantification of total intracellular iron content.

Quantification of intracellular iron content by heme uptake was carried out according to Riemer et al. [20] with minor modifications. Briefly, 100 μ l of the cytosolic fraction were mixed with 100 μ l 50mM NaOH, 100 μ l HCL, and 100 μ l iron releasing reagent (1:1 freshly mixed solution of 1.4 M HCl and 4.5 % (w/v) KMnO_4 in H_2O). Samples were incubated for 2 h at 60°C in a fume hood. 30 μ l iron detection reagent (6.5 mM ferrozine, 6.5 mM neocuproine, 2.5 M ammonium acetate, 1 M ascorbic acid) was mixed with the samples and incubated for 30 min at 37°C while shaking (1100 rpm). Samples were centrifuged for 3 min at 12000 x g to remove precipitates. 150 μ l of the supernatants were transferred to a 96-well microtiter plate and absorbance at 550 nm was measured in a plate reader (BMG Labtech). For determination of iron concentration, FeCl_3 standards in a range of 0 to 100 μ M were prepared.

Measurement of LhaS absorption spectra

LhaS was purified from LB (holo LhaS) or RPMI (apo LhaS) as described above. 2 μ l protein sample were loaded on an Eppendorf μ Cuvette and absorptions spectra were measured at 260 - 620 nm with a BioPhotometer (Eppendorf).

Characterization of LhaS and heme by mass spectrometry analysis

MALDI-TOF mass spectra were recorded with a Reflex IV (Bruker Daltonics, Bremen, Germany) in reflector mode. Positive ions were detected, and all spectra represent the sum of 50 shots. A peptide standard (Peptide Calibration Standard II, Bruker Daltonics) was used for external calibration. 2,5-dihydroxybenzoic acid (DHB, Bruker Daltonics) dissolved in water/acetonitrile/trifluoroacetic acid (50/49.05/0.05) at a concentration of 10 mg ml^{-1} was used as matrix. Before the measurements, the samples Lhas-apo (317 $\mu\text{g ml}^{-1}$) and Lhas+heme (377 $\mu\text{g ml}^{-1}$) were centrifuged and diluted with MilliQ- H_2O (1:25). An aliquot of 1 μ L of the samples was mixed with 1 μ L of the matrix and spotted onto the MALDI polished steel sample plate. As the solution dried, the organic solvent evaporated quickly. At this point, the remaining mini droplet was removed gently with a pipette and the remaining sample was air-dried at room temperature.

High resolution mass spectra of Lhas-apo (317 $\mu\text{g ml}^{-1}$) and Lhas+heme (377 $\mu\text{g ml}^{-1}$) were recorded on a HPLC-UV-HR mass spectrometer (MaXis4G with Performance Upgrade kit with ESI-Interface, Bruker Daltonics). The samples were diluted with

MilliQ-H₂O (1:25) and 3 μ L were applied to a Dionex Ultimate 3000 HPLC system (Thermo Fisher Scientific), coupled to the MaXis 4G ESI-QTOF mass spectrometer (Bruker Daltonics). The ESI source was operated at a nebulizer pressure of 2.0 bar, and dry gas was set to 8.0 L min⁻¹ at 200 °C. MS/MS spectra were recorded in auto MS/MS mode with collision energy stepping enabled. Sodium formate was used as internal calibrant. The gradient was 90 % MilliQ-H₂O with 0.1 % formic acid and 10 % methanol with 0.06 % formic acid to 100 % methanol with 0.06 % formic acid in 20 min with a flow rate of 0.3 mL/min on a Nucleoshell®EC RP-C₁₈ (150 x 2 mm, 2.7 μ m) from Macherey-Nagel.

[M+H]⁺ calculated for C₃₄H₃₂FeN₄O₄⁺: 616.1767; found 616.1778 (Δ ppm 1.78).

Calculation of binding stoichiometry

To calculate the putative binding stoichiometry of heme and LhaS the heme concentration in Fig.2A was determined utilizing the extinction coefficient of 58,4 mM⁻¹ cm⁻¹ at 384 nm for heme. The LhaS concentration was determined utilizing the extinction coefficient of 29910 M⁻¹ cm⁻¹ (calculated with ProtParam tool – ExPASy) at 280 nm.

Human Cardiac Myocytes (HCM)

Primary human cardiac myocytes were purchased from PromoCell (the identity of the cell line was not verified; the culture was negative for mycoplasma) and in 75-cm² culture flasks in 20 ml of myocyte growth medium (PromoCell). Cells were detached with accutase, washed once with RPMI containing 200 μ M EDDHA and resuspended in PRMI containing 200 μ M EDDHA. 40000 cells per well were used for bacterial growth assays as described above.

Assessing hemolytic activity of *S. lugdunensis* culture supernatants

S. aureus and *S. lugdunensis* were grown overnight in TSB. Cells were pelleted and culture supernatants were filter sterilized using a 0.22 μ M filter. A 100 μ L volume of supernatant was added into 1 mL of PBS containing either 5% v/v murine or human red blood cells. Mixtures were incubated at room temperature without shaking for 48 hours.

Declarations

Ethics approval and consent to participate: Animal experiments were performed in strict accordance with the European Health Law of the Federation of Laboratory Animal Science Associations. The protocol was approved by the Regierungspräsidium Tübingen (IMIT1/17). Human Erythrocytes were isolated from venous blood of healthy volunteers in accordance with protocols approved by the Institutional Review Board for Human Subjects at the University of Tübingen. Informed written consent was obtained from all volunteers.

Consent for publication: not applicable

Availability of data and materials: The datasets gained during the current study are available over dryad at <https://doi.org/10.5061/dryad.fgz612jqc>

Competing interests: The authors declare that they have no competing interests.

Funding: We acknowledge the funding of this project by the Deutsche Forschungsgemeinschaft (DFG) in form of an individual project grant (HE8381/3-1) to SH. SH was supported by infrastructural funding from the Deutsche Forschungsgemeinschaft (DFG), Cluster of Excellence EXC 2124 Controlling Microbes to Fight Infections. DJS was supported by NWO (TOP grant 714.018.003). DEH acknowledges support from the Canadian Institutes of Health Research (PJT-153308).

None of the funding bodies was involved in the design of the study, the performance of experiments, data evaluation, writing of the manuscript or the decision about submission.

Acknowledgements

We thank Timothy J. Foster and Libera Lo Presti for critically reading and editing this manuscript. We thank Andreas Peschel for helpful discussion. We thank Sarah Rothfuß and Vera Augsburger for excellent technical support and Imran Malik for the introduction to the ITC technology.

References

1. Roth, J.R., et al., *Characterization of the cobalamin (vitamin B12) biosynthetic genes of Salmonella typhimurium*. J Bacteriol, 1993. **175**(11): p. 3303-16.
2. Erkens, G.B., et al., *Energy coupling factor-type ABC transporters for vitamin uptake in prokaryotes*. Biochemistry, 2012. **51**(22): p. 4390-6.
3. Finkenwirth, F. and T. Eitinger, *ECF-type ABC transporters for uptake of vitamins and transition metal ions into prokaryotic cells*. Res Microbiol, 2019. **170**(8): p. 358-365.
4. Rempel, S., W.K. Stanek, and D.J. Slotboom, *ECF-Type ATP-Binding Cassette Transporters*. Annu Rev Biochem, 2019. **88**: p. 551-576.
5. Hood, M.I. and E.P. Skaar, *Nutritional immunity: transition metals at the pathogen-host interface*. Nat Rev Microbiol, 2012. **10**(8): p. 525-37.
6. Cassat, J.E. and E.P. Skaar, *Iron in infection and immunity*. Cell Host Microbe, 2013. **13**(5): p. 509-19.
7. Schaible, U.E. and S.H. Kaufmann, *Iron and microbial infection*. Nat Rev Microbiol, 2004. **2**(12): p. 946-53.
8. Weinberg, E.D., *Microbial pathogens with impaired ability to acquire host iron*. Biometals, 2000. **13**(1): p. 85-9.
9. Choby, J.E. and E.P. Skaar, *Heme Synthesis and Acquisition in Bacterial Pathogens*. J Mol Biol, 2016. **428**(17): p. 3408-28.
10. Liu, P.Y., et al., *Staphylococcus lugdunensis infective endocarditis: a literature review and analysis of risk factors*. J Microbiol Immunol Infect, 2010. **43**(6): p. 478-84.
11. Heilbronner, S., et al., *Genome sequence of Staphylococcus lugdunensis N920143 allows identification of putative colonization and virulence factors*. FEMS Microbiol Lett, 2011. **322**(1): p. 60-7.
12. Heilbronner, S., et al., *Competing for Iron: Duplication and Amplification of the *isd* Locus in Staphylococcus lugdunensis HKU09-01 Provides a Competitive Advantage to Overcome Nutritional Limitation*. PLoS Genet, 2016. **12**(8): p. e1006246.
13. Sheldon, J.R., H.A. Laakso, and D.E. Heinrichs, *Iron Acquisition Strategies of Bacterial Pathogens*. Microbiol Spectr, 2016. **4**(2).
14. El-Gebali, S., et al., *The Pfam protein families database in 2019*. Nucleic Acids Res, 2019. **47**(D1): p. D427-D432.
15. Coy, M. and J.B. Neilands, *Structural dynamics and functional domains of the fur protein*. Biochemistry, 1991. **30**(33): p. 8201-10.
16. Zapotoczna, M., et al., *Iron-regulated surface determinant (Isd) proteins of Staphylococcus lugdunensis*. J Bacteriol, 2012. **194**(23): p. 6453-67.
17. Fyrestam, J. and C. Ostman, *Determination of heme in microorganisms using HPLC-MS/MS and cobalt(III) protoporphyrin IX inhibition of heme acquisition in Escherichia coli*. Anal Bioanal Chem, 2017. **409**(30): p. 6999-7010.
18. Farrand, A.J., et al., *An Iron-Regulated Autolysin Remodels the Cell Wall To Facilitate Heme Acquisition in Staphylococcus lugdunensis*. Infect Immun, 2015. **83**(9): p. 3578-89.
19. Haley, K.P., et al., *Staphylococcus lugdunensis IsdG Liberates Iron from Host Heme*. J Bacteriol, 2011. **193**(18): p. 4749-57.
20. Riemer, J., et al., *Colorimetric ferrozine-based assay for the quantitation of iron in cultured cells*. Anal Biochem, 2004. **331**(2): p. 370-5.

21. Bowden, C.F.M., et al., *Structure-function analyses reveal key features in Staphylococcus aureus IsdB-associated unfolding of the heme-binding pocket of human hemoglobin*. J Biol Chem, 2018. **293**(1): p. 177-190.
22. Gianquinto, E., et al., *Interaction of human hemoglobin and semi-hemoglobins with the Staphylococcus aureus hemophore IsdB: a kinetic and mechanistic insight*. Sci Rep, 2019. **9**(1): p. 18629.
23. Deniau, C., et al., *Thermodynamics of heme binding to the HasA(SM) hemophore: effect of mutations at three key residues for heme uptake*. Biochemistry, 2003. **42**(36): p. 10627-33.
24. Wandersman, C. and P. Delepelaire, *Bacterial iron sources: from siderophores to hemophores*. Annu Rev Microbiol, 2004. **58**: p. 611-47.
25. Thomas, P.E., D. Ryan, and W. Levin, *An improved staining procedure for the detection of the peroxidase activity of cytochrome P-450 on sodium dodecyl sulfate polyacrylamide gels*. Anal Biochem, 1976. **75**(1): p. 168-76.
26. Spaan, A.N., et al., *Staphylococcus aureus Targets the Duffy Antigen Receptor for Chemokines (DARC) to Lyse Erythrocytes*. Cell Host Microbe, 2015. **18**(3): p. 363-70.
27. Beasley, F.C., et al., *Staphylococcus aureus transporters Hts, Sir, and Sst capture iron liberated from human transferrin by Staphyloferrin A, Staphyloferrin B, and catecholamine stress hormones, respectively, and contribute to virulence*. Infect Immun, 2011. **79**(6): p. 2345-55.
28. Sheldon, J.R. and D.E. Heinrichs, *Recent developments in understanding the iron acquisition strategies of gram positive pathogens*. FEMS Microbiol Rev, 2015. **39**(4): p. 592-630.
29. Brozyna, J.R., J.R. Sheldon, and D.E. Heinrichs, *Growth promotion of the opportunistic human pathogen, Staphylococcus lugdunensis, by heme, hemoglobin, and coculture with Staphylococcus aureus*. Microbiologyopen, 2014. **3**(2): p. 182-95.
30. Hargrove, M.S., D. Barrick, and J.S. Olson, *The association rate constant for heme binding to globin is independent of protein structure*. Biochemistry, 1996. **35**(35): p. 11293-9.
31. Tolosano, E. and F. Altruda, *Hemopexin: structure, function, and regulation*. DNA Cell Biol, 2002. **21**(4): p. 297-306.
32. Mazmanian, S.K., et al., *Passage of heme-iron across the envelope of Staphylococcus aureus*. Science, 2003. **299**(5608): p. 906-9.
33. Skaar, E.P., A.H. Gaspar, and O. Schneewind, *Bacillus anthracis IsdG, a heme-degrading monooxygenase*. J Bacteriol, 2006. **188**(3): p. 1071-80.
34. Lei, B., et al., *Identification and characterization of a novel heme-associated cell surface protein made by Streptococcus pyogenes*. Infect Immun, 2002. **70**(8): p. 4494-500.
35. Jin, B., et al., *Iron acquisition systems for ferric hydroxamates, haemin and haemoglobin in Listeria monocytogenes*. Mol Microbiol, 2006. **59**(4): p. 1185-98.
36. Duurkens, R.H., et al., *Flavin binding to the high affinity riboflavin transporter RibU*. J Biol Chem, 2007. **282**(14): p. 10380-6.
37. Eudes, A., et al., *Identification of genes encoding the folate- and thiamine-binding membrane proteins in Firmicutes*. J Bacteriol, 2008. **190**(22): p. 7591-4.

38. Erkens, G.B. and D.J. Slotboom, *Biochemical characterization of ThiT from Lactococcus lactis: a thiamin transporter with picomolar substrate binding affinity*. *Biochemistry*, 2010. **49**(14): p. 3203-12.
39. Berntsson, R.P., et al., *Structural divergence of paralogous S components from ECF-type ABC transporters*. *Proc Natl Acad Sci U S A*, 2012. **109**(35): p. 13990-5.
40. Santos, J.A., et al., *Functional and structural characterization of an ECF-type ABC transporter for vitamin B12*. *Elife*, 2018. **7**.
41. Rempel, S., et al., *Cysteine-mediated decyanation of vitamin B12 by the predicted membrane transporter BtuM*. *Nat Commun*, 2018. **9**(1): p. 3038.
42. Neubauer, O., et al., *Two essential arginine residues in the T components of energy-coupling factor transporters*. *J Bacteriol*, 2009. **191**(21): p. 6482-8.
43. Zhang, M., et al., *Structure of a pantothenate transporter and implications for ECF module sharing and energy coupling of group II ECF transporters*. *Proc Natl Acad Sci U S A*, 2014. **111**(52): p. 18560-5.
44. ter Beek, J., et al., *Quaternary structure and functional unit of energy coupling factor (ECF)-type transporters*. *J Biol Chem*, 2011. **286**(7): p. 5471-5.
45. Wang, T., et al., *Pyridoxamine is a substrate of the energy-coupling factor transporter HmpT*. *Cell Discov*, 2015. **1**: p. 15014.
46. Yu, Y., et al., *Planar substrate-binding site dictates the specificity of ECF-type nickel/cobalt transporters*. *Cell Res*, 2014. **24**(3): p. 267-77.
47. Kirsch, F. and T. Eitinger, *Transport of nickel and cobalt ions into bacterial cells by S components of ECF transporters*. *Biometals*, 2014. **27**(4): p. 653-60.
48. Wandersman, C. and P. Delepelaire, *Haemophore functions revisited*. *Mol Microbiol*, 2012. **85**(4): p. 618-31.
49. Letoffe, S., et al., *Interactions of HasA, a bacterial haemophore, with haemoglobin and with its outer membrane receptor HasR*. *Mol Microbiol*, 1999. **33**(3): p. 546-55.
50. Pilpa, R.M., et al., *Functionally distinct NEAT (NEAr Transporter) domains within the Staphylococcus aureus IsdH/HarA protein extract heme from methemoglobin*. *J Biol Chem*, 2009. **284**(2): p. 1166-76.
51. Torres, V.J., et al., *Staphylococcus aureus IsdB is a hemoglobin receptor required for heme iron utilization*. *J Bacteriol*, 2006. **188**(24): p. 8421-9.
52. Pishchany, G., et al., *IsdB-dependent hemoglobin binding is required for acquisition of heme by Staphylococcus aureus*. *J Infect Dis*, 2014. **209**(11): p. 1764-72.
53. Maresso, A.W., G. Garufi, and O. Schneewind, *Bacillus anthracis secretes proteins that mediate heme acquisition from hemoglobin*. *PLoS Pathog*, 2008. **4**(8): p. e1000132.
54. Choby, J.E., et al., *Molecular Basis for the Evolution of Species-Specific Hemoglobin Capture by Staphylococcus aureus*. *mBio*, 2018. **9**(6).
55. Pishchany, G., et al., *Specificity for human hemoglobin enhances Staphylococcus aureus infection*. *Cell Host Microbe*, 2010. **8**(6): p. 544-50.
56. Zambolin, S., et al., *Structural basis for haem piracy from host haemopexin by Haemophilus influenzae*. *Nat Commun*, 2016. **7**: p. 11590.
57. Hanson, M.S., et al., *Identification of a genetic locus of Haemophilus influenzae type b necessary for the binding and utilization of heme bound to human hemopexin*. *Proc Natl Acad Sci U S A*, 1992. **89**(5): p. 1973-7.
58. Grigg, J.C., et al., *Heme coordination by Staphylococcus aureus IsdE*. *J Biol Chem*, 2007. **282**(39): p. 28815-22.

59. Kim, S.J., et al., *Staphylococcus aureus* peptidoglycan stem packing by rotational-echo double resonance NMR spectroscopy. *Biochemistry*, 2013. **52**(21): p. 3651-9.
60. Turner, R.D., et al., *Peptidoglycan architecture can specify division planes in Staphylococcus aureus*. *Nat Commun*, 2010. **1**: p. 26.
61. Donvito, B., et al., *Synergistic hemolytic activity of Staphylococcus lugdunensis is mediated by three peptides encoded by a non-agr genetic locus*. *Infect Immun*, 1997. **65**(1): p. 95-100.
62. Rautenberg, M., et al., *Neutrophil responses to staphylococcal pathogens and commensals via the formyl peptide receptor 2 relates to phenol-soluble modulins release and virulence*. *FASEB J*, 2010.
63. Chatterjee, N., et al., *A novel heme transporter from the ECF family is vital for the Group A Streptococcus colonization and infections*. *J Bacteriol*, 2020.
64. Verplaetse, E., et al., *Heme uptake in *Lactobacillus sakei* evidenced by a new ECF-like transport system*. *bioRxiv*, 2019: p. 864751.
65. Monk, I.R., et al., *Transforming the untransformable: application of direct transformation to manipulate genetically Staphylococcus aureus and Staphylococcus epidermidis*. *MBio*, 2012. **3**(2).
66. Pishchany, G., K.P. Haley, and E.P. Skaar, *Staphylococcus aureus growth using human hemoglobin as an iron source*. *J Vis Exp*, 2013(72).
67. Tse, H., et al., *Complete genome sequence of Staphylococcus lugdunensis strain HKU09-01*. *J Bacteriol*, 2010. **192**(5): p. 1471-2.
68. Bruckner, R., *A series of shuttle vectors for Bacillus subtilis and Escherichia coli*. *Gene*, 1992. **122**(1): p. 187-92.

Supplementary Material

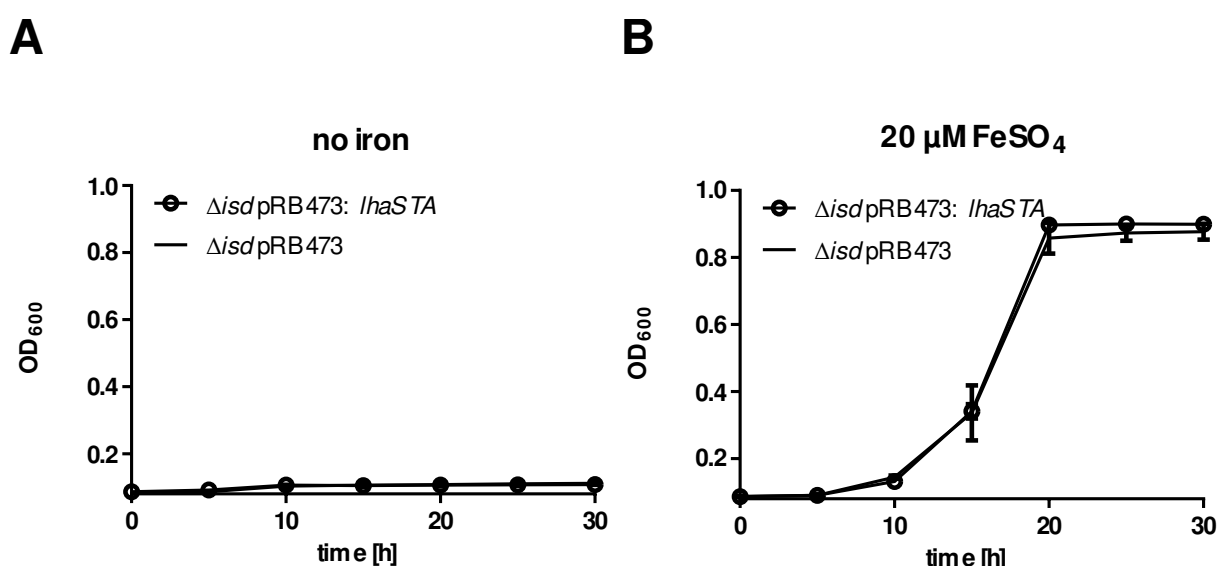


Figure 1- figure supplement 1. LhaSTA dependent growth.

A/B) Proliferation of *S. lugdunensis* N920143 Δisd pRB473 and Δisd pRB473:*lhaSTA* strains. The indicated strains were grown in the absence of nutritional iron (A) or in the

presence of 20 μM FeSO_4 (B). 500 μl of cultures were inoculated to an $\text{OD}_{600} = 0,05$ in 48 well plates and OD_{600} was monitored every 15 min using a Epoch1 plate reader. For reasons of clarity values taken every 5 hours are displayed. Mean and SD of three experiments are shown. Statistical analysis was performed using students unpaired t-test.

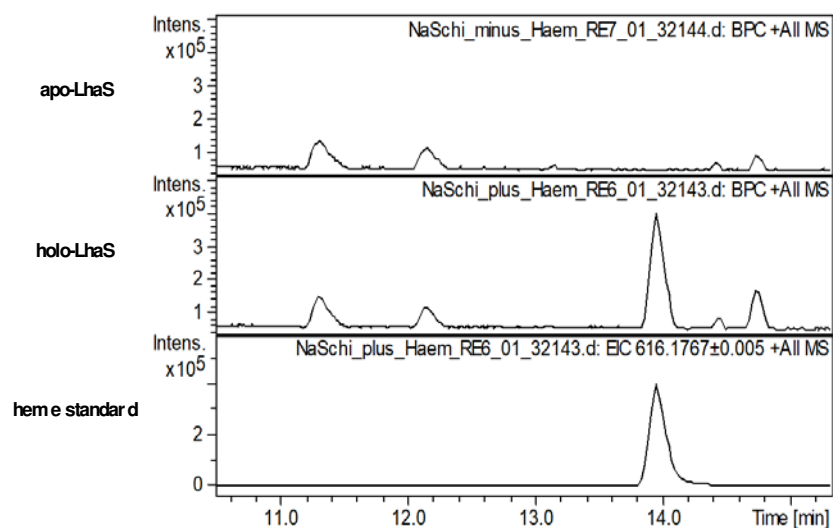


Figure 2 – figure supplement 1. High resolution mass spectra of apo- and holo-LhaS.

Spectra of apo-LhaS isolated from *E.coli* grown in RPMI medium (upper panel), holo-LhaS isolated from LB-medium (middle panel) and a heme standard (lower panel) were recorded on a HPLC-UV-HR mass spectrometer. The samples were diluted with MilliQ- H_2O and applied to a Dionex Ultimate 3000 HPLC system that is coupled to the MaXis 4G ESI-QTOF mass spectrometer.

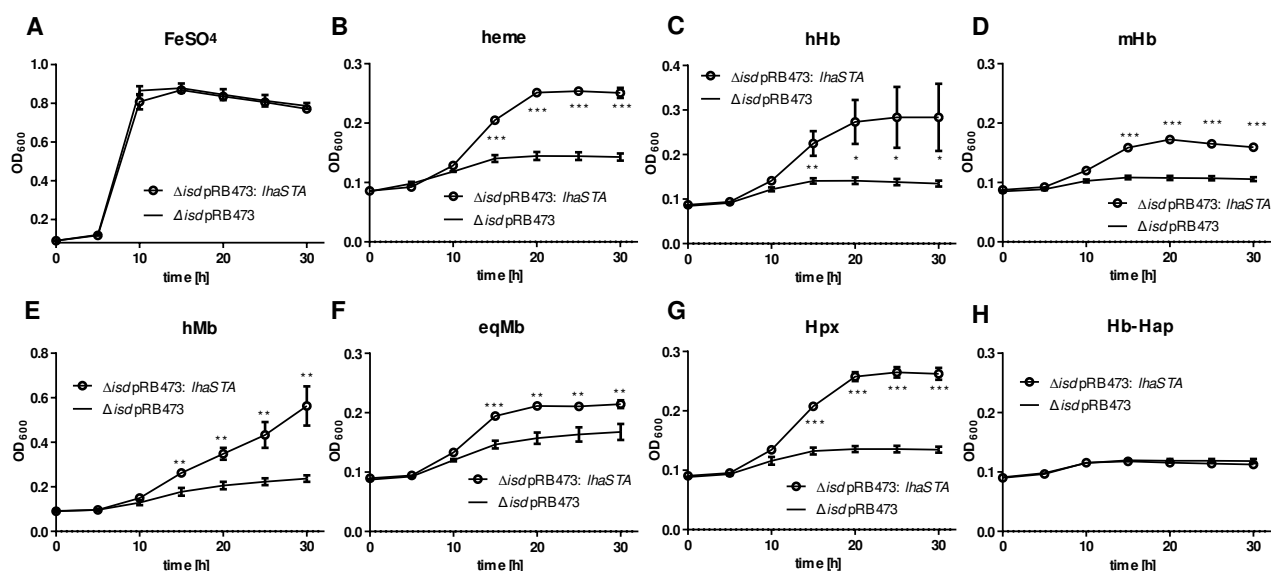


Figure 4 – figure supplement 1. Growth of *S. lugdunensis* N940135 Δ isd pRB473 and Δ isd pRB473:lhaSTA. The indicated strains were grown in the presence of 20 μ M FeSO₄ or 2.5 μ g/ml human hemoglobin (hHb), 2.5 μ g/ml or murine hemoglobin (mHb) or 10 μ g/ml human myoglobin (hMb) or 10 μ g/ml equine myoglobin (eqMb) or 200 nM human hemopexin (Hpx) or 117 nM Hb-Hap as a sole source of iron. 500 μ l of cultures were inoculated to an OD₆₀₀ = 0,05 in 48 well plates and OD₆₀₀ was measured every 15 min. For reasons of clarity values taken every 5 hours are displayed. Mean and SD of three experiments are shown. Statistical analysis was performed using students unpaired t-test.

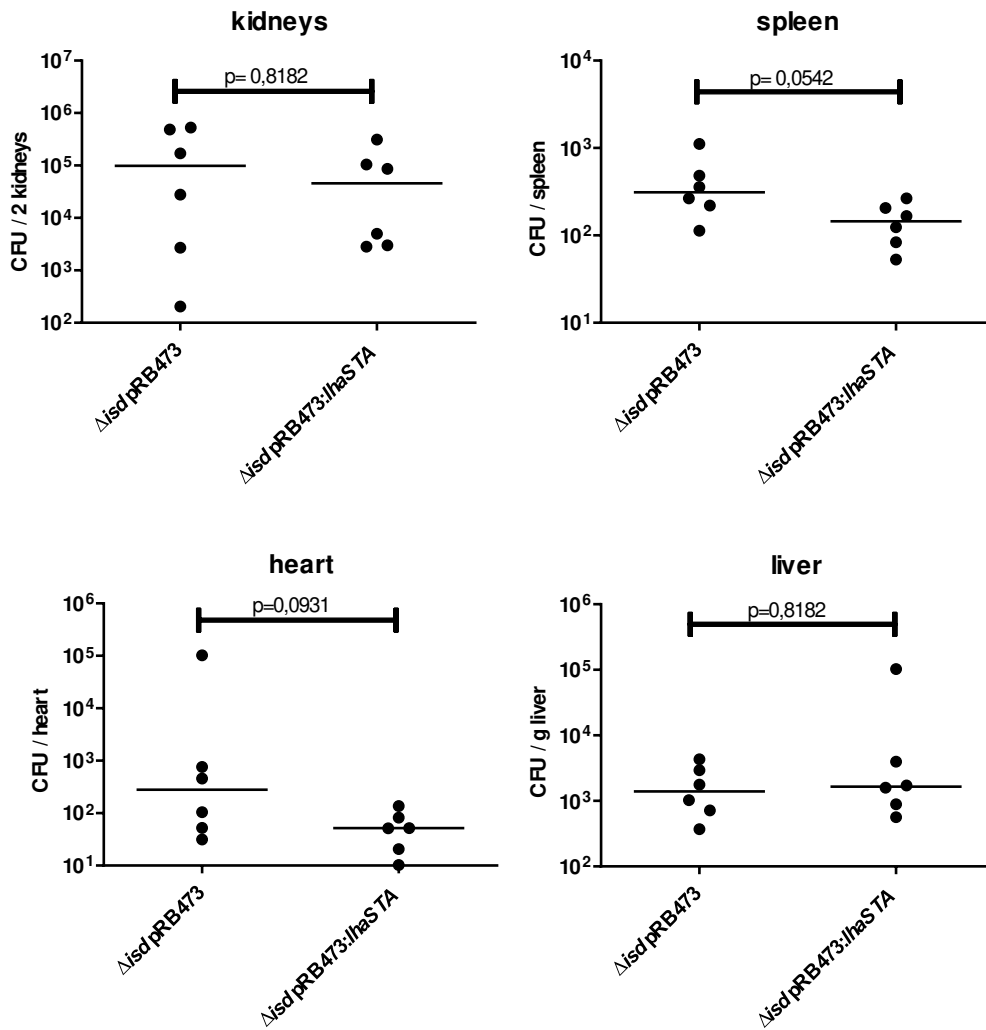


Figure 5 - figure supplement 1. Mouse systemic infection model.

C57BL/6 mice were infected either with 3×10^7 CFU per animal. Mice were sacrificed 72h post infection and CFUs within the indicated organs enumerated. Horizontal lines show the median. Statistical analysis was performed using Mann Whitney test.

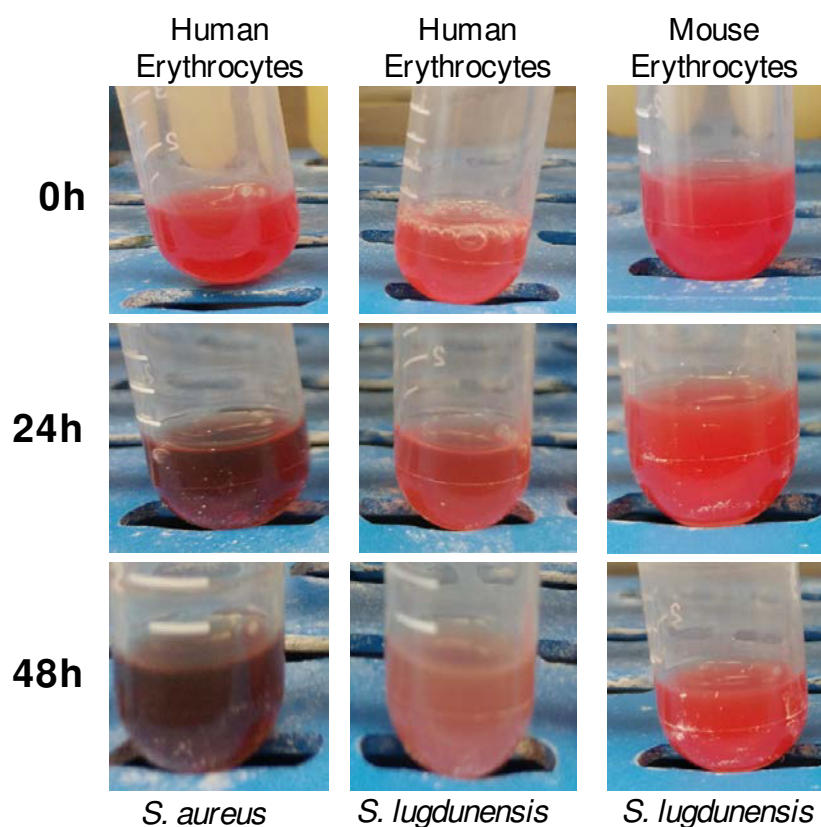


Figure 5 - figure supplement 2. Hemolysis of human and mouse erythrocytes.

Human (left and middle panels) or mouse erythrocytes (right panel) were incubated with the filtrated culture supernatants of *S. aureus* (left panel) or *S. lugdunensis* (middle and right panels) for 24 and 48 h.

Supplementary File 1. Key Resource Table PCR primers.

PCR and qPCR primers sequences used in this study.

| Key Resources Table | | | | |
|------------------------------------|-------------|---------------------|-------------|--|
| Reagent type (species) or resource | Designation | Source or reference | Identifiers | Additional information |
| Sequence based reagent | lhaSTA_A | This study | PCR primer | Deletion of the <i>lhaSTA</i> locus AGGGAACAAAAGCTGG GTACCGCAGGTGTATTA TTTTCTGATG |

| | | | | |
|------------------------|------------|------------|------------|--|
| Sequence based reagent | lhaSTA_B | This study | PCR primer | Deletion of the <i>lhaSTA</i> locus CATTTGTCACACTCCTT TAATG |
| Sequence based reagent | lhaSTA_C | This study | PCR primer | Deletion of the <i>lhaSTA</i> locus TTAAAGGAGTGTGACAA ATGTAAATAAATATTTAAA TAAGACG |
| Sequence based reagent | lhaSTA_D | This study | PCR primer | Deletion of the <i>lhaSTA</i> locus CTATAGGGCGAATTGGA GCTCCACCAAAGTAGT TCAACCTGC |
| Sequence based reagent | lhaSTA_ScF | This study | PCR primer | Screening of the <i>lhaSTA</i> deletion TTGTAGTTGTAGCTACT GTCTTG |
| Sequence based reagent | lhaSTA_ScR | This study | PCR primer | Screening of the <i>lhaSTA</i> deletion CACCTGTACCTGAATTA ACTACAG |
| Sequence based reagent | isdEFL_A | This study | PCR primer | Deletion of the <i>IsdEFL</i> locus AGGGAACAAAAGCTGG GTACCGAAAAACGTAAC AAAGATAAAC |

| | | | | |
|------------------------|---------------|------------|------------|--|
| Sequence based reagent | isdEFL_B | This study | PCR primer | Deletion of the <i>IsdEFL</i> locus CATTTTGTTACTCACCG CTTTC |
| Sequence based reagent | isdEFL_C | This study | PCR primer | Deletion of the <i>IsdEFL</i> locus GCGGTGAGTAACAAAAT GTGAAATTAGTGCTTCG ATTATG |
| Sequence based reagent | isdEFL_D | This study | PCR primer | Deletion of the <i>IsdEFL</i> locus CTATAGGGCGAATTGGA GCTCGATATTTTGTATC GAATTGAATGC |
| Sequence based reagent | isdEFL_ScF | This study | PCR primer | Screening of the <i>IsdEFL</i> deletion GCTAGGTGTAAACATC CAAATG |
| Sequence based reagent | isdEFL_ScR | This study | PCR primer | Screening of the <i>IsdEFL</i> deletion CTTTCGTCGTTGTTTGA TAAGC |
| Sequence based reagent | qPCR 5srRNA_F | This study | PCR primer | RT-qPCR quantification of <i>5srRNA</i> expression GCAAGGAGGTACACC TGTT |

| | | | | |
|------------------------|----------------------|------------|------------|---|
| Sequence based reagent | qPCR 5srRNAR_R | This study | PCR primer | RT-qPCR quantification of <i>5srRNA</i> expression GCCTGGCAACGTCCTA CTCT |
| Sequence based reagent | qPCR lhaS_F | This study | PCR primer | RT-qPCR quantification of <i>lhaS</i> expression |
| Sequence based reagent | qPCR lhaS_R | This study | PCR primer | RT-qPCR quantification of <i>lhaS</i> expression |
| Sequence based reagent | qPCR lhaA_F | This study | PCR primer | RT-qPCR quantification of <i>lhaA</i> expression AGCATTATCTGGTGGGC AAC |
| Sequence based reagent | qPCR lhaA_R | This study | PCR primer | RT-qPCR quantification of <i>lhaA</i> expression TTCATCCGTACAAGCCA TCA |
| Sequence based reagent | lhaS_F | This study | PCR primer | His-tagged expression of LhaS using pQE30 ATTAAAGGAGCATGCCA AATGAAGAGAC |
| Sequence based reagent | lhaS_R | This study | PCR primer | His tagged expression of LhaS using pQE30 ACCTAAGCTTTTAAATC ATACCTGCACGT |
| Sequence based reagent | Lha complement- F | This study | PCR primer | Expression of LhaSTA using pRB473 |

| | | | | |
|------------------------|------------------|------------|------------|--|
| | | | | CGTATTGAAGGATCCTG ATTTGG |
| Sequence based reagent | Lha complement-R | This study | PCR primer | Expression of LhaSTA using pRB473 CTCAACAGAAAAGTGG ATTCGTCTTATTTAAGC TTTATTTA |

Chapter 3

Methionine limitation impairs pathogen expansion and biofilm formation capacity

Authors

Jochim A¹, Shi T², Belikova D¹, Schwarz, S³, Peschel A^{1,4} and Heilbronner S^{1,4}

1 – Interfaculty Institute of Microbiology and Infection Medicine, Department of Infection Biology, University of Tübingen, Tübingen, Germany

2 – Roche Innovation Center Basel, Switzerland

3 – Interfaculty Institute of Microbiology and Infection Medicine, Department of Medical Microbiology and Hygiene, University of Tübingen, Tübingen, Germany

4 – German Centre for Infection Research (DZIF), Partner Site Tübingen, Tübingen, Germany

Abstract

Multi-drug resistant bacterial pathogens are becoming increasingly prevalent and novel strategies to treat bacterial infections caused by these organisms are desperately needed. Bacterial central metabolism is crucial for catabolic processes and provides precursors for anabolic pathways such as the biosynthesis of essential biomolecules like amino acids or vitamins. However, most essential pathways are not regarded as good targets for antibiotic therapy since their products might be acquired from the environment. This raises doubts about the essentiality of such targets during infection. A putative target in bacterial anabolism is the methionine biosynthesis pathway. In contrast to humans, almost all bacteria encode methionine biosynthesis pathways which have often been suggested as putative targets for novel anti-infectives. While the growth of methionine auxotrophic strains can be stimulated by exogenous methionine, the extracellular concentrations required by most bacterial species are unknown. Furthermore, several phenotypic characteristics of methionine auxotrophs are only partly reversed by exogenous methionine. We investigated methionine auxotrophic mutants of *Staphylococcus aureus*, *Pseudomonas aeruginosa*

and *Escherichia coli* (all differing in methionine biosynthesis enzymes) and found that each needed concentrations of exogenous methionine far exceeding that reported for human serum (~30 μM). Accordingly, these methionine auxotrophs showed a reduced ability to proliferate in human serum. Additionally, *S. aureus* and *P. aeruginosa* methionine auxotrophs were significantly impaired in their ability to form and maintain biofilms. Altogether, our data show intrinsic defects of methionine auxotrophs. This suggests that the pathway should be considered for further studies validating the therapeutic potential of inhibitors.

Importance

New antibiotics that attack novel targets are needed to circumvent widespread resistance to conventional drugs. Bacterial anabolic pathways such as the enzymes for biosynthesis of the essential amino acid methionine have been proposed as potential targets. However, the eligibility of enzymes in these pathways as drug targets is unclear because metabolites might be acquired from the environment to overcome inhibition. We investigated the nutritional needs of methionine auxotrophs of the pathogens *S. aureus*, *P. aeruginosa* and *E. coli*. We found that each auxotrophic strain retained a growth disadvantage at methionine concentrations mimicking those available *in vivo* and showed that biofilm biomass was strongly influenced by endogenous methionine biosynthesis. Our experiments suggest that inhibition of the methionine biosynthesis pathway has deleterious effects even in the presence of external methionine. Therefore, additional efforts to validate the effects of methionine biosynthesis inhibitors *in vivo* are warranted.

Introduction

The increasing prevalence of multi-drug resistant (MDR) bacterial pathogens and the limited efficacy of available antibiotics create an urgency for the development of alternative antimicrobial agents (1, 2). In particular, the ESCAPE-pathogens (*Enterococcus faecium*, *Staphylococcus aureus*, *Clostridium difficile*, *Acinetobacter baumannii*, *Pseudomonas aeruginosa*, and *Enterobacteriaceae*) are of increasing prevalence in clinical practice (3).

Staphylococcus aureus is a major cause of healthcare-associated infections leading to severe morbidity and mortality along with tremendous costs for healthcare systems (4). Methicillin-resistant *S. aureus* (MRSA) are resistant to most β -

lactam antibiotics and cause a substantial proportion of staphylococcal infections in hospitals and, in the USA and Asia, increasingly in the community. Antibiotics of last resort against MRSA such as vancomycin and daptomycin are much less effective than β -lactams. Only a few anti-MRSA drugs are in development pipelines but most of them do not have the right characteristics to solve the MRSA problem (5). Thus, MRSA will remain a pressing problem if no better preventive and therapeutic options become available. In addition, certain types of staphylococcal infections are particularly difficult to treat. This is the case for infections associated with artificial implants such as hip and knee joint replacements or artificial heart valves. Device-associated biofilms are largely insensitive to antibiotics and host defence factors (6). Infected implants usually have to be replaced. This leads to an enormous burden for patients and extra costs for health-care systems. *Pseudomonas aeruginosa* forms biofilms within the lungs of cystic fibrosis patients (7, 8) and within lung ventilators of intensive care patients (9-11). *E. coli* is another important ESCAPE pathogen. About 20% of all bacteraemia cases in the UK are caused by *E. coli* (12). The sharp increase in frequency of isolation of MDR ESCAPE pathogens including those expressing extended spectrum β -lactamases seems to be diminished by more careful use of antibiotics (13). Nonetheless, novel routes to treat MDR pathogens or to lower their pathogenic potential, for example by inhibiting biofilm formation, are needed.

The bacterial folate biosynthesis inhibitor trimethoprim combined with sulfamethoxazole is used to treat bacterial infections and the identification of additional targets in bacterial metabolic pathways has the potential for development of novel antibiotics (14). The methionine biosynthesis pathway is one, since it fulfils important criteria. Firstly, humans rely on exogenous methionine in their diet and no methionine biosynthesis pathway is encoded within the human genome. In contrast, almost all prokaryotes encode methionine biosynthesis pathways suggesting that inhibitors might have the potential to be broad-spectrum antibiotics. Secondly, methionine is crucial for bacterial protein biosynthesis and is required both for the initiation and elongation stages of translation. Finally, methionine limitation is expected to have broad impact on bacterial physiology since methionine is the precursor of the global methyl group donor S-adenosyl-L-methionine (SAM), which is required for DNA-methylation, protein-methylation, and polyamine biosynthesis.

A potential disadvantage of the methionine biosynthesis pathway as a drug target is the ability of bacteria to import exogenous methionine. The concentrations of

free methionine in different body fluids varies and might depend on the diet of the host. Human nasal secretions are devoid of methionine and a *S. aureus* methionine auxotroph is attenuated in an animal nasal colonization model (15). Human serum is reported to contain 25-48 μM methionine (16, 17). However, the concentrations of methionine required by different pathogens for optimal growth and virulence are mostly unknown.

The methionine biosynthesis pathways of many bacterial species are well characterized and are reviewed in detail elsewhere (18). The common precursor of methionine is homoserine, which is derived from aspartate. Biosynthesis of methionine occurs in three stages (Fig. 1).

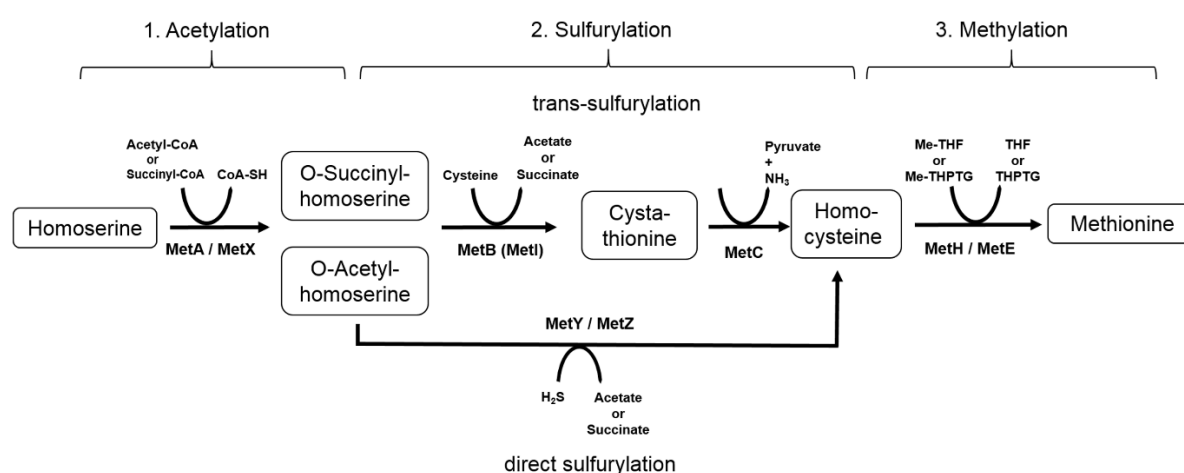


Figure 1 Schematic diagram of the bacterial methionine biosynthesis pathways

Me-THF - 5-methyl-tetrahydrofolat; Me-THPTG - 5-methyl-tetrahydropteroyl tri-L-glutamate

The first is the acetylation of homoserine. This reaction is performed by two protein families MetA and MetX that are unrelated both in amino acid sequence and protein structure. MetA-class enzymes can use either succinyl-CoA or acetyl-CoA to produce *O*-succinylhomoserine or *O*-acetylhomoserine, respectively. In contrast, MetX-class enzymes seem to use exclusively acetyl-CoA to produce *O*-acetylhomoserine. The second step is the sulfurylation of acylhomoserine to form the intermediate homocysteine. Sulfurylation reactions involved in methionine biosynthesis are more diverse than acetylation reactions, yet two types are most prominent. One pathway (called trans-sulfurylation) is a two-step reaction using cysteine as a sulfur donor. In this pathway, cystathionine- γ -synthases (MetB/MetI) incorporate cysteine to form the intermediated cystathionine. In a second step cystathionine- γ -lyases (MetC) create homocysteine. The second prominent type of sulfurylation (direct sulfurylation) uses

hydrogen sulfide by MetY and MetZ-class enzymes, allowing the creation of homocysteine in a single step. The third step in methionine biosynthesis is the methylation of homocysteine. MetH and MetE-class enzymes use the methyl group donors' 5-methyl-tetrahydrofolat (Me-THF) and 5-methyl-tetrahydropteroyl tri-L-glutamate (Me-THPTG), respectively, to form methionine from homocysteine.

It remains unclear whether bacteria that use different methionine biosynthesis pathways have different nutritional requirements and whether some steps of methionine biosynthesis represent more promising targets than others. Answering such questions is important if methionine biosynthesis is to be considered as a target for antibiotic development.

Results

Methionine auxotrophs need high concentrations of free methionine to overcome growth defects.

We chose three different model organisms, *E. coli*, *S. aureus*, and *P. aeruginosa*, for analysis of physiological effects associated with a lack of methionine biosynthesis. Each use distinct methionine biosynthesis pathways and enzyme classes to perform the reactions (Tab.1). *E. coli* performs the acetylation step using succinyl-CoA and a MetA-class enzyme. In contrast, *S. aureus* and *P. aeruginosa* use acetyl-CoA and a MetX-class enzyme. *E. coli* and *S. aureus* employ the trans-sulfurylation pathway to create homocysteine, while *P. aeruginosa* relies on the direct sulfurylation pathway. Finally, all model organisms perform the methylation of homocysteine using MetE and MetH-class enzymes.

Table 1 Methionine biosynthesis pathways of model organisms

| | <i>E. coli</i> | <i>S. aureus</i> | <i>P. aeruginosa</i> |
|--------------------------------|----------------------|--------------------|----------------------|
| 1. Acetylation | | | |
| - Co-Factor | Succinyl-CoA | Acetyl-CoA | Acetyl-CoA |
| - Product | O-Succinylhomoserine | O-Acetylhomoserine | O-Acetylhomoserine |
| - Encoded enzymes | MetA | MetX | MetX |
| 2A. Trans-sulfurylation | | | Not encoded |

| | | | |
|--|--------------------|--------------------|--------------------|
| - Encoded enzymes | MetB + MetC | MetI + MetC | |
| 2B. Direct sulfurylation - Encoded enzymes | Not encoded | Not encoded | MetY / MetZ |
| 3. Methylation - Encoded enzymes | MetE / MetH | MetE / MetH | MetE / MetH |

Isogenic mutants defective in key enzymes of the methionine biosynthesis pathways in each organism were obtained. Marker less deletion mutants in *S. aureus* (strains Newman, SH1000, USA300 LAC) were created by allelic replacement. Transposon insertion mutants of *P. aeruginosa* PA14 as well as *E. coli* BW25113 strains with *met* genes replaced by a kanamycin marker were acquired from mutant libraries (<https://cgsc2.biology.yale.edu/>, <http://pa14.mgh.harvard.edu/cgi-bin/pa14/home.cgi>). Each organism encodes the two redundant enzyme classes MetE and MetH. Mutants defective in either one alone would not be expected to be auxotrophic for methionine. Indeed *P. aeruginosa* mutants deficient in either MetE or MetH showed wildtype (WT) levels of growth yield in methionine-dependent growth assays (Fig. S1). Therefore, we focused on the other steps of the pathway.

All mutant strains grew in a similar fashion to the parental stain when cultivated in complex medium (data not shown) but were unable to grow when inoculated into defined medium without methionine, confirming methionine-auxotrophic phenotypes (Fig. 2). Only *E. coli* BW25113 $\Delta metC$ showed slow growth in the absence of methionine and reached an OD of ~ 0.5 after 50 h of incubation (Fig. S2). However, in our standard experiments (~12-15 h of growth) the increase in optical density was hardly detectable. Furthermore, the results showed that the *metY* gene of *P. aeruginosa* was dispensable, while *metZ* was essential for proliferation without external methionine. This was unexpected since both enzymes are supposedly able to perform the direct sulfurization reaction.

All of the mutants needed high amounts of methionine to reach the same density as the WT. Mutants of *S. aureus* strain Newman, USA300 LAC and SH1000 needed a concentration of 50-100 μ M methionine to overcome auxotrophy (Fig.2, Fig. S3). In contrast, *E. coli* and *P. aeruginosa* needed even higher concentrations (100-200 μ M). Furthermore, we observed that growth yields of *S. aureus* Newman and *P. aeruginosa* PA14 wild-type strains did not increase when additional methionine was available. This

suggests that autotrophic strains are actively synthesizing endogenous methionine rather than acquiring it from exogenous sources.

The individual methionine auxotrophs of each species showed very similar phenotypic characteristics. This makes unlikely that secondary site mutations or polar effects might be associated with mutagenesis. However, we thought to confirm this in one model organism and complemented the *E. coli* $\Delta metA$ strain by expression of the *metA* gene from the IPTG inducible vector pME6032. This abolished the observed differences in final bacterial density (Fig S4).

These experiments indicate that blockage of methionine biosynthesis cannot be easily overcome by using environmentally available methionine and that auxotrophic strains have growth disadvantages at concentrations reported to be available in human serum (25-48 μM).

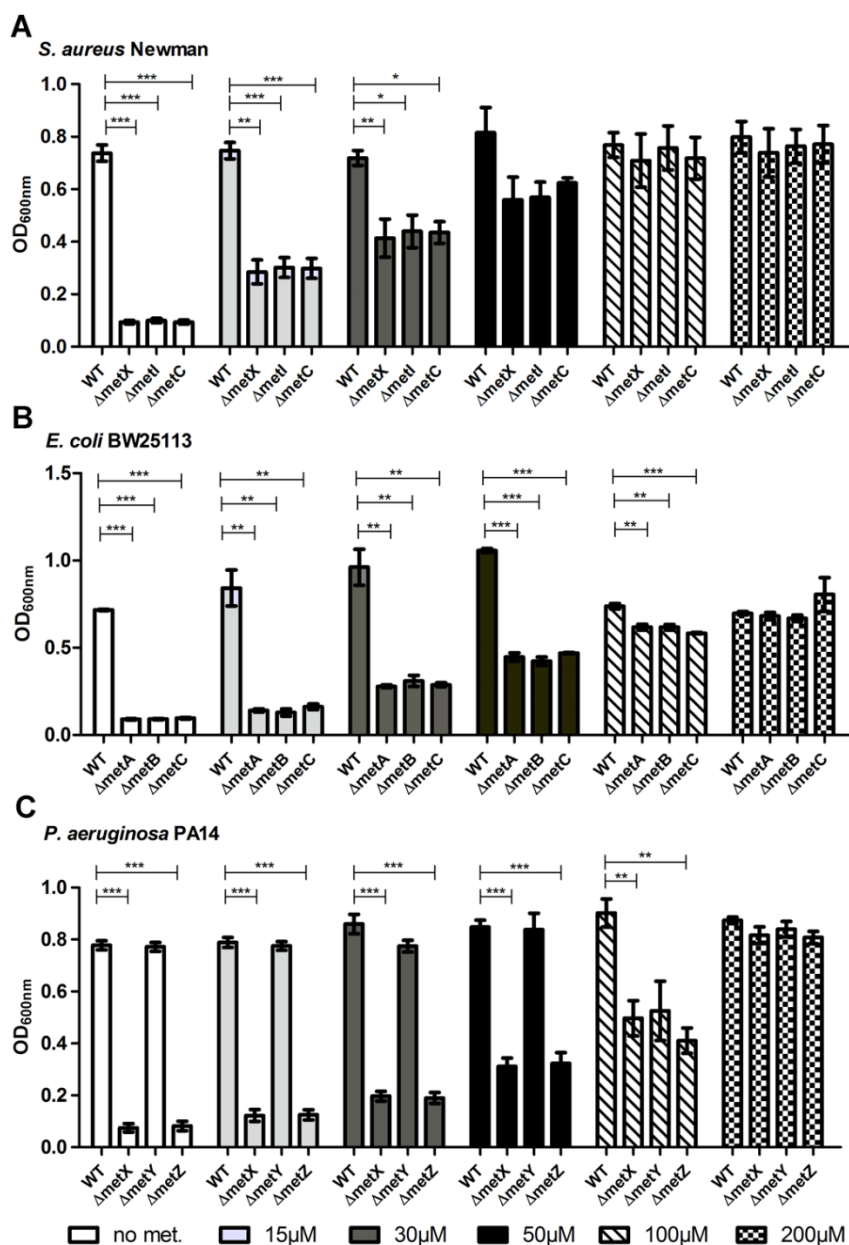


Figure 2 Growth of model organisms with defined amounts of methionine

In a 48-well microtiter plate, defined medium (SNM20 for *S. aureus* / M9 for *E. coli* and *P. aeruginosa*) was inoculated and supplemented with increasing concentrations of methionine. OD₆₀₀ was monitored over 48 h of growth. Optical densities when strains entered the stationary phase are shown. The mean and SEM of three independent experiments is shown. Statistical analysis was performed using Student's unpaired t-test. *, p<0.05; **, p<0.005; ***, p<0.001.

Human serum contains an insufficient source of methionine

Addition of 30 μM of methionine to defined medium was insufficient to restore a WT phenotype to methionine auxotrophs of all three organisms. However, it remained

unclear whether this finding would apply *in vivo* as human serum is a complex mixture of free amino acids, proteins, and peptides that might be used as a source of methionine by invading microorganisms. Therefore, we investigated the potential of heat inactivated pooled human serum to permit growth of methionine auxotrophic mutants. For each species we choose a representative mutant defective in the first step of methionine biosynthesis (acetylation). Therefore, all methionine precursors downstream of the acetylation reaction (compare Fig. 1) should be able to serve to bypass the blockage. Since all strains grew poorly in pooled human serum (data not shown) we supplemented human serum with methionine-free defined medium and compared the number of colony forming units after 24 h of incubation. As shown in Fig. 3, the mutants retained a distinct growth disadvantage over the entire range of serum concentrations tested and even 50% pooled human serum did not allow to reach WT levels of growth yield.

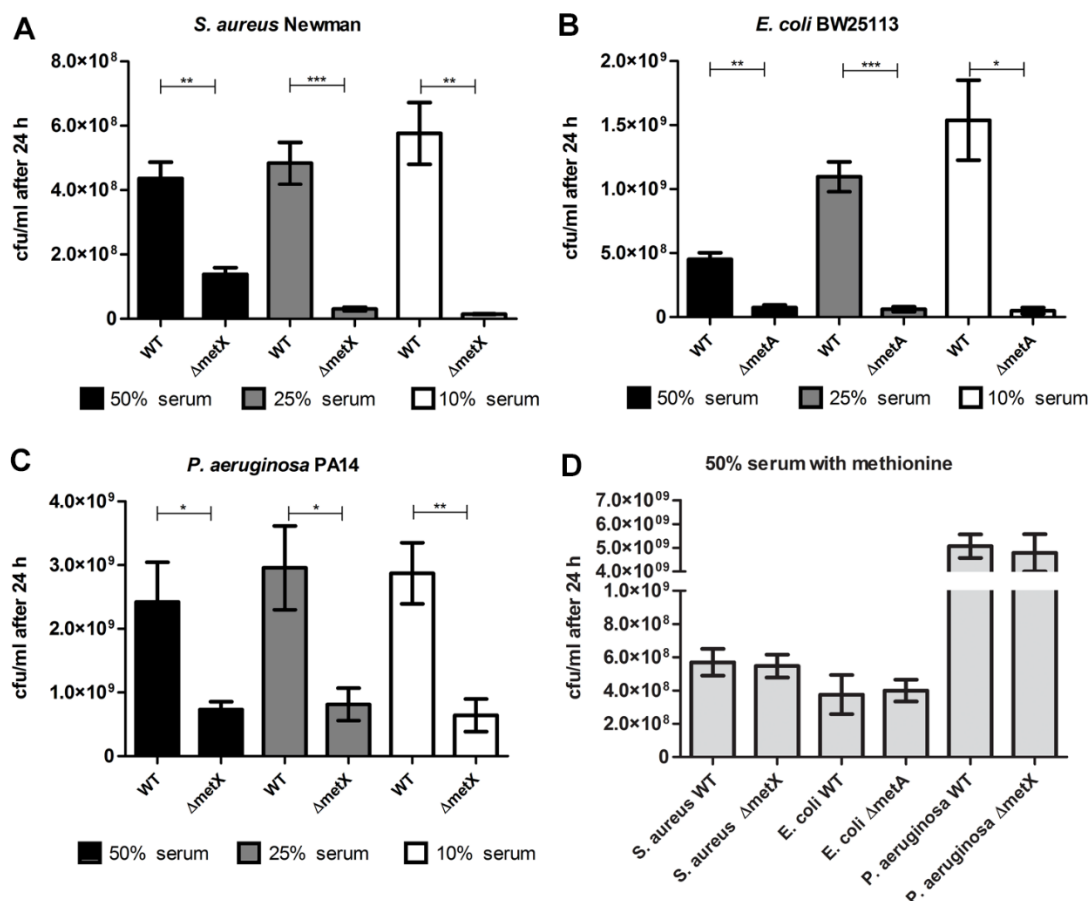


Figure 3 Growth yields of model organisms with pooled human serum as a source of methionine

A, B, C: Pooled human serum was diluted with defined medium (SNM20 for *S. aureus* / M9 for *E. coli* and *P. aeruginosa*) and inoculated to 5×10^6 CFU/ml. CFUs were enumerated after 24 h of growth.

D: Pooled human serum was diluted with defined medium (SNM20 for *S. aureus* / M9 for *E. coli* and *P. aeruginosa*) and supplemented with 30 μ M methionine (*S. aureus*) or 100 μ M methionine (*E. coli* and *P. aeruginosa*). The serum was inoculated to 5×10^6 CFU/ml. CFUs were enumerated after 24 h of incubation.

Shown are the mean and SEM of at least three independent experiments. Statistical analysis was performed using Student's unpaired t-test. *, $p < 0.05$; **, $p < 0.005$; ***, $p < 0.001$.

Importantly the addition of free methionine to human serum abolished the differences between the WT and mutant strains (Fig. 3D), indicating that methionine limitation was responsible for the observed defects.

These data indicate that the combined sources of methionine present in human serum are insufficient to restore a WT phenotype in mutant strains, suggesting that methionine biosynthesis might be a valid target for new antimicrobials.

Methionine auxotrophy reduces protein-dependent biofilm formation by staphylococci

Both, staphylococci, and pseudomonads form clinically relevant biofilm, for instance in catheter and joint-replacement associated infections (19). *S. aureus* SH1000 biofilm relies predominantly on proteins (20). Therefore, we speculated that the capacity to form biofilm might depend on the ability to synthesize methionine and investigated this using the methionine biosynthesis inhibitor propargylglycin (PG). PG specifically inhibits cystathionine- γ -synthase (21) which is well conserved among staphylococcal species. Indeed, in the absence of free methionine, PG reduced the growth yields of *S. aureus* SH1000 (Fig. 4A). PG concentrations reducing growth yields only partially had profound effects on biofilm formation of the strain (Fig 4A/B). To exclude that this effect reflected the decreased final growth yields in the presence of PG, we analysed the protein levels in the cell wall of SH1000. Cell wall-anchored proteins such as the fibronectin-binding proteins (22) or SasG (23) are associated with biofilm formation in different staphylococcal lineages. Therefore, we assumed that cell wall-associated proteins might also contribute to biofilm formation under our experimental conditions. We investigated this using cell wall-extracts of SH1000 grown under methionine limiting conditions in the presence or absence of PG. The extracts

were analysed by infra-red quantification of proteins separated by SDS-PAGE and stained with Coomassie Blue. PG treatment led to a decrease in cell wall-protein content (Fig 4C), supporting the idea that reduced protein amounts in the cell wall decreased the capacity to form proteinaceous biofilms.

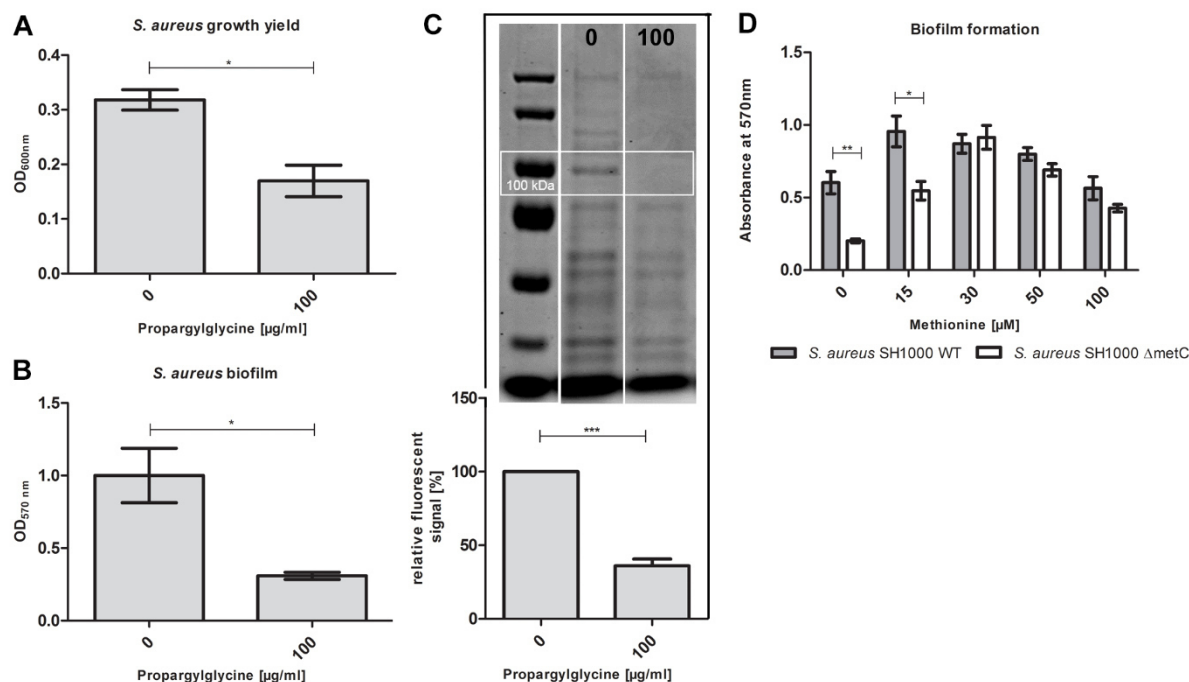


Figure 4 Impact of PG on proteinaceous biofilms formed by *S. aureus* SH1000

A: Growth inhibition by PG: In 96 well plates, *S. aureus* SH1000 was allowed to form biofilm in SNM3 with or without 100 $\mu\text{g/ml}$ PG for 24 h. OD₆₀₀ was quantified prior to biofilm staining. Values represent the mean and SEM of three independent experiments. Statistical analysis was performed using Student's unpaired t-test.

B: Inhibition of biofilm formation by PG: In 96 well plates, *S. aureus* SH1000 was allowed to form biofilm in SNM3 with or without 100 $\mu\text{g/ml}$ PG for 24 h. Biofilm was stained with crystal violet and the absorbance at 570 nm was measured.

Values represent the mean and SEM of three independent experiments. Statistical analysis was performed using Student's unpaired t-test.

C: Protein abundance within the *S. aureus* cell wall: *S. aureus* SH1000 was grown in SNM3 with or without 100 $\mu\text{g/ml}$ PG for 24 h. Cell wall extracts were isolated by digestion of the peptidoglycan in the presence of 0.5 M sucrose to protect protoplasts. Protoplasts were removed and cell wall extracts were analyzed by SDS-PAGE. Gels were stained with Coomassie Blue (a strong 700 nm fluorophore) and bands were quantified using infra-red fluorescent imaging. The upper picture shows a representative gel. The lower picture shows quantification of the prominent protein band indicated. The values represent mean and SEM

of four independent experiments. Statistical analysis was performed using Student's paired t-test.

D: Biofilm formation of *S. aureus* $\Delta metC$: In 96 well plates, *S. aureus* SH1000 was allowed to form biofilm in SNM3 containing different concentrations of methionine for 24 h. Biofilm was stained and quantified as in B. Values represent the mean and SEM of three independent experiments. Statistical analysis was performed using Student's unpaired t-test.

*****, $p < 0.05$; ******, $p < 0.005$; *******, $p < 0.001$.

We also created a $\Delta metC$ deletion mutant in the SH1000 background and tested the mutant for biofilm formation. Like the *S. aureus* Newman mutants described above, SH1000 $\Delta metC$ was auxotrophic for methionine and needed 50 μM methionine to reach the same growth yields as the WT (Fig S3). The auxotrophic mutant also showed a reduced biofilm formation and WT levels of biofilm were restored by the addition 30 – 50 μM methionine (Fig 4D)

Next, we investigated whether methionine limitation also effects the formation of polysaccharide dependent biofilms. *S. epidermidis* RP62A produces a biofilm dependent on the polysaccharide intracellular adhesion (PIA) (24). Similar to inhibition of SH1000, PG reduced growth yields of *S. epidermidis* RP62A in methionine deficient medium (Fig. 5A). However, the biomass of RP62A biofilms remained unaltered (Fig. 5B), suggesting that biosynthesis of the PIA matrix was not dependent on methionine biosynthesis. To validate this, we isolated the biofilm matrix of *S. epidermidis* RP62A grown in methionine deficient medium in the presence and absence of PG and assessed PIA semi quantitatively. Indeed, we found that the amount of PIA was not reduced by PG. In contrast, the amount of PIA seemed slightly increased in the presence of PG (Fig. 5C). Of note, no PIA was detected when an *icaA* deficient mutant was used, confirming the specificity of this assay (data not shown).

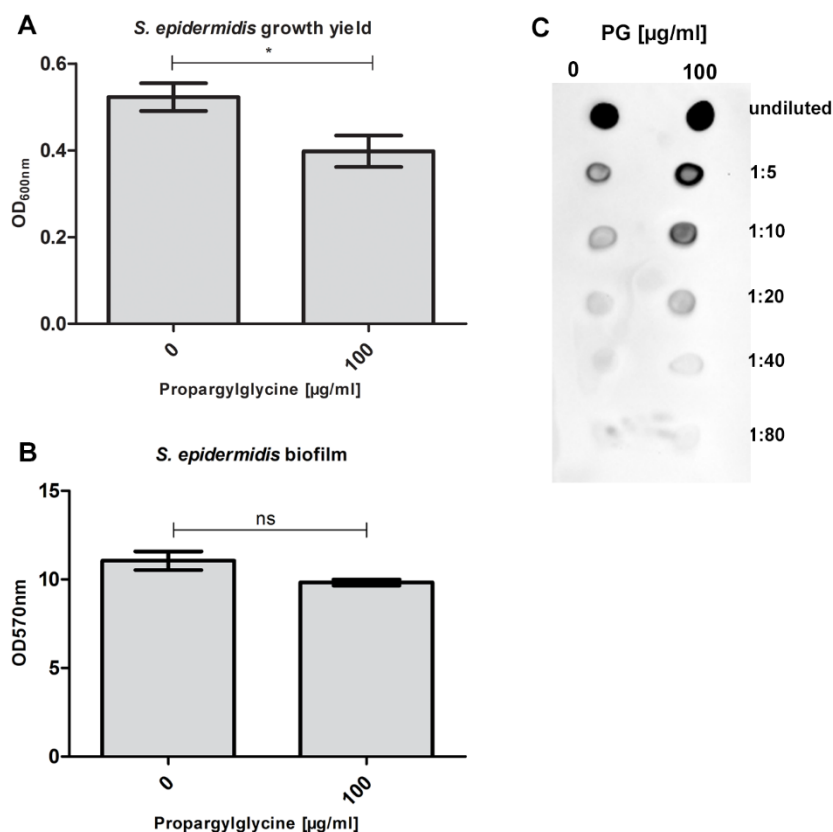


Figure 5 Impact of PG on polysaccharide biofilms formed by *S. epidermidis* RP62A

A: Growth inhibition by PG: In 96 well plates, *S. epidermidis* RP62A was allowed to form biofilm in methionine deficient mTMS with or without 100 $\mu\text{g/ml}$ PG for 24 h. OD₆₀₀ was quantified prior to biofilm straining.

B: Inhibition of biofilm formation by PG: In 96 well plates, *S. epidermidis* RP62A was allowed to form biofilm in methionine deficient mTMS with or without 100 $\mu\text{g/ml}$ PG for 24 h. Biofilm was stained with crystal violet and the absorbance at 570 nm was measured.

C: PIA in *S. epidermidis* biofilms: In 96 well plates, *S. epidermidis* RP62A was allowed to form biofilm in methionine deficient mTMS with or without 100 $\mu\text{g/ml}$ PG for 24 h. The biofilm matrix was isolated, serial dilutions were dotted on a nitrocellulose membrane and PIA was detected using wheat germ agglutinin coupled to horseradish peroxidase. The experiment was carried out three times with similar results.

Values represent the mean and SEM of three independent experiments. Statistical analysis was performed using Student's paired t-test. *, $p < 0.05$; **, $p < 0.005$; ***, $p < 0.001$.

In conclusion, these data indicate that in contrast to polysaccharide biofilms proteinaceous staphylococcal biofilm formation depends on the availability of sufficient amounts of methionine.

Methionine auxotrophy leads to the dispersal of *P. aeruginosa* biofilms

The capacity to form biofilms is key for *P. aeruginosa* to cause ventilator-associated pneumonia, catheter associated urinary tract infections and chronic lung infections in CF patients (9-11). Its biofilm consists of exopolysaccharides such as galactose and mannose-rich polysaccharide Psl (25) the glucose rich polysaccharide (Pel) (26) and alginate (27). In addition, extracellular DNA (eDNA) and proteins are present (28). Biofilm formation by the *P. aeruginosa* PA14 WT and the isogenic methionine auxotrophic mutants was compared. Defined medium was supplemented with 100 μ M methionine and biofilm formation was measured at the liquid/air-interface using the crystal violet microtiter plate method (29) which allows staining and quantification of biofilm mass comprising embedded cells and surrounding matrix. Only a minor difference in growth yield between the WT and the mutant strains was observed. (Fig. 6A). However, all mutants produced a significantly reduced biofilm mass under these conditions. Also, the *P. aeruginosa* $\Delta metY$ mutant which did not show any growth deficit compared to the parental strain, exhibited impaired biofilm formation (Fig. 6B).

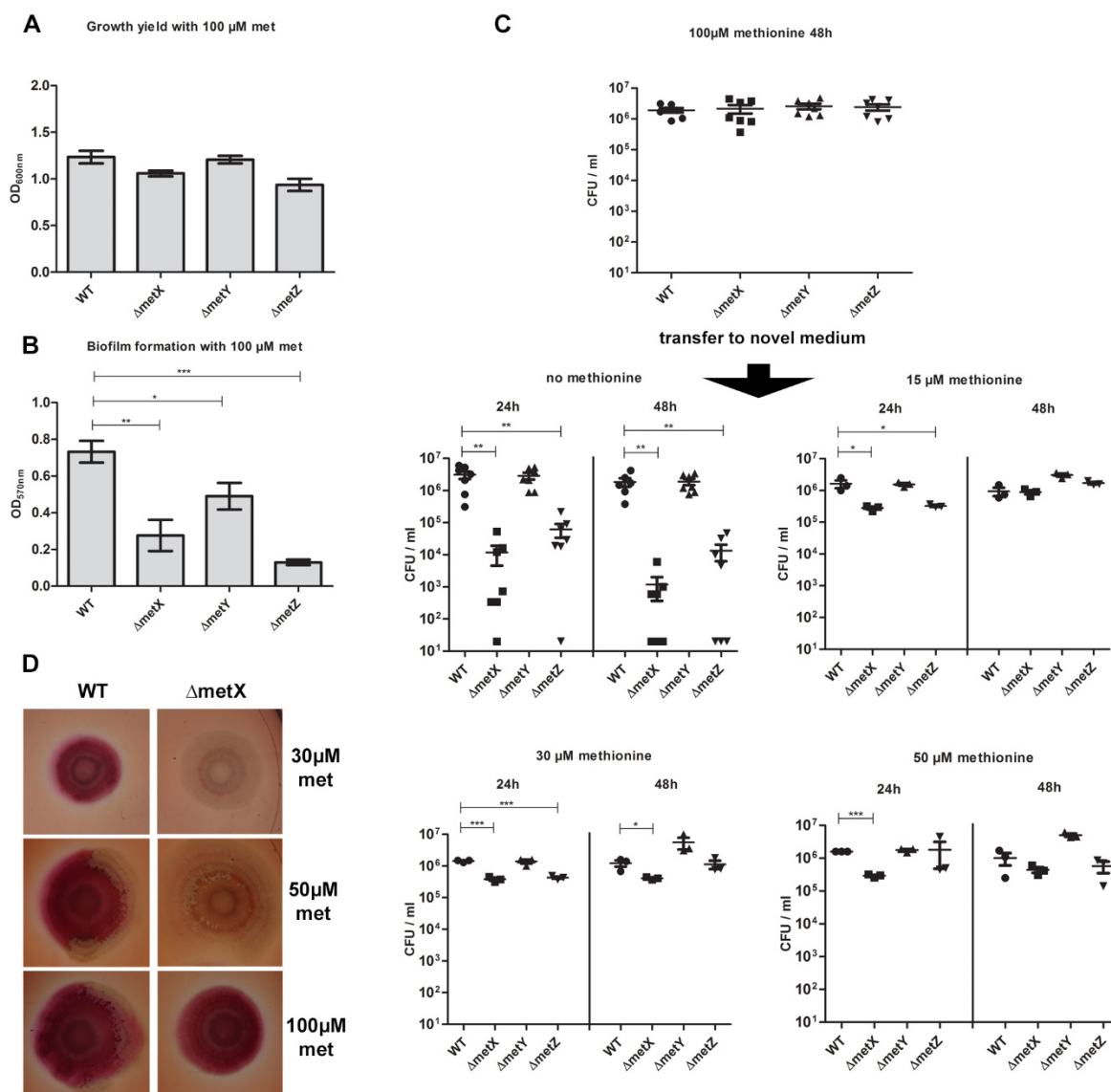


Figure 6 *Pseudomonas* biofilm formation and maintenance

A: Growth yields of *P. aeruginosa* under methionine limitation: Strains were cultivated for 24 h in 96 well plates containing M9 (100 μM methionine). OD_{600} was quantified prior to biofilm staining. Values represent the mean and SEM of triplicate wells. The experiment was carried out three times with similar results. Statistical analysis was performed using Student's unpaired t-test. *, $p < 0.05$; **, $p < 0.005$; ***, $p < 0.001$.

B: Biofilm formation by auxotrophic *P. aeruginosa* strains: Strains were cultivated for 24 h in 96 well plates containing M9 (100 μM methionine). Biofilm was stained with crystal violet and the absorbance at 570 nm was quantified. Values represent the mean and SEM of triplicate wells. The experiment was carried out three times with similar results. Statistical analysis was performed using Student's unpaired t-test. *, $p < 0.05$; **, $p < 0.005$; ***, $p < 0.001$.

C: Biofilm formation at the peg plates. *P. aeruginosa* biofilms were allowed to form on the lid of peg-plates in M9 medium containing 100 μM methionine. Biofilms were then transferred

to medium with various concentrations of methionine and incubated for an additional 24-48 h. Biofilms were disassociated at different time points and living cell counts were enumerated. CFU of at least three independent experiments are shown. Statistical analysis was performed using Student's unpaired t-test. * indicates $p < 0.05$, ** indicates $p < 0.005$, *** indicates $p < 0.001$

D: Congo red staining: *P. aeruginosa* strains were applied to M9 agar plates containing Congo red and various concentrations of methionine. Color of colonies was evaluated after 24h of incubation at 37 °C followed by 24h incubation on room temperature. The experiment was repeated thrice with similar results. A representative picture is shown.

Given the strong effects of methionine auxotrophy on *P. aeruginosa* biofilm formation, we asked whether this reflects differences in the production of the extracellular matrix or within the number of bacterial cells. To investigate this, the Calgary biofilm device was used consisting of a 96-well plate filled with defined medium and a lid containing pegs that reach into the medium (30). The biofilm formed on the pegs was dissociated to determine viable counts of bacteria located within the biofilm (31). In media containing 100 μM methionine, biofilms of methionine auxotrophs and the autotrophic parental strain harboured similar numbers of CFU (Fig 6C, upper panel), suggesting that differences between WT and mutants in the crystal violet assay were due to different quantities of extracellular matrix. This opened the question as to whether methionine biosynthesis is relevant for the initial formation of the biofilm or whether it is also important for biofilm growth and maintenance. To investigate this, *P. aeruginosa* biofilm was allowed to form on pegs in the presence of 100 μM methionine. After 48 h, the pegs were transferred to fresh medium containing different concentrations of methionine and incubated for 24 - 48 h after which CFU were enumerated. The WT and the ΔmetY mutant were able to maintain a constant number of CFUs over 48-96 h in medium lacking methionine. In contrast the viable counts of ΔmetX and ΔmetZ mutants decreased by 4-5 orders of magnitude in the same time frame. In half of the experiments, no viable bacteria were recovered from biofilms of the ΔmetX and ΔmetZ mutants (Fig. 6C). This effect was abolished when extracellular methionine (10 – 50 μM) was present in the medium. However, significantly fewer ΔmetX bacteria were recovered from the biofilm relative to the WT even in the presence of 30-50 μM methionine.

The biofilm matrix of *P. aeruginosa* PA14 binds Congo red giving WT strain colonies a distinct red colour in the presence of this dye. In contrast, Δpel mutants that are deficient in the carbohydrate processing Pel-proteins fail to stain with Congo red

(26). *P. aeruginosa* WT and the $\Delta metX$ mutants were grown on defined M9 agar plates containing 30-100 μ M methionine and Congo red. All strains formed comparable sized colonies. The PA14 WT strain showed an intense red colour on all concentrations of methionine indicating formation of a glycocalyx. In contrast, the colour of $\Delta metX$ colonies was dependent on the methionine concentration. The strain remained virtually colourless in presence of 30 to 50 μ M methionine, strongly resembling the reported phenotype of Pel-deficient mutants. This phenotype was reversed by increasing the concentration of methionine (Fig 6D).

These data suggest that the availability of sufficient levels of methionine is critical for both the development and maintenance of the biofilm, as well as for glycocalyx formation.

Discussion

Antibiotic resistant pathogens have become more and more prevalent. Especially members of the ESCAPE group such as *P. aeruginosa*, *E. coli*, *S. aureus*, *K. pneumonia* and *A. baumannii* are frequently highly resistant to multiple classes of antibiotics, making the development of alternative treatment strategies a pressing challenge (32). It has become more and more difficult to find new compounds active against the small number of known antibacterial targets and previous strategies for identification of new targets has had only limited success. Therefore, new routes for the identification of novel antibiotics or, as a first step, the identification of new targets are desperately needed. Such targets might exist within bacterial central metabolism or within biosynthetic pathways for essential biomolecules such as amino acids or vitamins. However, conventional antibiotic screening programs rely on the use of complex growth media. These contain an excess of essential nutrients, which may have to be synthesised endogenously during *in vivo* growth and infection. The methionine biosynthetic pathway represents an interesting target, as many aspects suggest it could be a valid target for novel anti-infectives (33, 34). However, whether the host can provide sufficient methionine to overcome auxotrophy is unclear.

Methionine auxotrophy and the regulation of methionine biosynthesis has been studied for decades (35-38) and important characteristics of auxotrophs are known. For auxotrophs of *E. coli*, the external methionine concentration governs the growth rate suggesting that this molecule is of central importance (39). Further it was reported that methionine limitation abolished chemotactic migration (40, 41). However,

knowledge regarding the roles of methionine and the phenotypic consequences of limitation in different species is incomplete.

S. aureus, *P. aeruginosa* and *E. coli* each differ in discrete steps in methionine biosynthesis and the enzyme classes employed. They represent the major pathways of methionine biosynthesis found among most bacterial pathogens. We found that methionine-auxotrophs of all three species needed higher levels of exogenous methionine than occur in human serum to reach WT levels of growth yield. The defect was most prominent in *E. coli* and *P. aeruginosa* where >100 μM methionine was needed. In contrast *S. aureus* needed 50-100 μM methionine to restore full growth. Human serum is reported to contain only between 25.6 and 48 μM methionine (16, 17, 42, 43). Such variations are most likely due to differences in the dietary intake. Additionally, diseases such as multiple sclerosis and liver failure are associated with increased levels of serum methionine (16, 44).

Pooled human serum was used to determine whether an average concentration of methionine in serum supports bacterial growth. In these experiments, we used mutants deficient in the first steps of methionine biosynthesis (acetylation) to allow any downstream intermediates such as acylhomoserine, cystathionine and homocysteine that might be available in human serum to serve as potential methionine precursors. A level of homocysteine in human serum of ~ 10.3 μM was measured (16), a concentration that needs to be considered in interpreting results. However, we found that human serum did not supply adequate methionine as it did not allow to overcome the growth disadvantage associated with methionine auxotrophy in any of the organisms tested. This observation correlates with the finding that methionine auxotrophs of *Salmonella enterica* serovar Typhimurium and of the fungus *Cryptococcus neoformans* are attenuated during invasive disease (45, 46). Interestingly, bronchoalveolar fluid (47) was found to be devoid of methionine and accordingly transposon insertion sequencing identified methionine biosynthesis as important during lung infection by *K. pneumoniae* (48) and *A. baumannii* (49). Also, human nasal secretions are devoid of methionine and *S. aureus* methionine auxotrophs are attenuated in the cotton rat model of nasal colonization (15).

As such methionine biosynthesis inhibitors might hold the potential to treat nasal colonisation of methicillin resistant *S. aureus* or to treat systemic infections. Several inhibitors of the individual steps of methionine biosynthesis are known. The clavams (50) and microcin 15m (51) inhibit acetylation reactions while propargylglycin and

several other inhibitors of the sulfurylation reaction are available (52, 53). Yet, to our knowledge, none of these inhibitors has been tested for toxic effects on eukaryotic cells, or for the potential to eliminate infections caused by MDR pathogens. The potential value of inhibiting the anabolic processes should not be underestimated. For instance, trimethoprim and sulfamethoxazole inhibit the biosynthesis of folate and are used for decades to treat bacterial infection.

The failure to produce methionine endogenously also impacts bacterial phenotypes that are not directly associated with the growth rate. Formyl-methionine is used by all bacteria for the initiation on translation. Furthermore, polypeptide elongation needs additional methionine if the mRNA possesses methionine codons. Methionine limitation will therefore reduce the translation rate and most likely reduce the amount of protein synthesised. Many bacterial species produce biofilms where bacterial cells are embedded in an extracellular matrix consisting of polysaccharides, extracellular DNA, and in many cases vast amounts of secreted and cell surface-associated proteins (6). Staphylococci classically produce two forms of biofilm. The first form is produced by *S. epidermidis* and many methicillin sensitive *S. aureus* strains and depends on the polysaccharide PIA (54). However, proteins are still important for the formation of the biofilm as they allow the primary attachment to surfaces and the accumulation of cells (i.e. the accumulation-associated protein Aap (55)). Most MRSA strains produce proteinaceous biofilms that are independent of polysaccharides while proteins allow the crosslinking of cells and allow formation of the extracellular matrix (i.e. the fibronectin-binding proteins FnbpA/B (22), the extracellular matrix binding protein Embp (56), the biofilm associated protein Bap (57)). We found that inhibition of methionine biosynthesis by PG impacted biofilm formation of *S. aureus* SH1000 a strain known to form proteinaceous biofilms. In contrast, PG had no impact on the biofilm formed by *S. epidermidis* RP62a, which forms a PIA-dependent biofilm. These experiments suggest that PG-mediated methionine limitation reduces the amount of produced and secreted proteins thereby reducing the biofilm quantity. Indeed, we discovered that the abundance of cell wall-associated proteins decreased after PG treatment of *S. aureus*, while the amount of PIA produced by *S. epidermidis* was not.

P. aeruginosa produces a biofilm that consist of various exopolysaccharides as well as of eDNA and proteins (28). We found that methionine limitation had a profound impact on biofilm formation of *P. aeruginosa*. Even with 200 μ M exogenous methionine, the biofilm formed by the auxotrophic mutants showed a significantly

reduced biomass compared to the biofilm formed by the WT. Interestingly we found that the number of viable cells within the biofilms did not differ between the WT and the individual mutants. However, when the biofilms were transferred to methionine-deficient conditions the biofilms formed by the mutants dissolved over a period of two days leading to a rapid decrease of live bacterial numbers. The mechanisms underlying the dependence of *P. aeruginosa* biofilms on methionine availability have yet to be investigated. However, we hypothesize that membrane associated proteins responsible for the processing of polysaccharides might contribute to the effects observed in our models. Under methionine limiting conditions methionine auxotrophic strains failed to incorporate Congo red stain into the surface of colonies. This phenotype is a hallmark of Pel deficient strains that cannot process carbohydrates to form biofilms (26). We suggest that methionine limitation might reduce the abundance of Psl/Pel-proteins, thereby reducing biofilm production. However, this hypothesis needs further experimental evidence to be validated and other explanations are possible. For example, the 220 kDa protein CdrA has been described to bind to Psl polysaccharides and to tether them to the cell envelope of *P. aeruginosa*, thereby strengthening and reinforcing biofilm integrity (58). It seems possible that a lack of methionine leads to insufficient biosynthesis of CdrA or similar biofilm-scaffolding proteins thereby preventing appropriate biofilm formation or restructuring.

Our results show that promising antimicrobial effects can be achieved by targeting bacterial methionine biosynthesis *in vitro*. Not only proliferation but also biofilm formation is affected when endogenous methionine biosynthesis is prevented, suggesting this biosynthesis pathway as an interesting target for antibiotic intervention. However, whether methionine biosynthesis inhibitors do indeed hold therapeutic potential *in vivo* is still unclear and further experiments using methionine biosynthesis blockers to treat infections *in vivo* will be required to answer this question.

Material and Methods:

If not stated otherwise, materials were purchased from Sigma Aldrich.

Bacterial strains and growth conditions

All bacterial strains used in this study are listed in Table 2. If not specified otherwise, *S. aureus* strains were grown at 37 °C in tryptic soy broth (TSB) (Oxoid) or on tryptic soy agar (TSA). *E. coli* and *P. aeruginosa* strains were grown at 37°C in lysogeny broth (LB) or on lysogeny agar (LA) (Oxoid).

All liquid overnight cultures for the experiments described below were grown in 20 ml volumes in 100 ml flasks containing one baffle. Cultures were incubated at 37 °C with 140 rpm agitation in an Innova44 incubator (New Brunswick Scientific). CO₂ content was not controlled.

Creation of marker-less deletion mutants in *S. aureus*

Targeted mutagenesis of *S. aureus* was performed using the thermosensitive plasmid pIMAY and allelic exchange. The procedure is described in detail elsewhere (59). In brief, 500 bp DNA fragments upstream and downstream of the genes of interest were amplified by PCR (oligonucleotides are summarized in Tab. 3). A sequence overlap was integrated into the fragments to allow fusion and creating an ATG-TAA scar in the mutant allele. The 1 kb deletion fragments were created using spliced extension overlap PCR and cloned into pIMAY. The deletion plasmids were used to transform *S. aureus* target strains using standard procedure at 30 °C. Integration of the plasmid was selected at 37 °C and excision was promoted by growing the strains in liquid culture overnight at 30 °C. Loss of plasmid was selected on plates containing 1 µg/ml anhydrotetracyclin and sensitivity of strains towards chloramphenicol was confirmed. Strains carrying the mutant allele were identified by colony PCR.

Construction of pME6032:metA

The *metA* gene was amplified from the chromosome of *E. coli* BW25113 by PCR (Tab. 3). The PCR product was purified and treated with EcoRI and BglII. After purification the DNA fragment was cloned into pME3032 treated with the same endonucleases. The recombinant plasmid was used to transform *E. coli* XL1-blue using standard techniques. The plasmid was validated by Sanger sequencing and transferred to *E. coli* BW25113Δ*metA*.

Bacterial growth in methionine-limited media

For overnight cultivation, *S. aureus* was grown in synthetic nasal medium SNM3 (15) containing 30 μM methionine. *E. coli* and *P. aeruginosa* strains were grown in M9 medium containing 100 μM methionine. Cells were harvested by centrifugation (10 min 5000 x g), washed with PBS, and adjusted to an $\text{OD}_{600} = 1$. In a 48 well plate (Nunclon Delta Surface) 500 μl volumes of defined medium (SNM20 for *S. aureus* and M9 for *E. coli*, *P. aeruginosa*) containing different methionine concentrations were inoculated to an $\text{OD}_{600} = 0.01$. The plates were sealed with adhesive covers (EXCEL Scientific) and incubated at 37 °C in an Epoch2 microplate reader (BioTek) for 20 h while agitating (807 rpm). OD_{600} was measured every 15 min.

For complementation of *E. coli* ΔmetA the overnight cultures were grown and harvested as described above. For the growth assay in the microtiter plate, M9 medium without methionine was supplemented with 1 mM IPTG. The plate was incubated as described above.

Growth in human serum

For overnight cultivation, staphylococci were grown in synthetic nasal medium SNM3 (15) containing 30 μM methionine. *E. coli* and *P. aeruginosa* strains were grown in synthetic M9 medium containing 100 μM methionine. Cells were harvested by centrifugation (10 min 5000 x g), washed with PBS, and adjusted to an $\text{OD}_{600} = 0.1$. Heat-inactivated pooled human serum derived from healthy males (Sigma Aldrich) was diluted in either SNM20 or M9 media to a final concentration of 50%, 25%, or 10% and 200 μl volumes were transferred to a 96-well plate (Greiner). Each well was inoculated with 15 μl of cells ($\text{OD}_{600} = 0.1 \sim 5 \times 10^6$ CFU/ml final concentration), sealed with adhesive covers and incubated at 37 °C with shaking (140 rpm) for 24 h in an Innova44 incubator. To enumerate CFUs, samples were taken and serial dilutions were plated on TSB agar plates.

Crystal violet assay for quantification of bacterial biofilms

S. aureus was grown overnight in SNM3 (15) containing 30 μM methionine. *S. epidermidis* was grown in modified Tris Minimal Succinate (mTMS) medium containing 30 μM methionine. mTMS was prepared according to (60) with the exception that casamino acids were replaced with proteinogenic amino acids (A:990 μM ; R:660 μM ; C:66 μM ; E: 660 μM ; G:990 μM ; H:330 μM ; L:1980 μM ; K:990 μM ; F:990 μM ; P:990

μM ; S:792 μM ; T:1320 μM ; W:132 μM ; V:660 μM) and Ornithine-HCL (660 μM). After overnight growth, cells were harvested by centrifugation (10 min 5000 x g), adjusted to $\text{OD}_{600} = 1$ in SNM3/mTMS containing 1% glucose. This suspension was diluted 1:200 in SNM3/mTMS containing 1% glucose. For *S. aureus* experiments 96 well Nunclon Δ surface microtiter plates (Thermo Fischer) were coated overnight at 4 °C with 100 μl of 0.045 $\mu\text{g/ml}$ fibrinogen (Calbiochem), to increase biofilm formation. After three washes with PBS, 200 μl of the inoculated defined medium was added to the wells. For inhibition experiments, a final concentration of 100 $\mu\text{g/ml}$ propargylglycine was added. The plate was incubated statically for 24 h at 37 °C. The plates were washed thrice with PBS, stained with 100 μl of 2.3% crystal violet (Sigma Aldrich) and washed five times with 300 μl PBS. Retained color was extracted in 100 μl 5% acetic acid. OD_{570} was quantified using a CLARIOstar device (BMG LABTECH).

For *P. aeruginosa* biofilms bacteria were grown overnight in M9 medium containing 100 μM methionine. Overnight cultures were harvested, adjusted to $\text{OD}_{600} = 1$ in M9 (100 μM methionine) and used to inoculate (1:200) M9 with appropriate concentrations of methionine. 200 μl were transferred to 96-well plates and grown statically at 37 °C for 48 h. The 96-well plate was washed and stained with crystal violet as described above.

Isolation of *S. aureus* cell wall-extracts.

S. aureus was grown overnight in SNM3 containing 30 μM methionine. Cells were harvested by centrifugation (10 min 5000 x g) and washed with SNM3 without methionine. A 20 ml volume SNM3 was inoculated to an $\text{OD}_{600} = 0.1$ and PG (0-100 $\mu\text{g/ml}$) was added. The culture was incubated with agitation for 24 h. Cells were collected (10 min 5000 x g) and washed once with buffer WB (10 mM Tris-HCl pH 7, 10 mM MgCl). 1 ml WB was adjusted to an $\text{OD}_{600} = 2$. Cells were collected and resuspended in 1 ml digestion buffer (10 mM Tris-HCl pH 7, 10 mM MgCl, 500 mM sucrose, 0.3 mg/ml lysostaphin, 250 U/ml mutanolysin, 30 μl protease inhibitor cocktail (Roche– 1 complete mini tablet dissolved in 1 ml H₂O), 1 mM phenylmethanesulfonylfluoride (PMSF)) and incubated at 37 °C for 1 h. The protoplasts were removed by centrifugation (8000 x g for 10 min and 4 °C). The supernatant (containing the cell wall-fraction) was collected and 15 μl were used for SDS-PAGE analysis using standard techniques. 7.5 % SDS gels were stained with Coomassie Brilliant Blue G 250 (SERVA). As Coomassie Blue protein stain is a strong 700 nm fluorophore, protein

amount within individual bands was quantified using an Odyssey CLx device (LI-CORE) which allows detection and accurate quantification of fluorescent signals in the near infra-red spectrum.

Isolation of *S. epidermidis* biofilm matrix

A 10 ml bacterial culture (mTMS, 30 μ M methionine) was grown overnight in a 50 ml flask containing one baffle at 37 °C. Bacteria were harvested and washed once with PBS. 2.5 ml methionine free mTMS was inoculated to an OD₆₀₀ = 0.01 and 0 – 100 μ g/ml PG was added. 200 μ l volumes of the inoculated medium were dispersed to 12 wells of a 96-well plate (Nunclon Delta Surface). The plate was incubated at 37 °C for 24 h. The plate was incubated for 30 min in an ultrasonic bath (BANDELIN, SONOREX RK 100). The biofilm was scratched off the wells and centrifuged at 3000 x g for 10 min. The pellet was resuspended in 200 μ l of 0.1 M EDTA (pH = 8). The suspension was incubated for 30 min in an ultrasonic bath and centrifuged at 8000 x g for 10 min. The supernatant was used for immunoblot analysis. Serial dilutions were prepared and 5 μ l were spotted on a nitrocellulose membrane (LI-COR). The membrane was blocked for 20 min with blocking buffer (Thermo Scientific) and incubated for 20 min with 130 ng/ml wheat germ agglutinin coupled to horseradish peroxidase (Biotium). The blot was washed twice with TBST and once with TBS. Detection was carried out using the WesternSure PREMIUM Chemiluminescent Substrate (LI-COR) and the BIORAD ChemiDoc™ XRS imaging system.

Peg plate assay of biofilm formation and detachment of *P. aeruginosa* PA14

P. aeruginosa strains were grown overnight in M9 media with 100 μ M methionine. Overnight cultures were diluted to OD₆₀₀ = 0.1 in M9 (with 100 μ M methionine) and 200 μ l were transferred to a 96-well plate (Thermo Scientific) with a transferable 96-peg solid phase (TSP) plate on top (Thermo Scientific). The pegs of the TSP plate reached into the inoculated medium and allowed initial bacterial adhesion. The plates were incubated statically for 2 h at 37 °C. The TSP plate was transferred to a new 96-well plate filled with 200 μ l of sterile M9 medium containing 100 μ M methionine and incubated statically for 48 h at 37 °C. If needed, the TSP was subsequently transferred to a new microtiter plate containing sterile M9 medium with various concentrations of methionine and incubated for an additional 24 to 48 h. For enumeration of living cells within the biofilms, TSP plates were transferred onto a 96-well plate containing 200 μ l

0.1 M EDTA, 0.1% CHAPS (3-[(3-Cholamidopropyl)dimethylammonio]-1-propanesulfonate) and incubated for 1 h on a rocking table. CFU were enumerated by plating serial dilutions of the bacterial suspensions on LB agar plates.

Congo red assay to detect *P. aeruginosa* glycocalyx

P. aeruginosa strains were grown overnight in M9 medium containing 100 μ M methionine. Cells were harvested, washed with methionine free M9 and adjusted to $OD_{600} = 0.025$ in the same medium. 5 μ l of bacterial suspension were spotted on defined M9 agar plates containing 30-100 μ M methionine as well as 40 μ g/ml Congo red and 20 μ g/ml Coomassie Brilliant Blue 250 G. Color of arising colonies was assessed after incubation at 37° C for 24 h followed by further incubation on room temperature for 24h.

Statistics

Statistical analysis was performed by using Graphpad Prism

Table 2: Bacterial strains and plasmids used in this study:

| Strain/ Plasmid | Genotype/ Description | Source |
|-----------------------------|--------------------------------------|--|
| Bacterial strains | | |
| <i>E. coli</i> K12 BW25113 | Wild type | Coli Genetic Stock Center (CGSC) – (Nr. 7636) |
| <i>E. coli</i> K12 BW25113 | $\Delta metA$ | CGSC – (Nr- 10856) |
| <i>E. coli</i> K12 BW25113 | $\Delta metB$ | CGSC – (Nr. 10824) |
| <i>E. coli</i> K12 BW25113 | $\Delta metC$ | CGSC – (Nr. 10286) |
| <i>E. coli</i> K12 BW25113 | $\Delta metA$ <i>pME6032</i> | This study |
| <i>E. coli</i> K12 BW25113 | $\Delta metA$ <i>pME6032:metA</i> | This study |
| <i>P. aeruginosa</i> PA14 | wildtype | PA14 Transposon Insertion Mutant Library |
| <i>P. aeruginosa</i> PA14 | $\Delta metX$ | PA14 Transposon Insertion Mutant Library (ID: 55735) |
| <i>P. aeruginosa</i> PA14 | $\Delta metY$ | PA14 Transposon Insertion Mutant Library (ID: 40250) |
| <i>P. aeruginosa</i> PA14 | $\Delta metZ$ | PA14 Transposon Insertion Mutant Library (ID: 31011) |
| <i>P. aeruginosa</i> PA14 | $\Delta metE$ | PA14 Transposon Insertion Mutant Library |
| <i>P. aeruginosa</i> PA14 | $\Delta metH$ | PA14 Transposon Insertion Mutant Library |
| <i>S. aureus</i> Newman | wildtype | (61) |
| <i>S. aureus</i> Newman | $\Delta metC$ | This study |
| <i>S. aureus</i> Newman | $\Delta metI$ | (15) |
| <i>S. aureus</i> Newman | $\Delta metX$ | This study |
| <i>S. aureus</i> SH1000 | wildtype | (62) |
| <i>S. aureus</i> SH1000 | $\Delta metC$ | This study |
| <i>S. aureus</i> USA300 LAC | wildtype | (63) |

| | | |
|-------------------------------|--|------------|
| <i>S. aureus</i> USA300 LAC | $\Delta metI$ | (15) |
| <i>S. epidermidis</i> RP62A | wildtype | (64) |
| <i>S. epidermidis</i> RP62A/3 | $\Delta icaA$ | (65) |
| Plasmids | | |
| pIMAY | Thermosensitive vector for allelic exchange | (59) |
| pIMAY: $\Delta metX$ | | This study |
| pIMAY: $\Delta metC$ | | This study |
| pME6032 | IPTG inducible expression plasmid | (66) |
| pME6032: <i>metA</i> | complementation of <i>metA</i> in <i>E. coli</i> | This study |

Table 3: Oligonucleotides used in this study

| Name | 5'-3' sequence | purpose |
|----------------|--|---|
| metC_A | AGGGAACAAAAGCTGGGTACCACTAG CAGGTGTCGTAACCGTC | Cloning of the <i>metC</i> deletion fragment for <i>S. aureus</i> |
| metC_B | CATACAATCTCTCCAATCTGAGC | Cloning of the <i>metC</i> deletion fragment for <i>S. aureus</i> |
| metC_P | AGATTGGAGAGATTGTATGTAATGTTT TAGTAGCTGATGGCG | Cloning of the <i>metC</i> deletion fragment for <i>S. aureus</i> |
| metC_P | CACTATAGGGCGAATTGGAGCTCAAG TAATTTGTGTTTGAAGCGGTTA | Cloning of the <i>metC</i> deletion fragment for <i>S. aureus</i> |
| metC_Scr. F | TTATCGACAATACTTTTTTAACACC | Screening of the <i>metA</i> deletion fragment for <i>S. aureus</i> |

| | | |
|----------------|--|---|
| metC_Scr. R | GTTGTTTTAATCCTTCATTGATTGC | Screening of the <i>metA</i> deletion fragment for <i>S. aureus</i> |
| metX_A | GGAACAAAAGCTGGGTACCCATCCCT TACATTATCGCGCTC | Cloning of the <i>metX</i> deletion fragment for <i>S. aureus</i> |
| metX_B | CATTGTTCTTTCCTCCTTAAAC | Cloning of the <i>metX</i> deletion fragment for <i>S. aureus</i> |
| metX_C | GGAGGAAAGAACAATGTAATAATATAT ATTTTCAAAGAATGAAGCC | Cloning of the <i>metX</i> deletion fragment for <i>S. aureus</i> |
| metX_D | CACTATAGGGCGAATTGGAGCTCGTT GTTATAATTAAGTGC | Cloning of the <i>metX</i> deletion fragment for <i>S. aureus</i> |
| metX_Scr.F | TGTCATTGACAGCATTATTCAACAG | Screening of the <i>metX</i> deletion fragment for <i>S. aureus</i> |
| metX_Scr. R | CTAATATGATGGCACTTAAAACGAAAG | Screening of the <i>metX</i> deletion fragment for <i>S. aureus</i> |
| MetA_F | TAATGAATTCATGCCGATTCGTGTG | Cloning of the MetA complementation fragment |
| MetA_R | cgatcgaAGatcTcagaagaTTAATCCAG | Cloning of the MetA complementation fragment |

Acknowledgement

We thank Bernhard Krismer and Junjun Gao for helpful discussion. We thank Timothy J. Foster for reading and editing this manuscript.

We acknowledge the support of Hoffmann-La Roche Ltd for providing a Roche Postdoctoral Fellowship to SH (EPBA 1615046-A17) and the support of the German Center of Infection Research (DZIF) to AP (HAARBI).

References

1. Ventola CL. 2015. The antibiotic resistance crisis: part 2: management strategies and new agents. *P T* 40:344-52.
2. Ventola CL. 2015. The antibiotic resistance crisis: part 1: causes and threats. *P T* 40:277-83.
3. Peterson LR. 2009. Bad bugs, no drugs: no ESCAPE revisited. *Clin Infect Dis* 49:992-3.
4. de Kraker ME, Davey PG, Grundmann H, group Bs. 2011. Mortality and hospital stay associated with resistant *Staphylococcus aureus* and *Escherichia coli* bacteremia: estimating the burden of antibiotic resistance in Europe. *PLoS Med* 8:e1001104.
5. van Hal SJ, Paterson DL. 2011. New Gram-positive antibiotics: better than vancomycin? *Curr Opin Infect Dis* 24:515-20.
6. Joo HS, Otto M. 2012. Molecular basis of *in vivo* biofilm formation by bacterial pathogens. *Chem Biol* 19:1503-13.
7. Ciofu O, Tolker-Nielsen T, Jensen PO, Wang H, Hoiby N. 2015. Antimicrobial resistance, respiratory tract infections and role of biofilms in lung infections in cystic fibrosis patients. *Adv Drug Deliv Rev* 85:7-23.
8. Bjarnsholt T, Jensen PO, Fiandaca MJ, Pedersen J, Hansen CR, Andersen CB, Pressler T, Givskov M, Hoiby N. 2009. *Pseudomonas aeruginosa* biofilms in the respiratory tract of cystic fibrosis patients. *Pediatr Pulmonol* 44:547-58.
9. Gil-Perotin S, Ramirez P, Marti V, Sahuquillo JM, Gonzalez E, Calleja I, Menendez R, Bonastre J. 2012. Implications of endotracheal tube biofilm in ventilator-associated pneumonia response: a state of concept. *Crit Care* 16:R93.
10. Adair CG, Gorman SP, Feron BM, Byers LM, Jones DS, Goldsmith CE, Moore JE, Kerr JR, Curran MD, Hogg G, Webb CH, McCarthy GJ, Milligan KR. 1999.

- Implications of endotracheal tube biofilm for ventilator-associated pneumonia. *Intensive Care Med* 25:1072-6.
11. Perkins SD, Woeltje KF, Angenent LT. 2010. Endotracheal tube biofilm inoculation of oral flora and subsequent colonization of opportunistic pathogens. *Int J Med Microbiol* 300:503-11.
 12. Livermore DM, Hope R, Brick G, Lillie M, Reynolds R, Surveillance BWPoR. 2008. Non-susceptibility trends among Enterobacteriaceae from bacteraemias in the UK and Ireland, 2001-06. *J Antimicrob Chemother* 62 Suppl 2:ii41-54.
 13. Livermore DM, Hope R, Reynolds R, Blackburn R, Johnson AP, Woodford N. 2013. Declining cephalosporin and fluoroquinolone non-susceptibility among bloodstream Enterobacteriaceae from the UK: links to prescribing change? *J Antimicrob Chemother* 68:2667-74.
 14. Murima P, McKinney JD, Pethe K. 2014. Targeting bacterial central metabolism for drug development. *Chem Biol* 21:1423-32.
 15. Krismer B, Liebeke M, Janek D, Nega M, Rautenberg M, Hornig G, Unger C, Weidenmaier C, Lalk M, Peschel A. 2014. Nutrient limitation governs *Staphylococcus aureus* metabolism and niche adaptation in the human nose. *PLoS Pathog* 10:e1003862.
 16. Deakova Z, Durackova Z, Armstrong DW, Lehotay J. 2015. Two-dimensional high performance liquid chromatography for determination of homocysteine, methionine and cysteine enantiomers in human serum. *J Chromatogr A* 1408:118-24.
 17. Psychogios N, Hau DD, Peng J, Guo AC, Mandal R, Bouatra S, Sinelnikov I, Krishnamurthy R, Eisner R, Gautam B, Young N, Xia J, Knox C, Dong E, Huang P, Hollander Z, Pedersen TL, Smith SR, Bamforth F, Greiner R, McManus B, Newman JW, Goodfriend T, Wishart DS. 2011. The human serum metabolome. *PLoS One* 6:e16957.
 18. Ferla MP, Patrick WM. 2014. Bacterial methionine biosynthesis. *Microbiology* 160:1571-84.
 19. Arciola CR, Campoccia D, Montanaro L. 2018. Implant infections: adhesion, biofilm formation and immune evasion. *Nat Rev Microbiol* doi:10.1038/s41579-018-0019-y.

20. Boles BR, Thoendel M, Roth AJ, Horswill AR. 2010. Identification of genes involved in polysaccharide-independent *Staphylococcus aureus* biofilm formation. PLoS One 5:e10146.
21. Johnston M, Jankowski D, Marcotte P, Tanaka H, Esaki N, Soda K, Walsh C. 1979. Suicide inactivation of bacterial cystathionine gamma-synthase and methionine gamma-lyase during processing of L-propargylglycine. Biochemistry 18:4690-701.
22. O'Neill E, Pozzi C, Houston P, Humphreys H, Robinson DA, Loughman A, Foster TJ, O'Gara JP. 2008. A novel *Staphylococcus aureus* biofilm phenotype mediated by the fibronectin-binding proteins, FnBPA and FnBPB. J Bacteriol 190:3835-50.
23. Corrigan RM, Rigby D, Handley P, Foster TJ. 2007. The role of *Staphylococcus aureus* surface protein SasG in adherence and biofilm formation. Microbiology 153:2435-46.
24. Mack D, Nedelmann M, Krokotsch A, Schwarzkopf A, Heesemann J, Laufs R. 1994. Characterization of transposon mutants of biofilm-producing *Staphylococcus epidermidis* impaired in the accumulative phase of biofilm production: genetic identification of a hexosamine-containing polysaccharide intercellular adhesin. Infect Immun 62:3244-53.
25. Ma L, Lu H, Sprinkle A, Parsek MR, Wozniak DJ. 2007. *Pseudomonas aeruginosa* Psl is a galactose- and mannose-rich exopolysaccharide. J Bacteriol 189:8353-6.
26. Friedman L, Kolter R. 2004. Genes involved in matrix formation in *Pseudomonas aeruginosa* PA14 biofilms. Mol Microbiol 51:675-90.
27. Franklin MJ, Nivens DE, Weadge JT, Howell PL. 2011. Biosynthesis of the *Pseudomonas aeruginosa* Extracellular Polysaccharides, Alginate, Pel, and Psl. Front Microbiol 2:167.
28. Wei Q, Ma LZ. 2013. Biofilm matrix and its regulation in *Pseudomonas aeruginosa*. Int J Mol Sci 14:20983-1005.
29. O'Toole GA. 2011. Microtiter dish biofilm formation assay. J Vis Exp doi:10.3791/2437.
30. Ceri H, Olson ME, Stremick C, Read RR, Morck D, Buret A. 1999. The Calgary Biofilm Device: new technology for rapid determination of antibiotic susceptibilities of bacterial biofilms. J Clin Microbiol 37:1771-6.

31. Harrison JJ, Stremick CA, Turner RJ, Allan ND, Olson ME, Ceri H. 2010. Microtiter susceptibility testing of microbes growing on peg lids: a miniaturized biofilm model for high-throughput screening. *Nat Protoc* 5:1236-54.
32. Boucher HW, Talbot GH, Bradley JS, Edwards JE, Gilbert D, Rice LB, Scheld M, Spellberg B, Bartlett J. 2009. Bad bugs, no drugs: no ESKAPE! An update from the Infectious Diseases Society of America. *Clin Infect Dis* 48:1-12.
33. Wahl MC, Huber R, Prade L, Marinkovic S, Messerschmidt A, Clausen T. 1997. Cloning, purification, crystallization, and preliminary X-ray diffraction analysis of cystathionine gamma-synthase from *E. coli*. *FEBS Lett* 414:492-6.
34. Brown ED, Wright GD. 2005. New targets and screening approaches in antimicrobial drug discovery. *Chem Rev* 105:759-74.
35. Davis BD, Mingioli ES. 1950. Mutants of *Escherichia coli* requiring methionine or vitamin B12. *J Bacteriol* 60:17-28.
36. Mulligan JT, Margolin W, Krueger JH, Walker GC. 1982. Mutations affecting regulation of methionine biosynthetic genes isolated by use of met-lac fusions. *J Bacteriol* 151:609-19.
37. Ahmed A. 1973. Mechanism of repression of methionine biosynthesis in *Escherichia coli*. I. The role of methionine, s-adenosylmethionine, and methionyl-transfer ribonucleic acid in repression. *Mol Gen Genet* 123:299-324.
38. Michaeli S, Mevarech M, Ron EZ. 1984. Regulatory region of the *metA* gene of *Escherichia coli* K-12. *J Bacteriol* 160:1158-62.
39. Diaz IBZ, Carreon FOC, Ellis WC, Ricke SC. 2007. Assessment of an *Escherichia coli* methionine auxotroph growth assay for quantifying crystalline methionine supplemented in poultry feeds. *Journal of Rapid Methods & Automation in Microbiology* 12:155-167.
40. Armstrong JB. 1972. Chemotaxis and methionine metabolism in *Escherichia coli*. *Can J Microbiol* 18:591-6.
41. Springer MS, Kort EN, Larsen SH, Ordal GW, Reader RW, Adler J. 1975. Role of methionine in bacterial chemotaxis: requirement for tumbling and involvement in information processing. *Proc Natl Acad Sci U S A* 72:4640-4.
42. Stein WH, Moore S. 1954. The free amino acids of human blood plasma. *J Biol Chem* 211:915-26.

43. Iriyama K, Yoshiura M, Iwamoto T. 1986. A method for the determination of methionine in human serum by high-performance liquid chromatography with electrochemical detection. *Journal of Liquid Chromatography* 9:2955-2968.
44. Sato K, Fukushima D, Doi H, Satomi S. 2013. Higher serum methionine levels as a predictive factor in patients with irreversible fulminant hepatic failure. *Transplant Proc* 45:1904-6.
45. Ejim LJ, D'Costa VM, Elowe NH, Loredano-Osti JC, Malo D, Wright GD. 2004. Cystathionine beta-lyase is important for virulence of *Salmonella enterica* serovar Typhimurium. *Infect Immun* 72:3310-4.
46. Nazi I, Scott A, Sham A, Rossi L, Williamson PR, Kronstad JW, Wright GD. 2007. Role of homoserine transacetylase as a new target for antifungal agents. *Antimicrob Agents Chemother* 51:1731-6.
47. Hofford JM, Milakofsky L, Pell S, Fish JE, Peters SP, Pollice M, Vogel WH. 1997. Levels of amino acids and related compounds in bronchoalveolar lavage fluids of asthmatic patients. *Am J Respir Crit Care Med* 155:432-5.
48. Bachman MA, Breen P, Deornellas V, Mu Q, Zhao L, Wu W, Cavalcoli JD, Mobley HL. 2015. Genome-wide identification of *Klebsiella pneumoniae* fitness genes during lung infection. *MBio* 6:e00775.
49. Wang N, Ozer EA, Mandel MJ, Hauser AR. 2014. Genome-wide identification of *Acinetobacter baumannii* genes necessary for persistence in the lung. *MBio* 5:e01163-14.
50. Rohl F, Rabenhorst J, Zahner H. 1987. Biological properties and mode of action of clavams. *Arch Microbiol* 147:315-20.
51. Aguilar A, Perez-Diaz JC, Baquero F, Asensio C. 1982. Microcin 15m from *Escherichia coli*: mechanism of antibiotic action. *Antimicrob Agents Chemother* 21:381-6.
52. Ejim LJ, Blanchard JE, Koteva KP, Sumerfield R, Elowe NH, Chechetto JD, Brown ED, Junop MS, Wright GD. 2007. Inhibitors of bacterial cystathionine beta-lyase: leads for new antimicrobial agents and probes of enzyme structure and function. *J Med Chem* 50:755-64.
53. Kong Y, Wu D, Bai H, Han C, Chen J, Chen L, Hu L, Jiang H, Shen X. 2008. Enzymatic characterization and inhibitor discovery of a new cystathionine {gamma}-synthase from *Helicobacter pylori*. *J Biochem* 143:59-68.

54. Mack D, Fischer W, Krokotsch A, Leopold K, Hartmann R, Egge H, Laufs R. 1996. The intercellular adhesin involved in biofilm accumulation of *Staphylococcus epidermidis* is a linear beta-1,6-linked glucosaminoglycan: purification and structural analysis. *J Bacteriol* 178:175-83.
55. Banner MA, Cunniffe JG, Macintosh RL, Foster TJ, Rohde H, Mack D, Hoyes E, Derrick J, Upton M, Handley PS. 2007. Localized tufts of fibrils on *Staphylococcus epidermidis* NCTC 11047 are comprised of the accumulation-associated protein. *J Bacteriol* 189:2793-804.
56. Christner M, Franke GC, Schommer NN, Wendt U, Wegert K, Pehle P, Kroll G, Schulze C, Buck F, Mack D, Aepfelbacher M, Rohde H. 2010. The giant extracellular matrix-binding protein of *Staphylococcus epidermidis* mediates biofilm accumulation and attachment to fibronectin. *Mol Microbiol* 75:187-207.
57. Cucarella C, Solano C, Valle J, Amorena B, Lasa I, Penades JR. 2001. Bap, a *Staphylococcus aureus* surface protein involved in biofilm formation. *J Bacteriol* 183:2888-96.
58. Borlee BR, Goldman AD, Murakami K, Samudrala R, Wozniak DJ, Parsek MR. 2010. *Pseudomonas aeruginosa* uses a cyclic-di-GMP-regulated adhesin to reinforce the biofilm extracellular matrix. *Mol Microbiol* 75:827-42.
59. Monk IR, Shah IM, Xu M, Tan MW, Foster TJ. 2012. Transforming the untransformable: application of direct transformation to manipulate genetically *Staphylococcus aureus* and *Staphylococcus epidermidis*. *MBio* 3.
60. Sebulsky MT, Speziali CD, Shilton BH, Edgell DR, Heinrichs DE. 2004. FhuD1, a ferric hydroxamate-binding lipoprotein in *Staphylococcus aureus*: a case of gene duplication and lateral transfer. *J Biol Chem* 279:53152-9.
61. Duthie ES, Lorenz LL. 1952. Staphylococcal coagulase; mode of action and antigenicity. *J Gen Microbiol* 6:95-107.
62. Horsburgh MJ, Aish JL, White IJ, Shaw L, Lithgow JK, Foster SJ. 2002. sigmaB modulates virulence determinant expression and stress resistance: characterization of a functional *rsbU* strain derived from *Staphylococcus aureus* 8325-4. *J Bacteriol* 184:5457-67.
63. Kazakova SV, Hageman JC, Matava M, Srinivasan A, Phelan L, Garfinkel B, Boo T, McAllister S, Anderson J, Jensen B, Dodson D, Lonsway D, McDougal LK, Arduino M, Fraser VJ, Killgore G, Tenover FC, Cody S, Jernigan DB.

2005. A clone of methicillin-resistant *Staphylococcus aureus* among professional football players. *N Engl J Med* 352:468-75.
64. Christensen GD, Simpson WA, Bisno AL, Beachey EH. 1982. Adherence of slime-producing strains of *Staphylococcus epidermidis* to smooth surfaces. *Infect Immun* 37:318-26.
65. Ziebuhr W, Krimmer V, Rachid S, Lossner I, Götz F, Hacker J. 1999. A novel mechanism of phase variation of virulence in *Staphylococcus epidermidis*: evidence for control of the polysaccharide intercellular adhesin synthesis by alternating insertion and excision of the insertion sequence element IS256. *Mol Microbiol* 32:345-56.
66. Heeb S, Blumer C, Haas D. 2002. Regulatory RNA as mediator in GacA/RsmA-dependent global control of exoproduct formation in *Pseudomonas fluorescens* CHA0. *J Bacteriol* 184:1046-56.

Chapter 4 – General Discussion

Restricted iron availability in host tissues is an effective mechanism to prevent bacterial infections [1-3]. Numerous bacterial strategies to cope with this iron restriction have been described. The production and secretion of siderophores with high affinity to ferric iron is the most prominent one. Siderophores like staphyloferrin A and B produced by *S. aureus* allow sequestration of small traces of iron to provide it to the bacteria during growth [4]. In contrast to *S. aureus*, *S. lugdunensis* does not produce such secreted iron-scavenging molecules [5]. Nevertheless, *S. lugdunensis* is involved in severe cases of endocarditis and bloodstream infections [6, 7]. This indicates that *S. lugdunensis* must have alternative mechanisms for iron acquisition. Like *S. aureus*, *S. lugdunensis* expresses the iron surface determinant system (Isd), which enables it to acquire iron from host proteins like hemoglobin or heme.

The Isd system of *S. lugdunensis* contains several cell wall-bound proteins for heme acquisition. IsdB is the major hemoglobin binding protein which extracts heme from hemoglobin. IsdC shuttles the extracted heme to the ABC importer IsdEFL for transport into the cytoplasm [8]. An *isd* locus is common in *S. aureus* and *S. lugdunensis*. But the loci of the species differ in several features. Three genes encoding for an ABC transporter of the energy coupling factor- type (ECF) are only present in *S. lugdunensis*. We showed that the three genes, named *lhaS*, *lhaT* and *lhaA* encode for an integral S-component, a T-domain, and an ATPase, respectively. Thereby, forming a novel ECF transporter that uses heme as a substrate for iron acquisition.

We demonstrated the ECF transporter Lha (*lugdunensis* heme acquisition) to be heme-specific, making it the first example of an ECF transporter involved in iron acquisition. The regulation of *lhaSTA* by the ferric uptake regulator (Fur) further confirmed its role in nutritional heme-acquisition.

Only few substrates are known to be transported by ECF transporters. They are described to mostly transport micronutrients as e.g. biotin, folate, pantothenate, pyridoxamine, riboflavin, thiamine, nickel and cobalt [9-15]. Those transporters show high affinities to their substrates in the low nanomolar range [16]. Heme is a new

described substrate for an ECF transporter. However, how does *S. lugdunensis* benefit from a high affinity heme transporter when a heme specific lipoprotein is already encoded within *Isd*?

We showed that the Lha system, in comparison to the *Isd* system, can not only extract heme from hemoglobin but also uses myoglobin and hemopexin as substrates. This enables *S. lugdunensis* to exploit more host proteins and expands the iron sources accessible during infection. The advanced substrate range is also demonstrated by a wide host range as not only human specific hemoproteins but also hemoproteins of murine or equine origin were accessible to LhaS. In contrast, *IsdB* of *S. lugdunensis* shows high substrate specificity and facilitates heme acquisition from human but not from mouse hemoglobin [8]. *IsdB* of *S. aureus* shows similar specificity [17]. *S. aureus* developed a strategy to expand its substrate range by expressing an additional protein *IsdH* to access heme from hemoglobin-haptoglobin complexes. But still, the specificity to hemoglobin or hemoglobin-haptoglobin complexes results in a limited substrate range and other host hemoproteins such as myoglobin remain inaccessible. An explanation for the high specificity of the *Isd* system to hemoglobin or hemoglobin-haptoglobin complexes is the binding mechanism of *IsdB*. Hemoglobin binding and heme extraction occur via two NEAT domains (*IsdB*-N1 and *IsdB*-N2). *IsdB*-N1 binds to hemoglobin and induces a conformational change in the hemoglobin molecule. This structural change results in an even tighter binding. Subsequently *IsdB*-N2 binds heme and extracts it from hemoglobin. The direct binding mechanism of the NEAT domains of *IsdB* to the proteinaceous backbone of hemoglobin results in a specific interaction limiting substrate range [8]. A unique feature of the *S. aureus* *Isd* system is the expression of an additional cell wall receptor *IsdH*. It has three NEAT domains, *IsdH*-N1 and N2 are involved in hemoglobin binding and N3 in heme extraction [18]. *IsdH* binds also to haptoglobin-hemoglobin complexes thereby expanding the substrate range of the *S. aureus* *Isd* system [19].

We demonstrated by saturation of heterologous expressed LhaS using human hemoglobin and myoglobin as well as murine hemoglobin, equine myoglobin, and human hemopexin-heme, that LhaSTA might represent a superior iron acquisition system with a very broad substrate range. This suggests that direct interactions with the hemoproteins are not occurring. We speculate, that the described extraordinary high affinity of the S-components to their substrates could allow diffusion-dependent heme-extraction from different hemoproteins. Such a binding mechanism might be

functional because of the non-covalent binding of heme to host-hemoproteins [20], allowing dissociation of heme and capture by LhaS [21]. Hence, if the k_{on} rate of LhaS for heme is bigger than the k_{on} of host hemoproteins competition for free heme occurs and may be sufficient for LhaS substrate binding. Together this argues for an affinity-driven binding mechanism of LhaS to its substrates.

The assumed affinity-driven heme acquisition of LhaS is also proposed for some hemophores as e.g. HasA from *Serratia marcescens*. Hemophores are small secreted proteins with a remarkably high affinity towards heme, comparable to the affinity of siderophores to Fe^{3+} . They are produced by both Gram-positive and Gram-negative species [22]. Prominent examples are HasA type hemophores from *S. marcescens* or *Pseudomonas aeruginosa* [23, 24]. HasA from *S. marcescens* is shown to bind heme with a K_d of 18 pM and scavenges heme from hemoglobin, leghemoglobin, myoglobin and hemopexin. Due to the high affinity and a slow heme binding constant, one assumes a passive binding of heme without any protein-protein contact [22]. The substrate range is akin to that of LhaS and such high affinities are also described for S-components, strengthening the idea of an affinity-driven mechanism for LhaS. We failed to determine the K_d of LhaS towards heme using ITC (isothermal titration calorimetry). Hence, further investigations are needed to verify this assumption.

One can speculate that LhaS might represent a membrane bound hemophore comparable to the HxuA, HxuC system from *Haemophilus influenzae*. HxuA is anchored to the outer membrane. As well as LhaS, HxuA uses hemopexin-heme as substrate, but in contrast to LhaS it does not show high affinity to heme but interacts with the proteinaceous part of hemopexin to foster heme release. HxuA provides the bacterial cells with free heme which is subsequently captured by HxuC [25-28]. In contrast to the passive binding mechanism of HasA, and LhaS, the binding mechanism of the Isd proteins depends on NEAT domain interaction. In the broadest sense, the NEAT domains responsible for hemoglobin binding and heme extraction can be counted to the family of hemophores, too. Besides the well-studied NEAT domain bearing Isd proteins in staphylococcal species also *Bacillus anthracis* encodes for NEAT proteins. In contrast to IsdB/H of *S. aureus*, IsdX1 and IsdX2 of *B. anthracis* are secreted proteins with either one (IsdX1) or five NEAT domains (IsdX2). Protein binding and heme extraction takes place through similar mechanisms as described for IsdB [29]. But this NEAT domain-driven heme acquisition has one prominent

disadvantage, it results in a limited substrate range only using hemoglobin or hemoglobin-haptoglobin as substrates.

Whether the passive-extraction mechanism proposed for LhaS or HasA is an advantage over heme acquisition systems that depend on specific interactions, is controversial. Although, it allows a wide substrate range, heme acquisition and extraction might be relatively slow since heme release from hemoproteins is rare [21, 30]. Whereas direct heme extraction by Isd proteins happens quite fast, it is limited to hemoglobin or hemoglobin-haptoglobin complexes [19, 31]. One can argue that Lha is the more efficient system with only three expressed proteins needed to perform a sufficient iron supply, especially if scores of hemoproteins are available. In contrast, the Isd system comprises at least nine proteins to fulfill the same job [32]. However, systems using NEAT domains for heme extraction, like the Isd system, are more common among bacteria [31, 33-35]. This strengthens the assumption it is the more worthwhile heme acquisition apparatus since hemoglobin is the biggest heme source during infection. Maybe one can think of the Lha system as an additional heme acquisition system to support iron supply during growth under extremely limited conditions. This might be one reason why *S. lugdunensis* is able to survive and infect the human host, although only few virulence factors have been described [32]. Still, *S. lugdunensis* would not express the Lha system without having any benefit. Maybe the Lha system enables *S. lugdunensis* to colonize specific niches, in which hemoprotein concentration favors the expression of *lha*. This additional system enables adaptation to the hostile surrounding of the human body even though no further iron scavenging molecules as e.g. the siderophores of *S. aureus* are expressed. The combination of Lha and Isd enables *S. lugdunensis* to access the biggest heme source in the human body (hemoglobin) as well as an expanded substrate range to use further host hemoproteins as myoglobin and hemopexin.

LhaSTA is localized in the bacterial membrane, which raises the question how the transporter accesses the host proteins through the peptidoglycan layers. Interestingly, hemoglobin-haptoglobin complexes did not serve as substrate for LhaSTA. One can speculate that this is due to the location of LhaS in the membrane and, in contrast to other hemoproteins, Hb-Hap might be too big to penetrate the peptidoglycan layers. However, we performed heme transfer assays from hemoglobin-haptoglobin to LhaS and did not detect transfer of heme to LhaS. This suggests that the affinity of heme to the hemoglobin-haptoglobin complex is too high for LhaS to compete with. It has been

observed that after hemoglobin is released from erythrocytes it dissociates to hemoglobin dimers. But heme is more stable bound to hemoglobin tetramers, than to hemoglobin mono- or dimers [30, 36]. It seems possible that hemoglobin dimers bound to haptoglobin show an increased affinity to heme which is higher than the affinity of LhaS and therefore hemoglobin-haptoglobin complexes do not serve as a substrate for Lha. In comparison to Lha, the Isd system encodes for cell wall bound proteins like IsdB and IsdC. IsdB reaches out into the extracellular environment for hemoglobin binding and IsdC is localized deeper in the cell wall for heme transport to the membrane [8]. It has been assumed that those cell wall anchored proteins are necessary to get access to the substrates in the extracellular milieu, but the Lha systems without any surface receptors, introduces a different way of heme acquisition. We showed that the LhaSTA transporter works independently of the Isd proteins. We used a mutant strain lacking all Isd related genes and found that LhaSTA has no need for cell wall-bound proteins for heme funneling to the membrane. However, one would assume that spatial proximity between host hemoproteins and the Lha transporter is necessary for effective heme acquisition by LhaS. The host proteins seem to be too large to penetrate the peptidoglycan layer of *S. lugdunensis*. Hemoglobin, myoglobin and hemopexin have sizes of ~ 64 kDa, 16 kDa and ~ 70,6 kDa, respectively. However, it has been described that the staphylococcal peptidoglycan layer contains pores with a diameter of ~ 23 Å [37-39]. The proposed structure of the staphylococcal peptidoglycan with cross-linked peptidoglycan stems in parallel orientation and thereby formed pores, also called tesserae, might allow host proteins to get access to the bacterial membrane and thus get in spatial proximity to the S-component of the ECF transporter Lha. Erickson et al. deduced from sizes and shapes of proteins a minimum radius for proteins of different sizes. According to his calculations hemoglobin, myoglobin and hemopexin have minimum diameters of ~ 25 Å, ~ 15 Å, and ~ 27 Å, respectively [40]. Considering this, it seems possible that host hemoproteins penetrate the cell wall using the intrinsic pores to reach membrane located LhaS.

Regarding the binding properties, the substrate range of the LhaSTA ECF transporter and its importance during growth, it can be considered as a virulence factor of *S. lugdunensis*. However, we did not see effects in a murine infection model for systemic disease. Reasons for this are unclear as not much is known about *S. lugdunensis* virulence factors. When comparing the *S. lugdunensis* genome to *S. aureus*, it becomes clear that *S. lugdunensis* possess only a small variety of

virulence genes encoded by *S. aureus* [32]. This might explain the reduced virulence of *S. lugdunensis* in mice. Additionally, we observed that *S. lugdunensis* lyses human but fails to lyse murine erythrocytes. This suggests human specific virulence factors and might explain low infectivity in murine models. It has been shown, that *S. aureus* creates human specificity by lysing erythrocytes via the bi-component system LukED and HlgAB targeting the duffy antigen receptor for chemokines (DARC) [41]. Similar but yet unknown mechanisms might apply to *S. lugdunensis*.

Our findings show that LhaSTA enables *S. lugdunensis* to use human erythrocytes and human cardiac myocytes for heme acquisition, thus affirming the importance of LhaSTA during invasive infection in human host. Considering all findings, the Lha system represents a novel high-affinity heme transport and acquisition system from the ECF-type, that enlarges the substrate range of *S. lugdunensis*. Recent studies describe similar transporter systems with affinity to heme from the ECF-type in *Streptococci* and *Lactococcus sakei* [42, 43]. Both S-components show low similarity to LhaS and therefore seem to have evolved independently. In group A *Streptococci* loss of the SiaGFH transporter resulted in a significant affectation in a murine mucosal colonization and systemic infection model. Homologs of this special ECF transporter were found in *Eggerthella lenta* and *Enterococcus faecalis* [42]. Diverse ECF transporters are found in many members of the phyla firmicutes. Hence a wide distribution of heme binding ECF transporters is possible. For example, *S. aureus* has been shown to use myoglobin as heme source. But the transporter or receptor involved in this heme uptake remains unknown [44].

Further investigations will be necessary to determine the biochemical binding properties of LhaS and heme. Additional experiments could help investigating whether heme binding ECF transporters are spread among bacterial pathogens and represent a so far undiscovered method in overcoming nutritional immunity.

Bacteria need to acquire nutrients to allow proliferation. This is also true during infection. However, which nutrients apart from metal ions are plentiful or limited during infection is largely unknown. Different studies showed that many genes involved in bacterial growth and survival during infection provide building blocks in metabolic pathways and are necessary for nutrient acquisition [45-47]. The proteinogenic amino acid methionine, together with cysteine, are the two sulfur-containing amino acids. Although methionine is infrequent in bacterial proteins compared to e.g. glycine and

leucine [48]. It plays an important role for protein biosynthesis, as formylated methionine is used to initiate protein synthesis. Additionally, it is involved in S-adenosylmethionine (SAM) mediated methylation of proteins, lipids, DNA and RNA [49, 50]. Considering the emerging number of multi drug resistant (MDR) pathogens and the limited number of effective last resort antibiotics, new strategies to treat bacterial infections are desperately needed [51]. Especially bacterial central metabolism seems to be an underestimated drug target, which gained more attention during the last years [52, 53]. But targeting the bacterial central metabolism requires knowledge about nutritional availability within the host micro environment as well as on the physiological effects of nutritional limitation [54].

The methionine biosynthesis pathway is in many respects a promising target for antibiotics. First, the *de novo* pathway for methionine biosynthesis is present amongst most bacterial pathogens. Among the different bacterial phyla some differences in the biosynthesis pathway exist. But, most of the involved enzymes are highly conserved [55]. This makes it a suitable target for broad spectrum antibiotics. Furthermore, the whole pathway is absent in vertebrate cells, which reduces the risk of toxic side effects of potential antibiotic compounds during patient treatment [56]. *S. aureus*, *E. coli* and *P. aeruginosa* all possess the methionine biosynthesis pathway, but differ in single biosynthesis steps and enzymes, therefore representing the most common biosynthesis types. Methionine levels in human serum range from 25 – 48 μM [57, 58]. However, it remained unclear whether this is sufficient for auxotrophic mutants to sustain a balanced metabolism. If these levels were sufficient, it would disqualify the pathway as a drug target.

We could show that a methionine auxotroph mutant of *S. aureus* needs 50-100 μM exogenous methionine to grow on wildtype level in methionine depleted medium. By comparison, methionine auxotroph mutants of *E. coli* and *P. aeruginosa* needed higher concentrations exceeding 100 μM to regain wildtype levels of growth. This exceeds methionine levels that human serum usually contains. Additionally, we showed that pooled human serum did not provide sufficient methionine to overcome the growth disadvantages associated with methionine auxotrophy. In our experiments we used mutants in *S. aureus*, *E. coli* and *P. aeruginosa* of the first step of methionine biosynthesis, the acetylation step, impaired in catalyzation of homoserine to O-Acetyl-homoserine or O-Succinyl-homoserine. But these mutants are able to utilize available methionine as well as precursors such as homocysteine in human serum. It is reported

for human serum to contain 13 μM homocysteine, and at least 25 μM methionine [57]. Our experiments revealed, that even with 50% pooled serum methionine auxotrophs show poor growth, indicating that the amount of free methionine and methionine precursors in human serum is not sufficient to bypass the blockage of the first acetylation step. Similar results have been observed for Group B *Streptococcus* in human plasma. A *mtaR* mutant lacking a major regulator of methionine biosynthesis in *Streptococcus* showed poor growth in human plasma, confirming that available nutrient concentration in human serum is not sufficient to restore full growth under methionine limited conditions [59]. Furthermore, studies with *Salmonella enterica* serovar Typhimurium and *Cryptococcus neoformans* revealed that methionine auxotrophs are attenuated in invasive infection models [60, 61]. Besides the effects of methionine biosynthesis inhibition on bacterial growth we found it to be important for biofilm formation. Staphylococcal biofilms comprise polysaccharides, eDNA and proteins and they are differentiated into polysaccharide intercellular adhesin (PIA)-dependent or PIA-independent biofilms. The latter strongly depends on proteins for cell-cell adhesion such as the *S. aureus* SasG, Fnbp, Aap or Embp proteins [62]. We showed that inhibition of methionine biosynthesis by the inhibitor PG results in significantly reduced amount biofilm formation of *S. aureus* SH1000, which is known to form a PIA-independent biofilm. Whereas *S. epidermidis* RP62A was unaffected by PG treatment, due to PIA-dependent biofilm formation [63]. We found methionine biosynthesis inhibition to result in a reduced protein biosynthesis. Most likely due to importance of formylated methionine for initiation of translation it can impact the amount of protein. An even more pronounced effect on biofilm formation was observed for *P. aeruginosa*. *P. aeruginosa* biofilms consist of similar building blocks as *S. aureus* biofilms, eDNA, proteins and polysaccharides. The three most important polysaccharides Alginate, Psl and Pel are involved in the structure and antibiotic resistance of biofilm [64, 65]. We demonstrated that not even 200 μM exogenous methionine could restore wildtype biofilm production of a methionine auxotroph mutant unable to convert homoserine into O-Acetyl-homoserine. Interestingly, living cell counts were similar between WT and mutant, but biofilm biomass was strongly reduced within the mutant. This is most likely explained with reduced protein biosynthesis resulting from methionine limitation. However, if mature *P. aeruginosa* biofilm was transferred to methionine limiting conditions, the biofilm dispersed over the following two days and living cell counts were reduced. We hypothesize that lack of membrane-associated proteins, involved in

polysaccharide processing such as PslA/PslO and PelA-F [66, 67] contributes to this phenotype. We confirmed this using the Congo red assay. Under methionine limiting conditions the methionine auxotroph mutant was unable to incorporate the red pigment Congo red. After exogenous methionine was added the mutant restored Congo red incorporation. Similar phenotypes are observed for Pel- deficient mutants. Pel-mutants are incapable in forming pellicles and solid surface biofilms [68]. Therefore, those mutants were not able to form an intact extracellular matrix [66]. According to this phenotype, we anticipate that methionine limitation alters the production of a principle component of *Pseudomonas* biofilm matrix comparable to Pel-mutants.

Pathogens colonizing different niches are differently affected if methionine biosynthesis is inhibited, as the methionine concentration varies in the different host micro-environments. Krismer et al. reported nasal secretions to be devoid of methionine, leaving pathogens colonizing the nasal cavities relying on endogenous methionine synthesis. Accordingly, a mutant was attenuated in a nasal colonization model [69]. Comparable to nasal secretions, bronchioalveolar fluids were shown to lack methionine. Hence, investigations revealed that during *K. pneumoniae* and *A. baumannii* infections endogenous methionine biosynthesis is important [70-72]. These studies demonstrated that methionine biosynthesis is important for bacterial proliferation, colonization and during infection. If methionine biosynthesis inhibitors are useful as therapeutic agents needs further investigations, but their use for *S. aureus* eradication from human nose seems possible. Methionine biosynthesis inhibitors as therapeutic agents would be comparable to successful antibiotics like trimethoprim. Trimethoprim inhibits the folate biosynthesis pathway resulting in an impaired nucleic acid- and amino acid biosynthesis. It is used to treat Gram-negative and Gram-positive bacterial infections [73]. There are numerous methionine biosynthesis inhibitors described, all targeting different steps of the biosynthesis pathway and produced by different species. The clavams, characterized 1987 by Röhl et al. were shown to be bacteriostatic and fungistatic. For example, the compound valclavam inhibits the homoserine- O-succinyl transferase (MetA) thereby blocking methionine biosynthesis. Although this pathway is absent from eukaryotic cells valclavam has shown to be toxic to human cells by interfering with RNA biosynthesis [74]. Additionally, the natural compound juglone, extracted from the leaves of *Juglancea*, inhibits the cystathionine γ -synthase (MetB) of *Helicobacter pylori* [75]. However, due to cytotoxicity in cell culture experiments juglone is not suitable for therapeutic treatment either [76]. A similar

problem has been reported for the inhibitor L-propargylglycine (PG), which also blocks the first step of the trans-sulfurylation reaction catalyzed by MetI/ MetB of methionine biosynthesis. Although, this reaction is not present in human cells the reverse reaction is, which is also inhibited by PG [77-79]. Several other methionine biosynthesis inhibitors are known, e.g. α -lapachone (NPLC518), 9-hydroxy- α -lapachone (NPLC519) Paulownin (NPLC604) and Yangambin (NPLC605). They are all described to inhibit the cystathione γ -synthase, too. They were discovered during a broad screening approach for methionine biosynthesis inhibitors in *Helicobacter pylori* [80]. Besides, inhibitors against the homoserine-O-acetyltransferase (MetX) in *Cryptococcus neoformans* and the homoserine-O-succinyl transferase (MetA) in *E. coli* have been investigated. Both inhibitors block the first step in methionine biosynthesis [60, 74]. Even though many methionine inhibitors are described, so far none of them was reported as a suitable therapeutic agent due to toxic side effects on eukaryotic cells. Still more and detailed investigations concerning their applicability during infections and side effects are necessary.

Our results strengthen the postulation of the methionine biosynthesis as a suitable target for novel antibiotics. We demonstrated that methionine limitation inhibits growth and biofilm formation of different human pathogens. Despite of the bacteriostatic inhibition of methionine biosynthesis inhibitors they can still be considered as an effective tool against bacterial infections. Comparable to trimethoprim or sulfamethoxazole, which also act bacteriostatic but in combination with both act bactericidal [81], one could hypothesize that a combined treatment with a methionine biosynthesis inhibitor and other antibacterial agents results in an effective treatment against bacterial pathogens. However, which methionine biosynthesis inhibitor is suitable for therapeutic applications remains unclear and requires further investigation. Methionine and iron are not the only nutrient limitations bacteria have to face when colonizing or infecting the human host. For example, phosphate is a limited nutrient in the human microenvironment, too. But pathogens such as *S. aureus* counter this limitation by special acquisition systems. *S. aureus* scavenges wall teichoic acids from other staphylococci and uses them as phosphate source by expressing a glycerophosphodiesterase GlpQ [82]. Similarly, GlpQ of *Mycoplasma pneumoniae* was shown to be crucial for bacterial glycerol metabolism and growth [83]. Besides iron, nutritional shortage for other transition metals such as zinc and manganese are well characterized [84].

In this light, inhibition of nutrient uptake systems or essential metabolic steps absent from the human host might be worthwhile in the steady search for novel antimicrobial targets to fight bacterial infections. But more investigations targeting these special systems are needed.

References

1. Andrews, S.C., A.K. Robinson, and F. Rodriguez-Quinones, *Bacterial iron homeostasis*. FEMS Microbiol Rev, 2003. **27**(2-3): p. 215-37.
2. Golonka, R., B.S. Yeoh, and M. Vijay-Kumar, *The Iron Tug-of-War between Bacterial Siderophores and Innate Immunity*. J Innate Immun, 2019. **11**(3): p. 249-262.
3. Bullen, J.J., H.J. Rogers, and E. Griffiths, *Role of iron in bacterial infection*. Curr Top Microbiol Immunol, 1978. **80**: p. 1-35.
4. Beasley, F.C., et al., *Staphylococcus aureus transporters Hts, Sir, and Sst capture iron liberated from human transferrin by Staphyloferrin A, Staphyloferrin B, and catecholamine stress hormones, respectively, and contribute to virulence*. Infect Immun, 2011. **79**(6): p. 2345-55.
5. Brozyna, J.R., J.R. Sheldon, and D.E. Heinrichs, *Growth promotion of the opportunistic human pathogen, Staphylococcus lugdunensis, by heme, hemoglobin, and coculture with Staphylococcus aureus*. Microbiologyopen, 2014. **3**(2): p. 182-95.
6. Vandenesch, F., et al., *Endocarditis due to Staphylococcus lugdunensis: report of 11 cases and review*. Clin Infect Dis, 1993. **17**(5): p. 871-6.
7. Pfaller, M.A., et al., *Survey of blood stream infections attributable to gram-positive cocci: frequency of occurrence and antimicrobial susceptibility of isolates collected in 1997 in the United States, Canada, and Latin America from the SENTRY Antimicrobial Surveillance Program. SENTRY Participants Group*. Diagn Microbiol Infect Dis, 1999. **33**(4): p. 283-97.
8. Zapotoczna, M., et al., *Iron-regulated surface determinant (Isd) proteins of Staphylococcus lugdunensis*. J Bacteriol, 2012. **194**(23): p. 6453-67.
9. Berntsson, R.P., et al., *Structural divergence of paralogous S components from ECF-type ABC transporters*. Proc Natl Acad Sci U S A, 2012. **109**(35): p. 13990-5.
10. Erkens, G.B. and D.J. Slotboom, *Biochemical characterization of ThiT from Lactococcus lactis: a thiamin transporter with picomolar substrate binding affinity*. Biochemistry, 2010. **49**(14): p. 3203-12.
11. Karpowich, N.K., et al., *ATP binding drives substrate capture in an ECF transporter by a release-and-catch mechanism*. Nat Struct Mol Biol, 2015. **22**(7): p. 565-71.
12. Wang, T., et al., *Structure of a bacterial energy-coupling factor transporter*. Nature, 2013. **497**(7448): p. 272-6.
13. Xu, K., et al., *Crystal structure of a folate energy-coupling factor transporter from Lactobacillus brevis*. Nature, 2013. **497**(7448): p. 268-71.

14. Zhang, P., J. Wang, and Y. Shi, *Structure and mechanism of the S component of a bacterial ECF transporter*. *Nature*, 2010. **468**(7324): p. 717-20.
15. Yu, Y., et al., *Planar substrate-binding site dictates the specificity of ECF-type nickel/cobalt transporters*. *Cell Res*, 2014. **24**(3): p. 267-77.
16. Duurkens, R.H., et al., *Flavin binding to the high affinity riboflavin transporter RibU*. *J Biol Chem*, 2007. **282**(14): p. 10380-6.
17. Pishchany, G., et al., *IsdB-dependent hemoglobin binding is required for acquisition of heme by Staphylococcus aureus*. *J Infect Dis*, 2014. **209**(11): p. 1764-72.
18. Gianquinto, E., et al., *Interaction of human hemoglobin and semi-hemoglobins with the Staphylococcus aureus hemophore IsdB: a kinetic and mechanistic insight*. *Sci Rep*, 2019. **9**(1): p. 18629.
19. Dryla, A., et al., *Identification of a novel iron regulated staphylococcal surface protein with haptoglobin-haemoglobin binding activity*. *Mol Microbiol*, 2003. **49**(1): p. 37-53.
20. Reeder, B.J., *The redox activity of hemoglobins: from physiologic functions to pathologic mechanisms*. *Antioxid Redox Signal*, 2010. **13**(7): p. 1087-123.
21. Szabo, A., *Kinetics of hemoglobin and transition state theory*. *Proc Natl Acad Sci U S A*, 1978. **75**(5): p. 2108-11.
22. Wandersman, C. and P. Delepelaire, *Haemophore functions revisited*. *Mol Microbiol*, 2012. **85**(4): p. 618-31.
23. Alontaga, A.Y., et al., *Structural characterization of the hemophore HasAp from Pseudomonas aeruginosa: NMR spectroscopy reveals protein-protein interactions between Holo-HasAp and hemoglobin*. *Biochemistry*, 2009. **48**(1): p. 96-109.
24. Letoffe, S., J.M. Ghigo, and C. Wandersman, *Iron acquisition from heme and hemoglobin by a Serratia marcescens extracellular protein*. *Proc Natl Acad Sci U S A*, 1994. **91**(21): p. 9876-80.
25. Cope, L.D., et al., *Binding of heme-hemopexin complexes by soluble HxuA protein allows utilization of this complexed heme by Haemophilus influenzae*. *Infect Immun*, 1998. **66**(9): p. 4511-6.
26. Cope, L.D., et al., *The 100 kDa haem:haemopexin-binding protein of Haemophilus influenzae: structure and localization*. *Mol Microbiol*, 1994. **13**(5): p. 863-73.
27. Fournier, C., A. Smith, and P. Delepelaire, *Haem release from haemopexin by HxuA allows Haemophilus influenzae to escape host nutritional immunity*. *Mol Microbiol*, 2011. **80**(1): p. 133-48.
28. Wong, J.C., et al., *Affinity, conservation, and surface exposure of hemopexin-binding proteins in Haemophilus influenzae*. *Infect Immun*, 1995. **63**(6): p. 2327-33.
29. Maresso, A.W., G. Garufi, and O. Schneewind, *Bacillus anthracis secretes proteins that mediate heme acquisition from hemoglobin*. *PLoS Pathog*, 2008. **4**(8): p. e1000132.
30. Hargrove, M.S., et al., *Quaternary structure regulates hemin dissociation from human hemoglobin*. *J Biol Chem*, 1997. **272**(28): p. 17385-9.
31. Mazmanian, S.K., et al., *Passage of heme-iron across the envelope of Staphylococcus aureus*. *Science*, 2003. **299**(5608): p. 906-9.
32. Heilbronner, S., et al., *Genome sequence of Staphylococcus lugdunensis N920143 allows identification of putative colonization and virulence factors*. *FEMS Microbiol Lett*, 2011. **322**(1): p. 60-7.

33. Daou, N., et al., *IlsA, a unique surface protein of Bacillus cereus required for iron acquisition from heme, hemoglobin and ferritin*. PLoS Pathog, 2009. **5**(11): p. e1000675.
34. Gat, O., et al., *Characterization of Bacillus anthracis iron-regulated surface determinant (Isd) proteins containing NEAT domains*. Mol Microbiol, 2008. **70**(4): p. 983-99.
35. Honsa, E.S., et al., *The five near-iron transporter (NEAT) domain anthrax hemophore, IsdX2, scavenges heme from hemoglobin and transfers heme to the surface protein IsdC*. J Biol Chem, 2011. **286**(38): p. 33652-60.
36. Mocny, J.C., J.S. Olson, and T.D. Connell, *Passively released heme from hemoglobin and myoglobin is a potential source of nutrient iron for Bordetella bronchiseptica*. Infect Immun, 2007. **75**(10): p. 4857-66.
37. Kim, S.J., J. Chang, and M. Singh, *Peptidoglycan architecture of Gram-positive bacteria by solid-state NMR*. Biochim Biophys Acta, 2015. **1848**(1 Pt B): p. 350-62.
38. Kim, S.J., et al., *Staphylococcus aureus peptidoglycan stem packing by rotational-echo double resonance NMR spectroscopy*. Biochemistry, 2013. **52**(21): p. 3651-9.
39. Turner, R.D., et al., *Peptidoglycan architecture can specify division planes in Staphylococcus aureus*. Nat Commun, 2010. **1**: p. 26.
40. Erickson, H.P., *Size and shape of protein molecules at the nanometer level determined by sedimentation, gel filtration, and electron microscopy*. Biol Proced Online, 2009. **11**: p. 32-51.
41. Spaan, A.N., et al., *Staphylococcus aureus Targets the Duffy Antigen Receptor for Chemokines (DARC) to Lyse Erythrocytes*. Cell Host Microbe, 2015. **18**(3): p. 363-70.
42. Chatterjee, N., et al., *A novel heme transporter from the ECF family is vital for the Group A Streptococcus colonization and infections*. J Bacteriol, 2020.
43. Verplaetse, E., et al., *Heme Uptake in Lactobacillus sakei Evidenced by a New Energy Coupling Factor (ECF)-Like Transport System*. Appl Environ Microbiol, 2020. **86**(18).
44. Torres, V.J., et al., *Staphylococcus aureus IsdB is a hemoglobin receptor required for heme iron utilization*. J Bacteriol, 2006. **188**(24): p. 8421-9.
45. Fields, P.I., et al., *Mutants of Salmonella typhimurium that cannot survive within the macrophage are avirulent*. Proc Natl Acad Sci U S A, 1986. **83**(14): p. 5189-93.
46. Groisman, E.A. and H. Ochman, *How to become a pathogen*. Trends Microbiol, 1994. **2**(8): p. 289-94.
47. Lau, G.W., et al., *A functional genomic analysis of type 3 Streptococcus pneumoniae virulence*. Mol Microbiol, 2001. **40**(3): p. 555-71.
48. Krick, T., et al., *Amino Acid metabolism conflicts with protein diversity*. Mol Biol Evol, 2014. **31**(11): p. 2905-12.
49. Pasamontes, A. and S. Garcia-Vallve, *Use of a multi-way method to analyze the amino acid composition of a conserved group of orthologous proteins in prokaryotes*. BMC Bioinformatics, 2006. **7**: p. 257.
50. Ferla, M.P. and W.M. Patrick, *Bacterial methionine biosynthesis*. Microbiology, 2014. **160**(Pt 8): p. 1571-1584.
51. Coates, A.R. and Y. Hu, *Novel approaches to developing new antibiotics for bacterial infections*. Br J Pharmacol, 2007. **152**(8): p. 1147-54.

52. Munger, J., et al., *Systems-level metabolic flux profiling identifies fatty acid synthesis as a target for antiviral therapy*. Nat Biotechnol, 2008. **26**(10): p. 1179-86.
53. Rabinowitz, J.D., et al., *Metabolomics in drug target discovery*. Cold Spring Harb Symp Quant Biol, 2011. **76**: p. 235-46.
54. Murima, P., J.D. McKinney, and K. Pethe, *Targeting bacterial central metabolism for drug development*. Chem Biol, 2014. **21**(11): p. 1423-32.
55. Fontecave, M., M. Atta, and E. Mulliez, *S-adenosylmethionine: nothing goes to waste*. Trends Biochem Sci, 2004. **29**(5): p. 243-9.
56. Guedes, R.L., et al., *Amino acids biosynthesis and nitrogen assimilation pathways: a great genomic deletion during eukaryotes evolution*. BMC Genomics, 2011. **12 Suppl 4**: p. S2.
57. Deakova, Z., et al., *Two-dimensional high performance liquid chromatography for determination of homocysteine, methionine and cysteine enantiomers in human serum*. J Chromatogr A, 2015. **1408**: p. 118-24.
58. Psychogios, N., et al., *The human serum metabolome*. PLoS One, 2011. **6**(2): p. e16957.
59. Shelver, D., et al., *MtaR, a regulator of methionine transport, is critical for survival of group B streptococcus in vivo*. J Bacteriol, 2003. **185**(22): p. 6592-9.
60. Nazi, I., et al., *Role of homoserine transacetylase as a new target for antifungal agents*. Antimicrob Agents Chemother, 2007. **51**(5): p. 1731-6.
61. Ejim, L.J., et al., *Cystathionine beta-lyase is important for virulence of Salmonella enterica serovar Typhimurium*. Infect Immun, 2004. **72**(6): p. 3310-4.
62. Otto, M., *Staphylococcal infections: mechanisms of biofilm maturation and detachment as critical determinants of pathogenicity*. Annu Rev Med, 2013. **64**: p. 175-88.
63. Jochim, A., et al., *Methionine Limitation Impairs Pathogen Expansion and Biofilm Formation Capacity*. Appl Environ Microbiol, 2019. **85**(9).
64. Ma, L., et al., *Assembly and development of the Pseudomonas aeruginosa biofilm matrix*. PLoS Pathog, 2009. **5**(3): p. e1000354.
65. Ryder, C., M. Byrd, and D.J. Wozniak, *Role of polysaccharides in Pseudomonas aeruginosa biofilm development*. Curr Opin Microbiol, 2007. **10**(6): p. 644-8.
66. Friedman, L. and R. Kolter, *Genes involved in matrix formation in Pseudomonas aeruginosa PA14 biofilms*. Mol Microbiol, 2004. **51**(3): p. 675-90.
67. Ma, L., et al., *Pseudomonas aeruginosa Psl is a galactose- and mannose-rich exopolysaccharide*. J Bacteriol, 2007. **189**(22): p. 8353-6.
68. Friedman, L. and R. Kolter, *Two genetic loci produce distinct carbohydrate-rich structural components of the Pseudomonas aeruginosa biofilm matrix*. J Bacteriol, 2004. **186**(14): p. 4457-65.
69. Krismer, B., et al., *Nutrient limitation governs Staphylococcus aureus metabolism and niche adaptation in the human nose*. PLoS Pathog, 2014. **10**(1): p. e1003862.
70. Bachman, M.A., et al., *Genome-Wide Identification of Klebsiella pneumoniae Fitness Genes during Lung Infection*. mBio, 2015. **6**(3): p. e00775.

71. Hofford, J.M., et al., *Levels of amino acids and related compounds in bronchoalveolar lavage fluids of asthmatic patients*. Am J Respir Crit Care Med, 1997. **155**(2): p. 432-5.
72. Wang, N., et al., *Genome-wide identification of Acinetobacter baumannii genes necessary for persistence in the lung*. mBio, 2014. **5**(3): p. e01163-14.
73. Wisell, K.T., G. Kahlmeter, and C.G. Giske, *Trimethoprim and enterococci in urinary tract infections: new perspectives on an old issue*. J Antimicrob Chemother, 2008. **62**(1): p. 35-40.
74. Rohl, F., J. Rabenhorst, and H. Zahner, *Biological properties and mode of action of clavams*. Arch Microbiol, 1987. **147**(4): p. 315-20.
75. Kong, Y.H., et al., *Natural product juglone targets three key enzymes from Helicobacter pylori: inhibition assay with crystal structure characterization*. Acta Pharmacol Sin, 2008. **29**(7): p. 870-6.
76. Paulsen, M.T. and M. Ljungman, *The natural toxin juglone causes degradation of p53 and induces rapid H2AX phosphorylation and cell death in human fibroblasts*. Toxicol Appl Pharmacol, 2005. **209**(1): p. 1-9.
77. Johnston, M., et al., *Suicide inactivation of bacterial cystathionine gamma-synthase and methionine gamma-lyase during processing of L-propargylglycine*. Biochemistry, 1979. **18**(21): p. 4690-701.
78. Rao, A.M., M.R. Drake, and M.H. Stipanuk, *Role of the transsulfuration pathway and of gamma-cystathionase activity in the formation of cysteine and sulfate from methionine in rat hepatocytes*. J Nutr, 1990. **120**(8): p. 837-45.
79. Steegborn, C., et al., *Kinetics and inhibition of recombinant human cystathionine gamma-lyase. Toward the rational control of transsulfuration*. J Biol Chem, 1999. **274**(18): p. 12675-84.
80. Kong, Y., et al., *Enzymatic characterization and inhibitor discovery of a new cystathionine {gamma}-synthase from Helicobacter pylori*. J Biochem, 2008. **143**(1): p. 59-68.
81. Smilack, J.D., *Trimethoprim-sulfamethoxazole*. Mayo Clin Proc, 1999. **74**(7): p. 730-4.
82. Jorge, A.M., et al., *Staphylococcus aureus counters phosphate limitation by scavenging wall teichoic acids from other staphylococci via the teichoicase GlpQ*. J Biol Chem, 2018. **293**(38): p. 14916-14924.
83. Schmidl, S.R., et al., *A trigger enzyme in Mycoplasma pneumoniae: impact of the glycerophosphodiesterase GlpQ on virulence and gene expression*. PLoS Pathog, 2011. **7**(9): p. e1002263.
84. Kehl-Fie, T.E. and E.P. Skaar, *Nutritional immunity beyond iron: a role for manganese and zinc*. Curr Opin Chem Biol, 2010. **14**(2): p. 218-24.

Contributions to publications

Chapter 2- An ECF-type transporter scavenges heme to overcome iron-limitation in *Staphylococcus lugdunensis*

Jochim A, Adolf LA, Belikova D, Schilling NA, Setyawati I, Chin D, Meyers S, Verhamme P, Heinrichs DE, Slotboom DJ and Heilbronner S

For this publication, I performed all experiments except the MALDI-TOF and ESI-MS analysis (Nadine-Anna Schilling), the hemolysis of human and mouse erythrocytes (David Heinrichs and Denny Chin) , the construction of the expression plasmid pQE30::LhaS (Lea Adolf), the qPCR analysis (Darya Belikova) and the intracellular iron accumulation assay (Lisa Dengler).

Chapter 3- Methionine limitation impairs pathogen expansion and biofilm formation capacity

Jochim A, Shi T, Belikova D, Schwarz, S, Peschel A and Heilbronner S

For this publication, I performed all experiments (by myself or in cooperation) but the following:

Growth yields of model organisms with pooled human serum (Darya Belikova), construction of the complementation plasmid pME6032::*metA* (Darya Belikova).